CORRELATION OF SEA SURFACE TEMPERATURE WITH CLOUD PATTERNS OFF THE WEST COAST OF NORTH AMERICA DURING THE UPWELLING SEASON

Anthony Leo Gerst

United States
Naval Postgraduate School

THESIS

CORRELATION OF SEA SURFACE TEMPERATURE
WITH CLOUD PATTERNS OFF THE WEST COAST
OF NORTH AMERICA
DURING THE UPWELLING SEASON

by

Anthony Leo Gerst

October 1969

Correlation of Sea Surface Temperature with Cloud Patterns off the West Coast of North America During the Upwelling Season

by

Anthony Leo Gerst
Lieutenant, United States Navy
B. S., The Pennsylvania State University, 1964

Submitted in partial fulfillment of the
requirements for the degree of

MASTER OF SCIENCE IN OCEANOGRAPHY

from the

NAVAL POSTGRADUATE SCHOOL
October 1969

ABSTRACT

The possibility of a correlation between sea surface temperature (SST) and cloud patterns was investigated using cloud photos from the satellites NIMBUS II (1967) and ESSA VI (1968). Five types of correlation were found to exist: the correlation between stratus and the California Current and upwelling areas in a warm air mass, between clearing and the California Current and upwelling areas in a cold air mass, between stratus and the upwelling areas under favorable conditions, between frontal clouds and warm tongues of surface water, and between vortices and cold tongues of surface water. A sixth type of correlation was found between the surface isobaric pattern and the orientation of cold and warm tongues of surface water. Finally, the divergence of the surface isobars was found not to correlate with the stratus pattern. An awareness of the physical conditions off the coast was vital to seeing and understanding these correlations. A model SST analysis, using the six types of correlation observed, represented the actual SST analysis significantly better than the historical SST analysis.

TABLE OF CONTENTS

LIST OF TABLES

LIST OF FIGURES

NEPHANALYSIS LEGEND*

BOUNDARIES

 Major Cloud System ———— Definite

- — — — — Indefinite

CLOUD AMOUNT (COVERAGE)

O	Open	Less than 20%
MOP	Mostly Open	20% to 50%
MCO	Mostly Covered	51% to 80%
C	Covered	More than 80%

SYMBOLS

 Vortex  Vorticity Center

 Bright (Highly reflective cloud mass)

 Thin

 Striations

CLOUD TYPES

 Cumuliform  Stratiform

 Strato-cumuliform Cirriform

---

* From Bittner (1967)

ACKNOWLEDGEMENTS

The author wishes to express his appreciation to Professor Glenn H. Jung and Professor Dale F. Leipper of the Naval Postgraduate School for their guidance and assistance in this study. Appreciation is also expressed to those of the library staff for their cooperation in obtaining background material.

I. INTRODUCTION

The principal objects of this research were to determine (1) if a correlation exists between the sea surface temperature (SST) and the cloud patterns off the coast of North America during the upwelling season, and (2) if upwelling areas can be delineated through the use of satellite cloud photos.

Since normally only scant synoptic SST observations are available, a description of the SST patterns is difficult to obtain in detail, especially on a day-to-day basis. It does not appear that the availability of synoptic SST data will increase significantly in the near future; therefore it appears desirable to explore relationships between the SST patterns and more readily available data. With the advent of the satellite with photographic telemetry capability, cloud patterns over the ocean are readily available to readout stations on a synoptic basis. Thus any correlation between these cloud patterns and SST patterns would improve our description of the sea surface temperature distribution.

In a cold air mass, cloudiness (cumuliform) would be expected over the warmer areas of the ocean and less cloudiness or clearing over the colder areas. In a warm air mass, cloudiness (stratiform) would be expected over the colder areas of the ocean with less cloudiness or clearing

over the warmer areas. Confirmation of this type of correlation has been suggested in three recent reports. In a cruise report by the Bureau of Commercial Fisheries (1968), a cloud-free area (in a cold air mass) along the southwest coast of Africa was observed to appear consistently in satellite photos. It was suggested that this cloud-free area was associated with cold water from upwelling or with the cold Benguela Current. Two reports from the Naval Oceanographic Office (LaViolette and Seim, 1968 and 1969a) noted that persistent cloud patterns over the ocean can be associated with the sea surface temperatures and thus with the oceanographic features of the ocean. Examples presented in these papers included the Peru Current region, the north wall region of the Gulf Stream, and upwelling areas off the coasts of the Somali Republic and India. It was suggested that a good working knowledge of the physical conditions in the area concerned is necessary to discern these correlations.

The area off the west coast of North America is an area of a cold ocean current and relatively strong upwelling; there is an excellent opportunity to study this air-sea interaction phenomenon through use of locally received satellite photos of cloudiness cover along with synoptic SST data reported for that region.

II. BACKGROUND

To obtain a good working knowledge of the physical conditions in the area off the west coast of North America in the upwelling season, a detailed investigation of what is known about the normal SST distribution and the atmospheric conditions near the sea surface is necessary. The normal distribution of the SST with geographic location and with time, along with the criteria required for cloud formation under certain conditions in certain areas, must be known in order to determine if correlations do, in fact, exist.

A. DISTRIBUTION OF SEA SURFACE TEMPERATURE

The spatial distribution of the sea surface temperatures in the California Current and upwelling areas is not zonal, as it is in the mid-ocean regions. Therefore, a knowledge of the influencing factors (which include the flow of the California Current and countercurrent, the radiation and heat exchanges with the atmosphere, and upwelling) is essential to fully understand the distribution of the SST. The process of mixing combines the effects of these influencing factors. The distribution of SST with time can be described in terms of range and variation.

1. The Spatial Distribution of Sea Surface Temperatures

Sverdrup and Fleming (1941) classified the surface water off southern California into three types. These are

the offshore surface water which has a normal temperature (typical for that location in the California Current); the upwelling water which has a low temperature; and the countercurrent water which has a high temperature. This subdivision of the surface water can be applied to all the water off the west coast of the United States and Baja California.

Sverdrup and Fleming found large horizontal differences in sea surface temperature and a tongue-like distribution existing down the depths of 25 m. A more recent technical report from the Oceanographic Office by LaViolette and Seim (1969b) presents monthly mean sea surface temperatures for the Pacific Ocean based on over six million observations taken over 105 years. Fig. 1 shows the mean SST for the eastern North Pacific area and during the months concerned in this research.

2. Factors Influencing the Distribution of Sea Surface Temperatures

Several factors must be considered in studying the temperature distribution along the west coast of North America; of these factors, the most important are the flow of the California Current, the flow of the countercurrent, radiation and heat exchanges with the atmosphere, and upwelling.

Skogsberg (1936) in his classic study of upwelling in Monterey Bay divided the year into three seasons for coastal water. First is the period of the countercurrent which

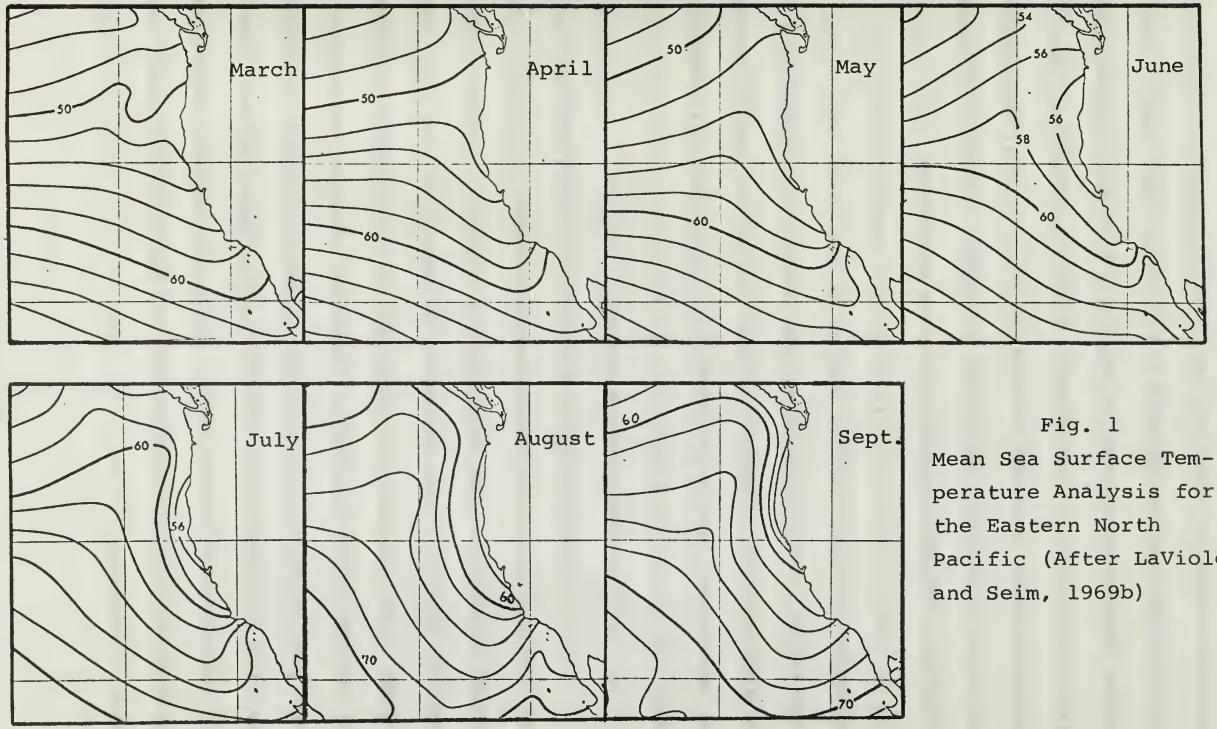

Fig. 1
Mean Sea Surface Temperature Analysis for the Eastern North Pacific (After LaViolette, and Seim, 1969b)

occurs during late fall to the middle of winter. This period is typical of a low vertical gradient of temperature and sinking of surface water along the coast. Next is the cold water phase, the period of coastal upwelling, which continues to late summer. Finally there is the oceanic season in which the California Current dominates the coastal waters. Although radiation and heat exchanges with the atmosphere predominate in mid-ocean areas, they play a lesser relative role near the coast. Upwelling dominates the area within 100 km of the coast while the California Current dominates the water further offshore. The effect of the countercurrent during the upwelling season is minimal, but a discussion is included for completeness.

a. The California Current

The California Current is a wind-driven current flowing southeast off the western North American coast between a cell of high atmospheric pressure to the west over the ocean and low pressure to the east over land. This current turns westward between 20N and 30N where it becomes part of the North Equatorial Current. Except when high winds persist for several days, the speed of the Current is less than one-half knot (Pattullo and others, 1958). The cool subarctic waters of the California Current cause the SST isotherms to bend south as they approach the west coast of North America.

b. The Countercurrent

The countercurrent flows along the coast at ocean depths below 200 m from the tip of Baja California to north of Cape Mendocino (Reid and others, 1958). In late fall and early winter it appears at the surface on the inshore side of the California Current and flows north to Point Conception; there it is called the Davidson Current.

c. Radiation and Heat Exchanges with the Atmosphere

The four principal processes to be considered in this ocean region are discussed by Tabata (1957) and James (1966). First of these is solar radiation, which is a function of the sun's altitude and cloudiness. The seasonal effects of insolation are counteracted by the high frequency of fog and stratus in the summer and the relatively clear conditions in the winter (Skogsberg, 1936).

Second of the considered processes is the effective back radiation. This is a function of temperature of the sea surface, the temperature of the air, and the moisture content of the air. Leipper (1947) asserted that radiation is unimportant in altering the pattern of sea surface temperature since in cloudly regions both incoming and back radiation are reduced and therefore the net radiation is not significantly different from that of clear areas.

Third is evaporation and condensation which depend upon the difference between the vapor pressure at the sea

surface and in the air above it; evaporation and condensation also depend on the velocity of the wind. Since evaporation tends to cool warmer areas of the ocean more than colder areas (since a larger amount of vapor is required to saturate the warm air overlying warm ocean areas) and condensation tends to warm colder areas of the ocean more than warmer areas, they both tend to diminish the SST gradient (Leipper, 1947).

Finally there is the conduction of sensible heat between the ocean surface and the atmosphere. This depends mainly on the vertical temperature gradient across the air-sea interface and the stability above the sea surface which in turn depends on the type of air mass above the sea surface. A cold air mass,which will have instability and thus a high conductive efficiency, will lower the sea surface temperature; while a warm air mass, which will have a high stability and thus a low conductive stability, may slightly warm the sea surface.

d. Upwelling

One of the objectives of this research is to better describe and understand the oceanic processes associated with upwelling; as background material, a detailed consideration of past research is presented.

Upwelling is that process wherein water from subsurface layers is drawn to the surface at a continuous or intermittent rate, where it spreads outward from the originating area (Sverdrup and Fleming, 1941). The process

and its mechanism have been investigated considerably along the west coast of North America, especially by McEwen (1934), Skogsberg (1936), Sverdrup and Fleming (1941), Yoshida (1955) and (1958), Yoshida and Mao (1957), Arthur (1965), and Smith and others (1966).

(1) Nearshore Circulation. One of the early attempts to describe the flow near the California Coast was by Skogsberg (1936) in his investigation of the hydrography of Monterey Bay. He attributed upwelling to the combined effects of the offshore deflection of the wind-driven current flowing south, and subsurface motion perpendicular to and directed toward the coast. This subsurface motion presumably caused a pressure upward when encountering a deep southerly-flowing current, such as the California Current. He concluded that upwelling did not occur against the continental slope, but instead it occurs against this deep current.

Sverdrup (1938) presented observations (Fig. 2) off southern California and adapted them to a model. He described upwelling as due primarily to the northerly winds. The area in Fig. 2 marked by plus signs is an area of swift current and is an offshore boundary. An inner cell exists between the coast and the offshore boundary, and this reaches a depth of about 80 m. Another cell is observed between the outer edge of the offshore boundary and some diffuse boundary away from the coast.

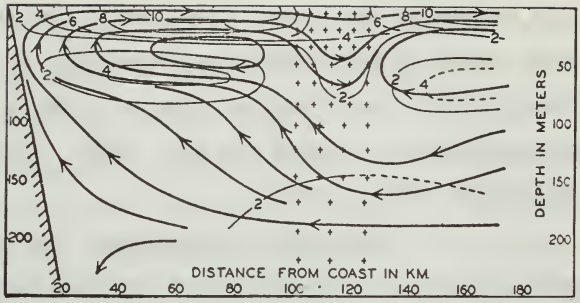

Fig. 2. Nearshore Circulation as Presented by Sverdrup (1938).

(Direction shown by heavy lines with arrows; horizontal velocities shown by thin lines in cm/sec.)

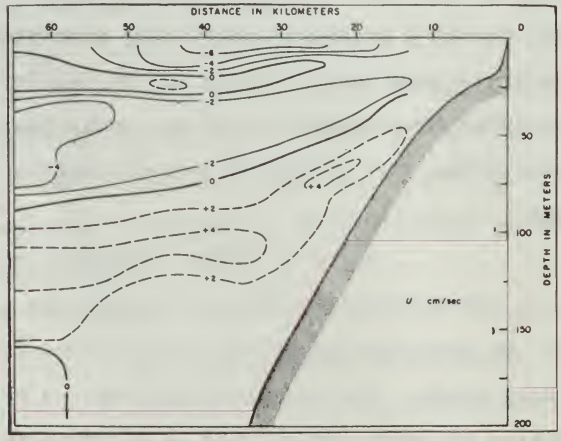

Fig. 3. Mean Onshore Flow
(After Smith and others, 1966)

The inner cell is fed from below by water flow toward the coast at greater depths as the boundary moves slowly seaward. The maximum depth of the inflow to the inner cell is 200 m. The boundary is not considered a solid surface, but one which is continuously reforming. The velocity of the boundary surface is determined to be about 2 cm/sec. Great shearing motion occurs on both sides of the boundary, and eddies may be produced.

Smith and others (1966) presented a nearshore circulation, computed from temperature and salinity data off the Oregon Coast, similar to that of Sverdrup (Fig. 3). The minimum encountered at 25 m is attributed to the fact that an initial assumption, whereby there is no cross-isogram transport (mixing), is not strictly correct.

Hidaka (1954) presented a theoretical model describing the nearshore circulation resulting from either a longshore flow or from an offshore flow (see Figs. 4 and 5). He derives the stream function in Eq. (1), composed of components due to the wind stress perpendicular to the coast (τ_x) and the wind stress parallel to the coast (τ_y).

$$\Psi(x,z) = \left(\frac{2\pi\tau_x}{\rho\omega \sin\phi}\right) \Phi_x(x,z) + \left(\frac{2\pi\tau_y}{\rho\omega \sin\phi}\right) \Phi_y(y,z) \quad . \tag{1}$$

If the wind stress perpendicular to the coast is zero ($\tau_x = 0$), then the circulation shown in Fig. 4 results from

the remaining wind stress parallel to the coast (longshore flow). The circulation in Fig. 5 results from offshore flow, i.e., when the wind stress parallel to the coast is zero ($\tau_y = 0$). The longshore flow can be shown to produce more intense upwelling than that due to the offshore flow. Hidaka further calculates the direction of the wind that will produce the most intense upwelling. He found this direction depends on the width of the wind belt; when this width is greater than the friction distance (D_h), the angle approaches 21.5° asymptotically.

While Sverdrup (1938) does not consider his outer cell as upwelling (see Fig. 2), Yoshida and Mao (1957) consider this to be upwelling of a large horizontal extent. They assumed a two-layer ocean wherein they derived the vertical change in the vertical velocity.

$$\frac{\partial w}{\partial t} = \frac{\beta v}{f} + \frac{1}{f} \frac{\partial \mathrm{Curl}_z \tau}{\partial z} \quad . \tag{2}$$

Then from dimensional analysis they show that the horizontal divergence (W_h) balances the stress vorticity in the surface layer,

$$W_h = - \frac{1}{f} \mathrm{Curl}_z \tau \quad , \tag{3}$$

and the planetary vorticity in the lower layer

$$W_h = - \frac{\beta}{f} \int_H^D v dz \quad . \tag{4}$$

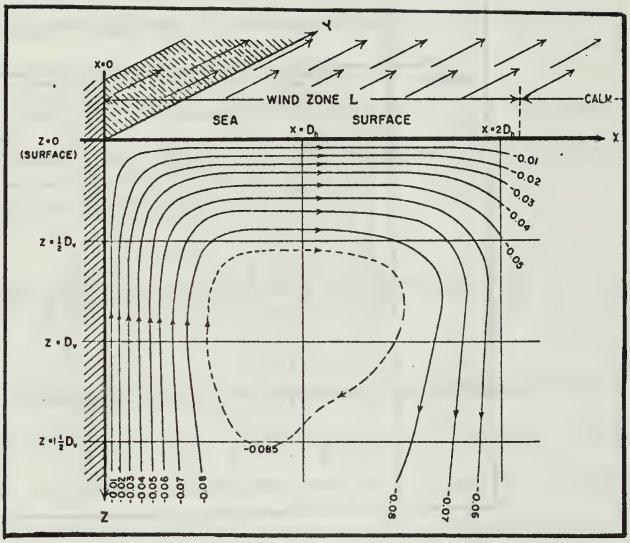

Fig. 4. Streamlines Resulting from Wind Parallel to the Coast (After Hidaka, 1954)

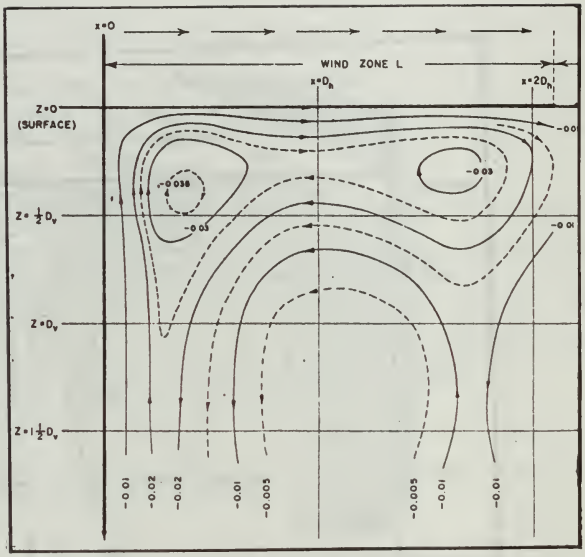

Fig. 5. Streamlines Resulting from on Offshore Wind (After Hidaka, 1954)

In these equations, H is the depth of the interface of the two layers, h is the depth of the mixed layer, and D is the total depth. From (4) it can be seen that ascending motion is associated with a subsurface poleward-moving current while descending motion is associated with a southerly subsurface flow. From (3) it can be seen that upwelling of a large horizontal extent is the result of the curl of the wind stress and will take place when this curl is greater than zero.

Arthur (1965) obtained a result (5) similar to that of Yoshida and Mao [see (2)], except that he retained the relative vorticity term,

$$(\zeta+f)\frac{\partial w}{\partial z} = \frac{D\zeta}{Dt} + \beta_v - A_H\left(\frac{\partial^2\zeta}{\partial x^2} + \frac{\partial^2\zeta}{\zeta_y{}^2}\right) + A_v\frac{\partial^2\zeta}{\zeta_z{}^2}. \qquad (5)$$

Yoshida (1955 and 1958) compared coastal upwelling with upwelling of a large horizontal extent. Coastal upwelling is more intense and smaller in scale. Although the two regions of upwelling often occur simultaneously, they are separated by a trough of sinking water. Coastal upwelling is attributed to the wind stress itself rather than to the curl of the wind stress, and it is not considered by Yoshida to be purely wind-driven. To obtain an intensity such as that obtained in a narrow coastal zone, the coastal barrier and the stratification of the water must be considered.

(2) Transport. Most transport values presented for the west coast of North America are similar in magnitude. Using the Ekman transport equation

$$M_N = \frac{\tau_y}{f} \tag{6}$$

and the integration of the vertical velocity,

$$M_N = \int_o^h v dt \ . \tag{7}$$

Sverdrup and Fleming (1941) computed transports (M_N) normal to the coast of southern California as 2.28×10^4 gm/(cm-sec) and 2.62×10^4 gm/cm-sec respectively. Smith and others (1966) used temperature and salinity data to compute the transport which ranged from 1.56 to 3.80×10^4 gm/(cm-sec) off the Oregon Coast.

Smith (1967) showed that Yoshida's transport equation (8) could reduce to the Ekman transport equation if L, a characteristic width, is taken large enough (e.g. L = 50 km where coastal upwelling becomes insignificant)

$$M_N(x=-L) = \int_o^{-L} PN_{-h} dx = \frac{\tau_y}{f} (1-e^{-KL}) . \tag{8}$$

He concluded that the Ekman transport gives a valid estimate of the offshore transport in the early (non-equilibrium) stages of coastal upwelling.

(3) Velocity of Upwelling. Upwelling velocity values reported by different authors are similar; these are summarized in Table I. A value of 10^{-3} cm/sec. appears to be a representative order of magnitude.

(4) Period of Upwelling. The period of strongest upwelling differs along different parts of the coast. For San Diego, McEwen (1934) gives the upwelling period as April to September with a maximum during June and July. Skogsberg (1936) for Monterey Bay gives the upwelling period as the middle of February to the beginning of September. Maximum upwelling occurs before the end of July in his investigations. Reid and others (1958) suggested that upwelling is the strongest when the north and northwest winds are most marked. This is in April and May off Baja California, May and June off southern California, June and July off northern California, and August off Oregon. Wyrtki (1960) said that upwelling off Baja California occurs all year long.

A theoretical consideration for large scale upwelling was given by Yoshida and Mao (1957). They used their equation for vertical velocity in the surface layer [see (3)] to show that intense upwelling should occur only in the spring in southern areas, because the curl of the wind stress has only positive values in this area in the spring; intense upwelling occurs only during the summer and fall in the northern areas, where the curl of the wind stress has only positive values at that time.

AUTHOR	METHOD	LOCATION	DEPTH	VELOCITY	MONTHS
McEwen (1934)	Calculated from the Fourier Heat Equation	San Diego	Surface	(0.8 to 2.9)x 10^{-3}cm/sec	April to September
Skogsberg (1936)	Measured	Monterey Bay	Surface	2.0 x 10^{-3}cm/sec	Summer
Sverdrup and Fleming (1941)	Measured	Southern California	Surface	1.5 x 10^{-3}cm/sec	Summer
Yoshida and Mao (1957)	Calculated from Model	West Coast	Surface	2.0 x 10^{-3}cm/sec	Summer
			150 m	0.7 x 10^{-3}cm/sec	Summer
Arthur (1965)	Calculated from Model	West Coast	100 m	0.8 x 10^{-3}cm/sec	Summer
Smith & others (1966)	Calculated from Yoshida's (1955) Eq.	Oregon	Surface*	8.5 x 10^{-3}cm/sec	Summer
			Surface**	0.1 x 10^{-3}cm/sec	Summer
	Calculated from Temperature and Salinity Data	Oregon	Surface*	7.0 x 10^{-3}cm/sec	Summer
			Surface**	0.2 x 10^{-3}cm/sec	Summer

* 9 km from the coast
** 65 km from the coast

TABLE I - Summary of Upwelling Velocities.

(5) Depth of Upwelling. Skogsberg (1936) indicated that upwelling was limited normally to the upper 300 m; but during years of intense upwelling, the depth could be greater. Sverdrup and Fleming (1941) have indicated this figure to be about 200 m. Roden and others (1962), using statistical data off northern California, concluded that water from depths greater than 100 m does not ascend frequently to the sea surface in that area.

(6) Width of Upwelling. Sverdrup (1938) found evidence of coastal upwelling out to 100 km from the coast. Yoshida and Mao (1957) implied that upwelling of a large horizontal extent could occur out as far from the coast as 600 km. Yoshida's (1955) theory of coastal upwelling described a narrow strip of upwelling about 50 km in width close to the coast. The width of the coastal upwelling is controlled by two parameters. The first is the axis of the northerly winds; when the axis is closer to the shore, the upwelling zone width will be narrower and vice versa. The second parameter is the latitude; the calculations presented from Yoshida's model showed that the upwelling area width decreased with increasing latitude.

(7) Most Intense Areas of Upwelling. Sverdrup and others (1944) indicated centers of upwelling along the coast at 24N, 35N, and 41N. Hidaka (1954) suggested that since his velocity components all included the sine of the latitude in the denominator, the intensity should increase

with decreasing latitude. Reid and others (1958) noted that upwelling was more intense south of capes and seaward extensions (Cape Mendocino, Point Conception, and Punta Eugenia). Pattullo and others (1960) reported a similar situation off the coast of Oregon, while Dawson (1951) reported this effect off the coast of Baja California. Arthur (1965), using his equation, [see (5)], for upwelling velocity, showed theoretically why this occurs. The planetary vorticity term is always negative on the west coast of continents (see Fig. 6). The relative vorticity

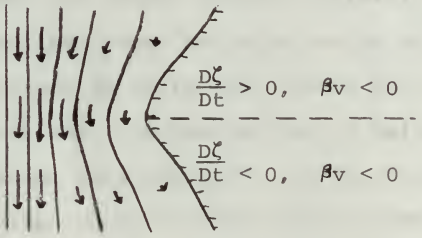

Fig. 6

Flow Across a Seaward Extension (After Arthur, 1965)

is positive north of the point or cape (opposing the planetary vorticity) and thus contributes to a smaller upwelling velocity; the vorticity term is negative south of the point or cape, and therefore contributes to a higher upwelling velocity. Holly (1968) showed that the most

persistent areas of coastal upwelling seem to be where the continental shelf slope is the greatest. These are approximately at 29N, 31N, and 33N.

(8) Summary. During the period from April to September, coastal upwelling is the principal controlling factor of sea surface temperature within 100 km of the west coast of North America; large scale upwelling is an influential factor in the California Current region further offshore. When comparing coastal and large scale upwelling, coastal upwelling is smaller in scale and more intense. The two types of upwelling frequently occur at the same time and are separated by a trough of sinking water. The nearshore circulation resulting from coastal upwelling is determined mainly by the wind stress; but the stratification of the water, topography, and latitude are influential factors. The winds may be either longshore or offshore to produce coastal upwelling. A predominantly longshore flow with a small offshore component produces the most intense upwelling. Intensity also increases, as does width, with decreasing latitude. Large scale upwelling is produced by the curl of the wind stress. The ascending motion of the water produced by the curl of the wind stress results in a subsurface poleward moving current. Also an increase in intensity south of capes and seaward extensions can be observed and shown theoretically to occur with a current flowing southward on a west coast.

3. Mixing

The mixing processes are discussed by James (1966). Wind mixing is rapid and irregular while convective mixing is slower and more steady. Convective mixing will always increase the mixed layer when it occurs, although this is not true of wind mixing.

Sverdrup and Fleming (1941) considered mixing as a process of diffusion. Horizontal mixing was found to be much more significant than vertical mixing. Skogsberg (1936), Yoshida (1955), and Sverdrup and Fleming suggested that horizontal mixing is maintained by quasi-horizontal eddies. The size of these eddies are 10 to 20 km or even greater and appear to grow in size with increasing upwelling intensity. Increased vorticity in the surface layer and local topography are suggested as the causes of the eddies.

4. Distribution of Sea Surface Temperatures with Time

a. Range of Sea Surface Temperatures

The maximum surface temperature is found in the fall and the minimum is found in early spring. Roden (1962), who analyzed data from 1935 to 1960, found the mean temperature off northern California coast to be lower in summer than in winter. The minimum observed was 7C. For southern California, the minimum observed was 10C, and temperatures of less than 13C were found in both summer and winter. Reid and others (1958) reported a range of 5C in

the monthly average temperature with a maximum range of 7C. He noted that the frequency distributions were not symmetrical; during the months of minimum temperature, the mean SST was closer to the minimum than to the maximum. He concluded that the large temperature departures in the cold months are the result of intrusions of warm water into the surrounding cold water rather than conversely. An opposite asymmetry was observed in late summer, although it was not as obvious.

The waters offshore vary in a simple pattern, with an increasing range of temperature occurring with higher latitude (Reid, 1960). Near the coast upwelling reduces the seasonal range of temperature and lenghtens the period for lower sea surface temperature. The maximum temperature in the fall is increased because of the (northward-flowing) countercurrent and the minimum in the spring is delayed because of it.

b. Variation of Sea Surface Temperature

Reid (1960) discussed anomalies of sea surface temperatures and suggested they are related to upwelling variations, atmospheric anomalies, and changes in the height of the sea surface. The intensity of the upwelling was noted to vary significantly from year to year by Skogsberg (1936). As the atmospheric pressure gradient weakens along the west coast, the flow of the California Current and the intensity of upwelling are diminished; thus the isotherms are displaced less to the south. Stewart

(1960) investigated the relation between sea level and temperature anomalies. As upwelling occurs, the level of the sea near the coastline is at a reduced level. If the upwelling diminishes in intensity to a significant extent, the surface waters are no longer pushed away from the coast and the sea level tends to establish a new equilibrium. This relation, Stewart noted, becomes poorer toward the north.

Arthur (1954), Leipper (1955), and Stevenson and Gorsline (1959) investigated unusual temperature variations for the continental shelf areas not related to upwelling. These erratic changes occur within a few miles of the coast; they appear to be due to internal waves of large amplitude. The intensity of the temperature differences depends on several factors in the bordering ocean; the most important factors are characteristics of the tide, the orientation of the topography, and the stratification of the water.

B. ATMOSPHERIC CONDITIONS NEAR THE SEA SURFACE

An understanding of the atmospheric conditions near the sea surface may begin with a description of the cloud cover; this is predominantly stratiform off the west coast of North America during the upwelling season. In studying the processes involved in the formation of fog and stratus, the vertical structure of the atmosphere should be considered. During the upwelling season, the nearly permanent inversion and the stability of the air mass are the most important

aspects of the vertical structure. The vertical structure, and thus formation of fog and stratus, are influenced by the synoptic situation and the sea surface temperatures.

1. Description of Cloud Cover

An overcast of stratus clouds is prevalent near the west coast of North America while further seaward, where the inversion is higher, the cloud layer becomes broken and the clouds are predominantly cumuliform (Neiburger, 1960). A manual on fog and stratus by the Air Weather Service (1954) states that the area affected by the fog and stratus extends from southern Oregon to Baja California, with a maximum frequency occurring between Point Reyes (near San Francisco) and Baja California. The season of highest frequency of fog and stratus is late spring to early fall.

2. The Vertical Structure of the Atmosphere

The typical structure of the atmosphere for the west coast during the upwelling season is presented in Fig. 7. A temperature inversion separates a marine layer at low level from warm dry air above (Petterssen, 1938). The marine layer has temperature and humidity characteristics influenced by the sea surface. The warm dry air above is related to subsidence of the upper level air within the Pacific anticyclone.

a. The Inversion

The inversion is composed of very stable air, so there is no turbulence and only molecular diffusion occurs vertically across it. It is produced dynamically

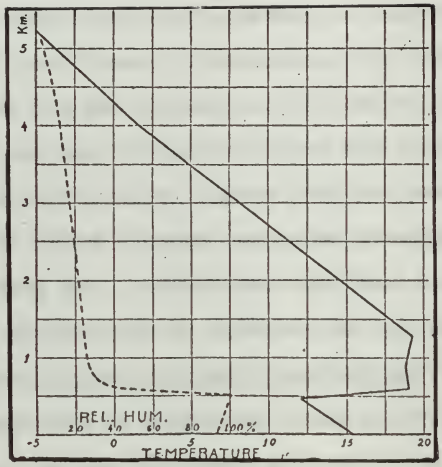

Fig. 7

Typical Structure of the Atmosphere off the West Coast of the United States (After Petterssen, 1938)

by subsidence and thermally by passage of the air mass over the cold surface waters (Patton, 1956). The air mass above and below it exchange properties primarily through radiation processes (Petterssen, 1938).

From June through September the inversion is almost a permanent feature in the eastern North Pacific ocean. Neiburger (1960) presented data on the frequency of soundings where the subtropical inversion is not present (Fig.8). The zero frequency isopleth (where the inversion always exists) encloses a substantial area off the North American coast. Neiburger and others (1961) presented data showing the average inversion height (Fig. 9). The inversion height is about 400 to 600 m along the coast with first a rapid increase as one proceeds seaward (to approximately 130W), and then there is a more gradual increase with distance offshore. These inversion height variations may be explained by the heating of the air as it moves from colder to warmer surface waters, which tends to offset the sinking motion through the inversion so that the inversion rises westward (Neiburger and others, 1961). From day to day the inversion height changes little over the ocean.

The inversion tends to make itself more permanent through radiation after formation of the stratus cloud (Petterssen, 1938). After the stratus has formed, the outgoing radiation from the cloud upper surface is that of a blackbody, while that of the warm dry air above is gray body radiation, which rarely amounts to more than

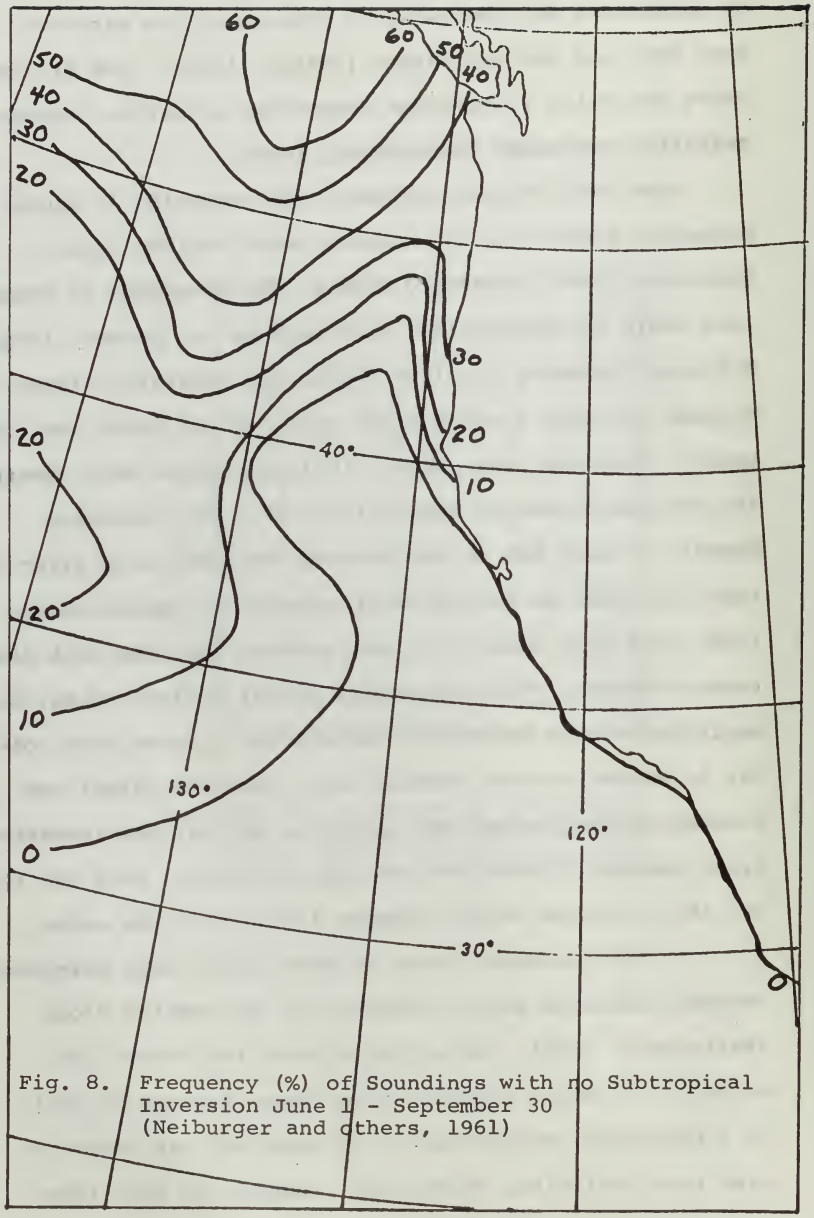

Fig. 8. Frequency (%) of Soundings with no Subtropical Inversion June 1 - September 30 (Neiburger and others, 1961)

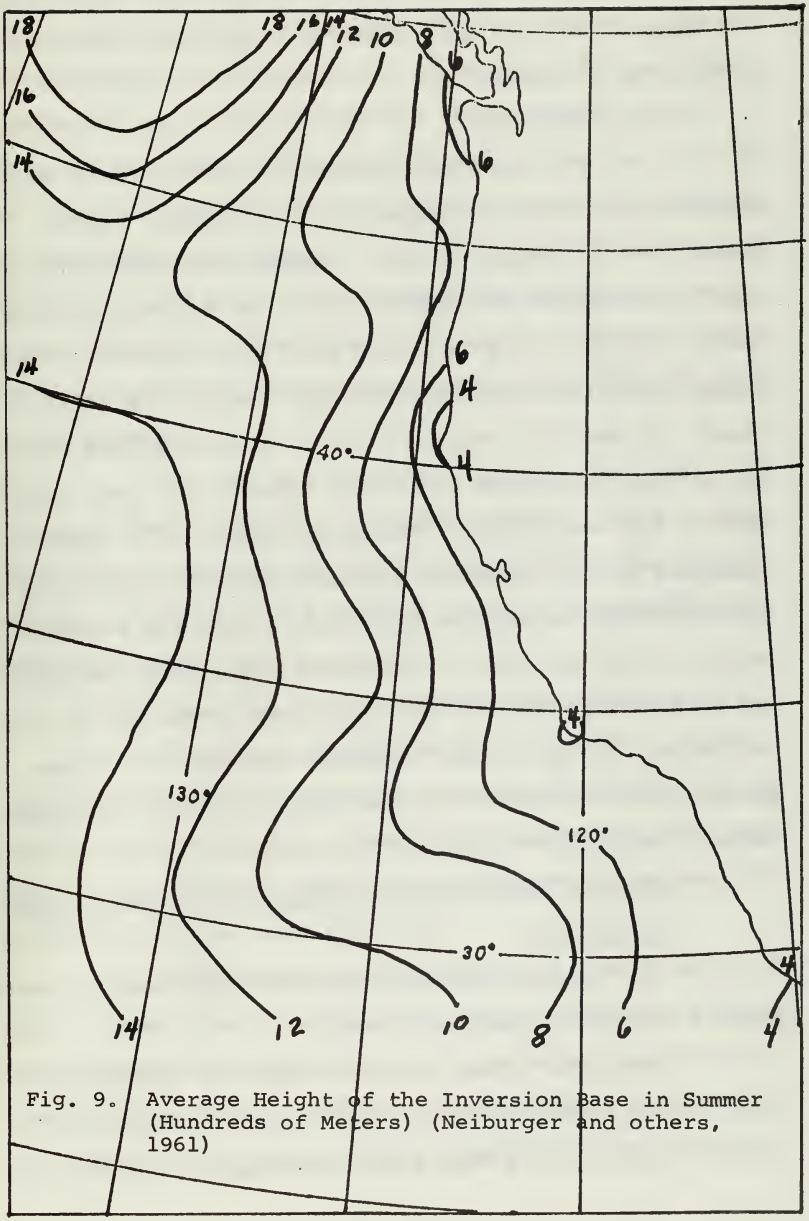

Fig. 9. Average Height of the Inversion Base in Summer (Hundreds of Meters) (Neiburger and others, 1961)

sixty-six percent of the blackbody radiation. Therefore, the temperature gradient becomes more positive, thus intensifying the inversion.

b. Stability

Fog and stratus along the west coast of North America is of a convective nature (Petterssen, 1938), (Wood, 1938), (Leipper, 1948). Leipper discussed this process in presenting his fog model for the Southern California Coast. After the fog is formed over the cold water, the incoming solar radiation is reflected from the top of the cloud. In addition, enough heat is radiated by the cloud top to cool the marine layer to a temperature lower than that of the sea surface. The marine layer, as a result, undergoes heating from the sea surface below, creating a superadiabatic convective lapse rate within the marine layer next to the ocean. Convective mixing then begins, and this mixing controls the thickness of the fog or stratus layer. Edinger (1963) observed that the top of the marine layer coincides with the level of maximum stability rather than with the base of the inversion.

3. Factors Influencing the Vertical Structure of the Atmosphere

a. Synoptic Conditions on the West Coast of North America During the Upwelling Season

Neiburger (1960) indicated that the normal position for the eastern Pacific anticyclone is 38N and 150W. Fig. 10 indicates the mean position of surface isobars

associated with this feature in July. According to Neiburger, it usually is not far from its normal location and intensity, but occasionally large deviations do occur. Subsidence occurs in the east and south sectors of the anticyclone. Thus, a favorable condition for fog and stratus formation normally exists over the California Current and upwelling areas depending on the intensity of the high and the passage of synoptic weather features (i.e., lows, fronts, troughs, convergence of the surface isobars) which have associated horizontal convergence of atmospheric flow at the surface.

For fog and stratus to move on the coast, the wind must have an onshore component (Patton, 1956). Offshore flow dissipates the fog and stratus near the coast because it brings to the coastal region a dryer warmer air mass which lowers the inversion.

b. Importance of Sea Surface Temperatures

The exact importance of sea surface temperatures is debated with respect to the formation and dissipation of fog and stratus. Some authors emphasize the importance of sea surface temperatures while others suggest different factors are more important.

Petterssen (1938) asserted that cold water is not the direct cause of fog and stratus, although it favors the formation by keeping the air temperature low and relative humidity high. According to Petterssen, the flux of heat after the formation of the inversion is upward from

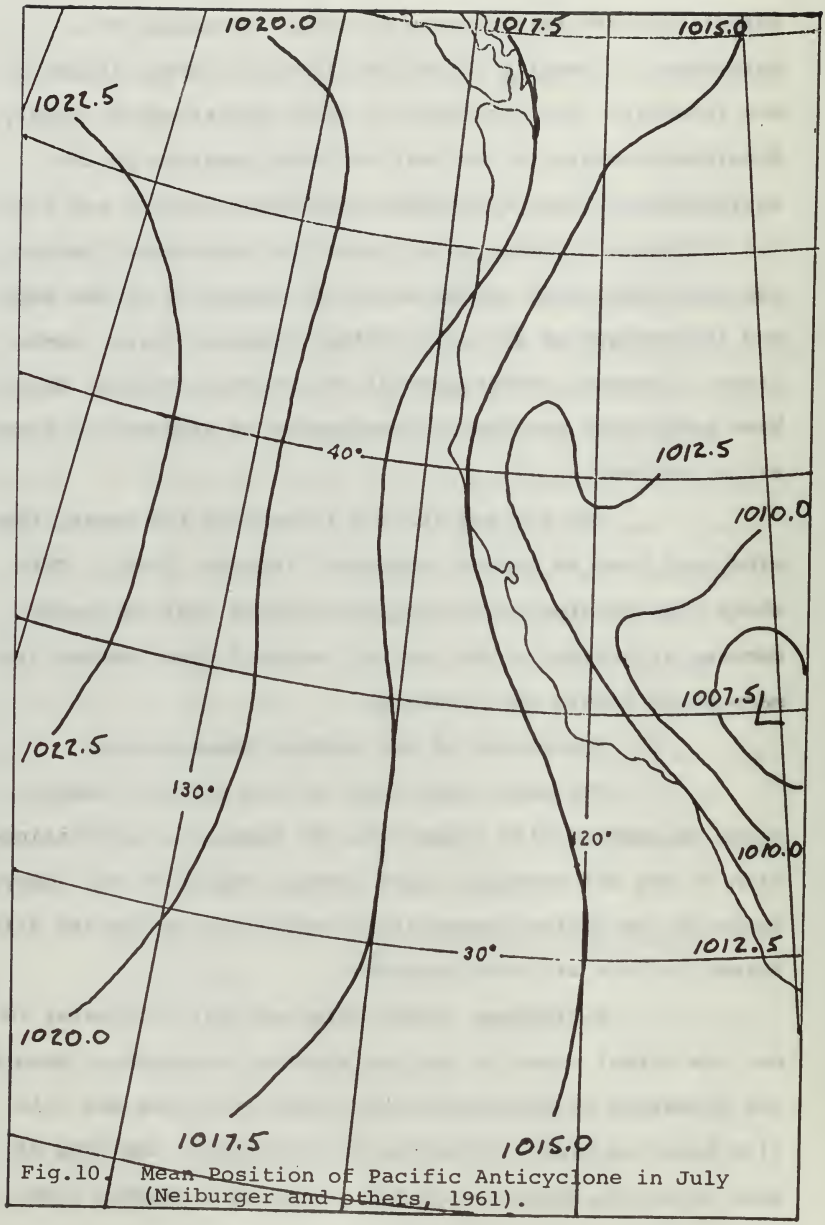

Fig.10. Mean Position of Pacific Anticyclone in July (Neiburger and others, 1961).

the cold moist air toward the warm dry air. When the surface or marine layer is sufficiently cooled, the stratus forms. Wood (1938) assumed that adiabatic cooling through convection is the immediate cause of the formation of stratus beneath a turbulence inversion.

Among those emphasizing the importance of sea surface temperature are Leipper (1947), Pincock and Turner (1955), and Patton (1956). Leipper investigated the influence of sea surface temperatures in fog and stratus formation off southern California. He concluded that the SST gradient in the direction of the air movement is very important in stratus and fog formation and dissipation. He stated that areas of coldest surface water should also be areas of greatest cloudiness since cloudiness increases as air is cooled. Patton asserted that stratus and fog cannot occur without cooling of the marine layer by contact with cold water. Pincock and Turner described the formation of fog over cold water along the British Columbia coast. With the onset of northwesterly winds along the coast of British Columbia, upwelling occurs and a SST gradient is established. This then leads to the rapid formation of a strip of advection fog over the colder waters near the coast. This takes place when the Pacific high is ridging into the Gulf of Alaska. On the western side of the ridge, warm marine air from south of 40N is brought over colder water at about 53N; this results in the formation of another

area of fog and stratus, well offshore. These two cloud masses tend to merge since, as shown from calculations by Pincock and Turner, the surface water that separates the two stratus areas are not warm enough to dissipate the clouds.

III. DATA AND PROCEDURE

A comparison was made of SST analyses and nephanalyses for the years 1967 and 1968. Nephanalyses were used because in this manner, to facilitate comparison, the cloud patterns could be transferred to a scale equal to that of the SST analyses. The distribution of the data is presented in Table II.

Two types of SST analysis were made. Daily analyses were made for each nephanalysis for the area outlined in Fig. 11. Data for these analyses were obtained from the National Weather Records Center, Asheville, North Carolina. Unfortunately, data from the National Weather Records Center were not obtained for the remainder of the area shown in Fig. 11. Therefore, composite analyses of varying time lengths were made using sea surface temperatures copied from ship reports on U.S. Weather Bureau surface weather charts. The composite analyses are included with certain available daily analyses. The daily analysis is selected for that time period nearest to the middle day of the period covered by the composite analysis. To support the assumption that the SST patterns did not change significantly over the composite time period, an attempt was made (by inspection) to cover a relatively constant synoptic situation with each composite chart.

Nephanalyses were made in accordance with instructions by Bittner (1967). The photos of 1968 (mostly from the

Month	Number of Photos Nephed	Number of Sea Surface Temperature Analyses
1967		
March	6	6
April	3	3
May	NO DATA AVAILABLE	
June	8	8
July	8	8
August	10	8
September	4	3
	39	36
1968		
March	2	2
April	9	9
May	NO DATA AVAILABLE	
June	11	11
July	16	16
August	13	13
September	14	14
	65	65

Table II

Data Distribution

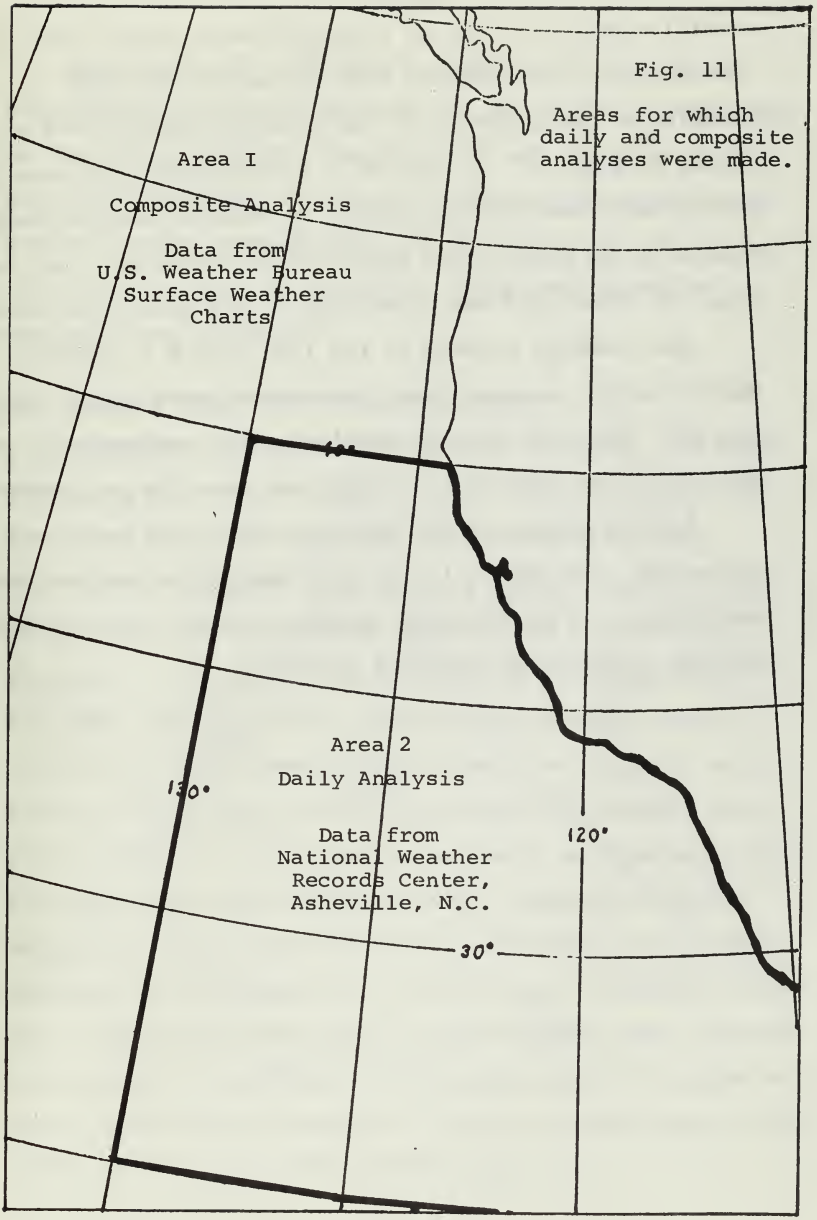

Fig. 11

Areas for which daily and composite analyses were made.

satellite ESSA VI) were of a significantly better quality than those of 1967 (mostly from the satellite NIMBUS II). Examples of the photos from the satellite ESSA VI are presented in Figs. 17, 28, and 31. Pictures were not received at the Naval Postgraduate School on weekends and holidays. Also only one pass of the satellite was received; and that pass, at times, did not cover much of the area of interest.

The isobaric pattern of the 1200 Zulu U.S. Weather Bureau surface weather chart was superimposed on the nephanalysis. This was done to supplement the nephanalysis in describing the atmospheric conditions near the sea surface.

Since analysis of the satellite photos is much less subjective than SST analysis, the temperature analyses were made first to eliminate any tendency to bias the isothermal pattern in favor of the cloud patterns.

IV. RESULTS

Five types of correlations between the sea surface temperatures and cloud patterns and one type of correlation between the sea surface temperatures and the isobaric pattern were observed. One type of non-correlation (between the sea surface temperatures and the divergence of the surface isobars) was also observed. These are described in the following paragraphs.

A. STRATUS OVER THE CALIFORNIA CURRENT

An inexact correlation between stratus and cold water underlying the warm air mass (the air mass is warmer than the water) over the California Current could be seen. Fig. 12 is a schematic diagram of a typical stratus cloud pattern with its correlating isobaric and SST patterns. The width of the stratus band increased with decreasing latitude. The tip of the stratus body normally occurred south of the sharp bend in the isobars, as depicted in the diagram, and it was located most frequently between latitudes 35N and 41N. A cold tongue of water existed under the stratus while a warm tongue of water formed the seaward boundary of the stratus or was aligned with a significant decrease in the intensity of the stratus. At times a warm spot occurred near the coast at about 33.5N, and a decrease in intensity or clearing of the clouds could be related to this. There were 38 examples illustrating this model; Figs. 25 and 28 illustrate the typical case.

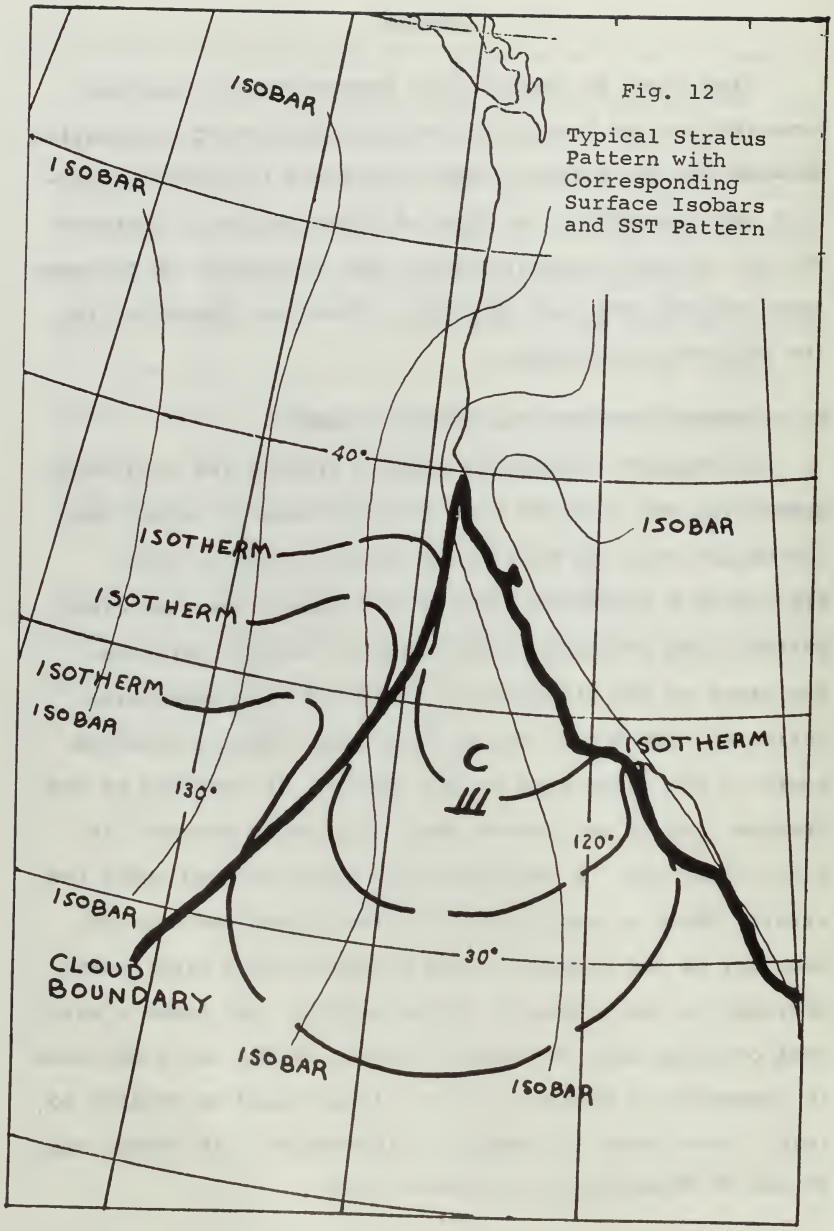

Fig. 12

Typical Stratus Pattern with Corresponding Surface Isobars and SST Pattern

Figs. 32 and 35 include a decrease in cloudiness which correlates with the warm spot near 33.5N. Fig. 36 shows the typical pattern on the upper part of the coast while Fig. 24 shows the pattern off Baja California. Fig. 34 shows the pattern covering the entire coast. Other examples can be seen in Figs. 21, 29, 30, and 33.

The rate of warming of SST in degrees per month for the period between April and August was computed for 1967, 1968, and for mean sea surface temperature data (data for the mean from LaViolette and Seim, 1969b). These are presented in Figs. 13, 14, and 15. Comparing the three, they appear to be similar in pattern. A frequency of occurrence of stratus was superimposed on Figs. 13 and 14 for the respective years; again a correlation can be noted. It appears that the SST pattern is very important in determining the spatial coverage of the stratus.

B. STRATUS AND UPWELLING AREAS

Only under specific conditions would clouds be observed that could be attributed to upwelling. They were masked by the stratus of the California Current many times, or were prevented from appearing due to a passing front or low, or because of offshore flow (offshore flow brings into the area a dry air mass which is not favorable to stratus formation). The cloud body generally appeared with a sharp eastern edge outlining the coast, and it extended seaward up to 100 miles. The clouds over the upwelling area

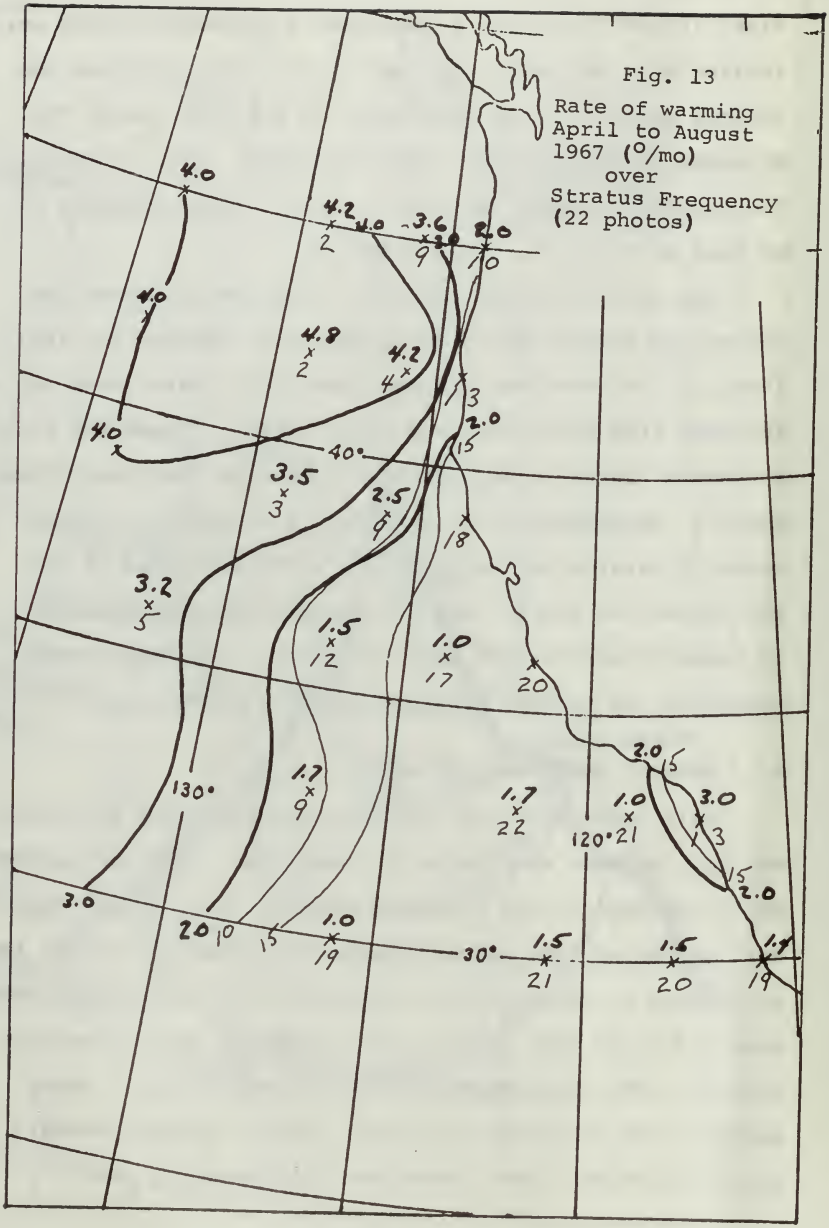

Fig. 13
Rate of warming
April to August
1967 (°/mo)
over
Stratus Frequency
(22 photos)

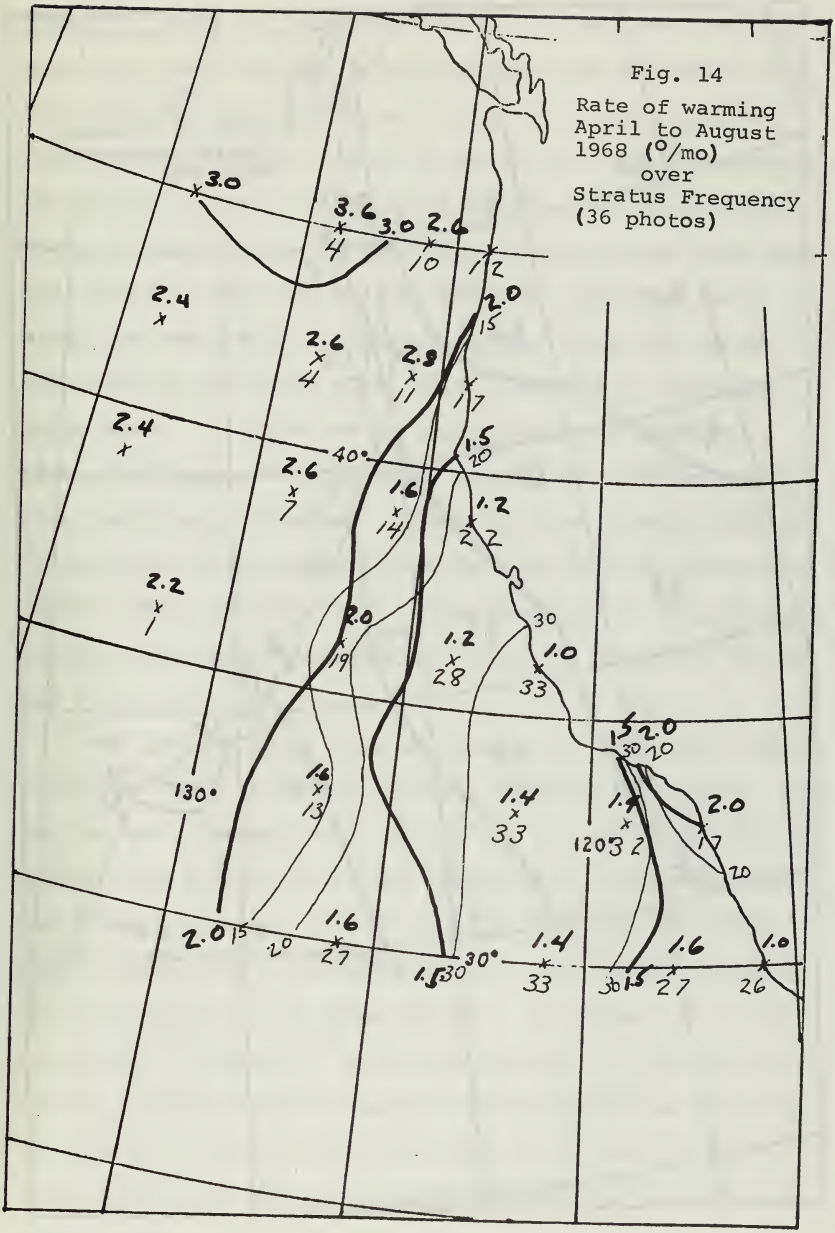

Fig. 14
Rate of warming
April to August
1968 (°/mo)
over
Stratus Frequency
(36 photos)

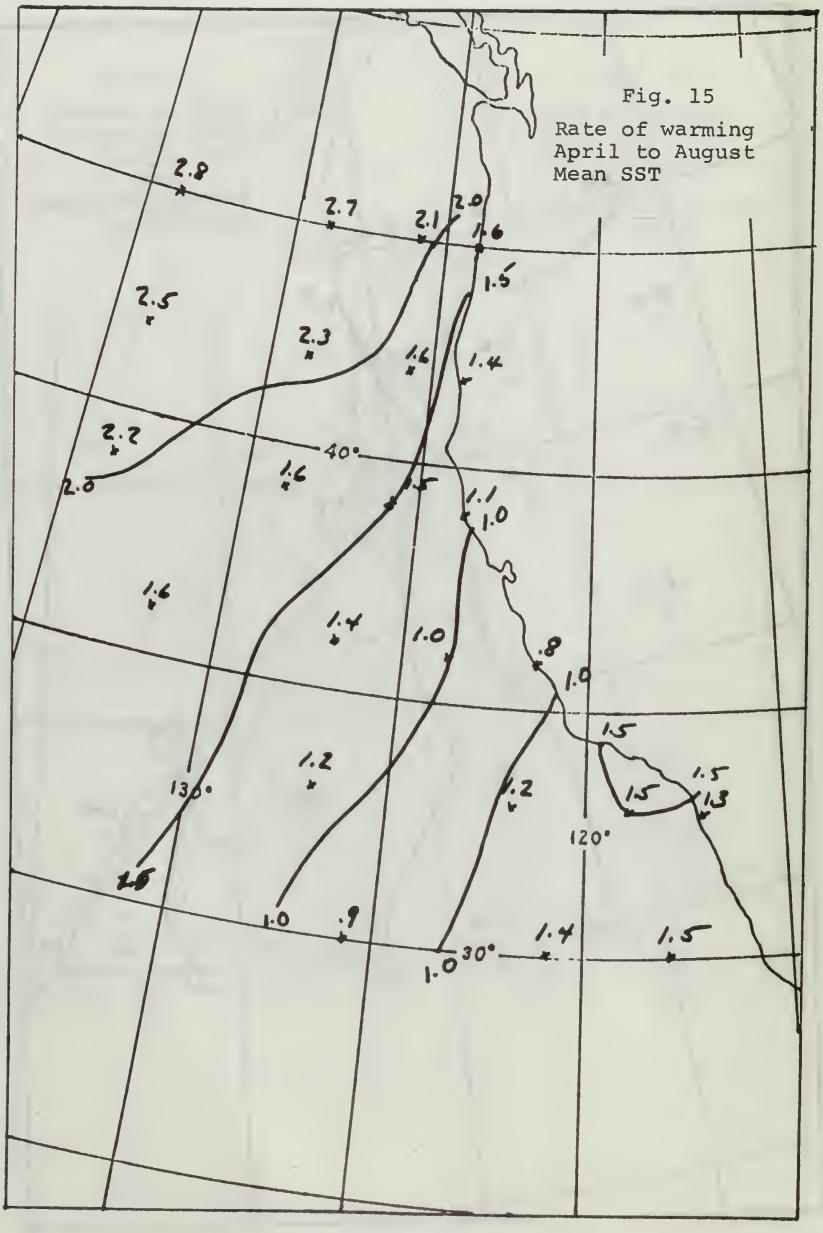

Fig. 15
Rate of warming
April to August
Mean SST

sometimes took the form of a long neck along the shore northward from the body of the stratus over the California Current. Thirty examples were found to illustrate cloud forms from upwelling. Figs. 32 and 33 are typical examples of stratus occurring close to the coast over the upwelling area. In both cases the main body of the stratus over the California Current has a long neck-like extension north along the coast with a varying width of up to 100 miles. The width of the cloud band can be observed to increase going south. It also can be noted that with longshore flow, cold tongues of water are associated with Cape Mendocino and Point Conception. These last two observations are in agreement with theoretical models by Yoshida (1955) and Arthur (1965) respectively. Other examples of stratus occurring over upwelling water are found in Figs. 27, 29, 34, and 37.

The periods of maximum occurrence for particular areas along the coast (e.g., off Oregon, northern California, etc.) and the most intense areas during any particular period or season were difficult, if not impossible, to observe from the cloud patterns; this was due to a variety of atmospheric conditions existing along the coast which disrupted the continuity of the cloud pattern. No attempt was made to relate the intensity of the cloud cover to the intensity of the upwelling (thus possibly the transport and velocity of upwelling) because the cloud photos were not of sufficient quality to observe intensity variations except on a gross basis.

C. CLEARING OVER THE CALIFORNIA CURRENT AND UPWELLING AREAS

After the passage of a cold front, the situation was set up where a cold air mass existed over the California Current and upwelling areas. In this situation, a clear area was observed over the colder waters of the California Current and upwelling areas, while cumuliform type clouds were normally present over warmer water to the west. There were a great number of examples illustrating this process in the northern portion of the area of interest. Six examples in 1968 illustrated the process extending completely along the coast. Fig. 21 shows a cold front passing through the area bringing in the cold air mass. Fig. 22 (also Fig. 23 for a later date) shows cloud free areas over the California Current and upwelling waters.

D. SURFACE ISOBARIC PATTERN WITH SEA SURFACE TEMPERATURE PATTERN

Tongues of cold and warm water were observed to line up well with the isobaric pattern. This could be the result of wind driven surface currents. The currents are about 20° to the right of the wind, which in turn, is about 20° to the left of the surface isobars (James, 1966). The tongues probably extend along the axis of maximum velocity. Good correlation was seen in almost every analysis examined. Figs. 22 and 32 have the orientation of the tongues

superimposed on the nephanalysis for easy correlation. When discrepancies from correlation occur, they can be explained usually through the history of the flow. The large cold tongue built up by the offshore flow on April 3, 1968 (Fig. 18b), located near 36N and 125W, is pushed south and narrowed by the northerly flow on the 4th (Fig. 19); it is aligned with the northerly flow by the 5th (Fig. 20). At least a two-day time period appears to be needed to realign the SST pattern orientation after a change in flow.

E. FRONTAL CLOUDS WITH SEA SURFACE TEMPERATURE

Frontal clouds were observed normally to be associated with (aligned with) warm tongues in the SST patterns. Twenty-four examples illustrating this correlation were observed. Figs. 17 and 37 show frontal clouds approaching southern California. Each of these nephanalysis has a corresponding daily SST analysis. In each case the frontal clouds extend along the tongue of warm water. Fig. 31 shows a similar situation, but with a break in the frontal clouds apparently correlated with the narrow neck in the warm tongue. Figs. 23, 25, 27, 28, and 29 are examples also illustrating this correlation. Most of these are in the area of composite SST analysis.

One factor that could contribute to this correlation is that the cold frontal clouds are more intense over warmer water. Warmer water results in the marine layer having a warmer temperature, thus a greater temperature contrast

occurs vertically across the frontal surface; cold water results in just the opposite situation.

A second factor is the flow. Fig. 16b illustrates the flow around the cold frontal clouds. The flow behind the front brings colder water from the north, while that ahead of the front brings warmer water from the southwest against the cold water of the California Current and upwelling area. This will tend to bend the isotherms ahead and behind the frontal clouds southward in an orientation similar to that of the front. Another process, which tends to reinforce the above, is the transfer of heat from the water to the air behind the frontal clouds in the cold air mass and the possible slight transfer of heat from the air to the water ahead of the frontal clouds in the warm air mass.

Cold frontal situations (as described by the cloud patterns) appeared to drag the main warm tongue of surface water off the northern coast of the United States eastward against the colder California Current and upwelling waters. The process is described schematically in Fig. 16. Fig. 16a shows the frontal clouds entering the area. Fig. 16b shows the flow pushing the warm tongue of water up against the cold California Current and upwelling waters as described in the preceding paragraph. Then the frontal clouds weaken or dissipate over the cold waters as shown in 16c. Only composite analyses were available to examine this model. On April 3, 1968 (Fig. 18), a wide band of frontal

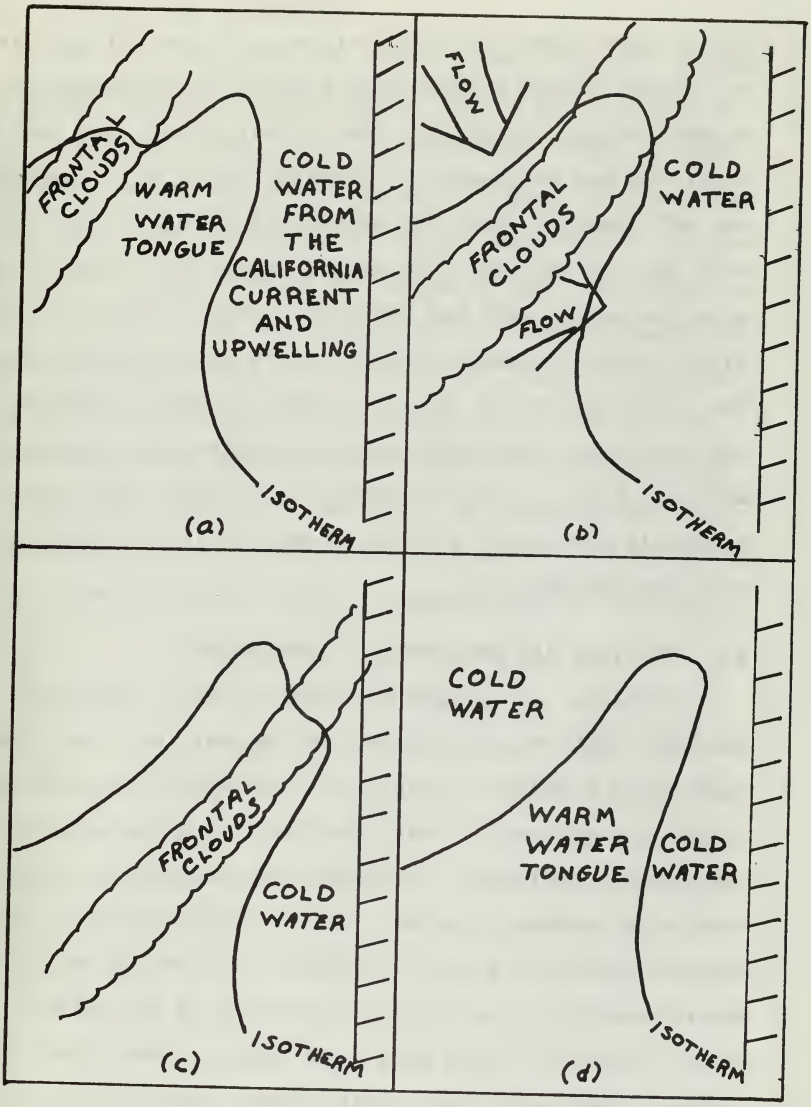

Fig. 16

Passage of Cold Frontal Clouds off Northwest Coast of United States.

clouds approached the northwest coast of the United States. It was associated already with the major warm tongue of surface water. By April 4 the frontal clouds were over the coast and had decreased in intensity (Fig. 19). Comparing the SST composite analysis of the 3rd of April (Fig. 18b) with that of the next time period (Fig. 20), it can be seen that the warm tongue has moved east from its previous position. Another example of this can be seen in Figs. 25 and 26. In Figs. 28, 29, and 30 frontal clouds approaching the northwest coast are observed to dissipate over the cold waters. Again, as in the previous two cases, the warm tongue is moved east from its former position (comparing Figs.28c and 30b).

F. VORTICES AND SEA SURFACE TEMPERATURES

Vortices, as defined by Bittner (1967), are cloud patterns with one major cloud band spiralling into a center, indicating a definite center of circulation (at least one closed contour for at least one level in a conventional atmospheric analysis). Vortices were observed to occur over cold tongues of water. This could be caused by upwelling resulting from the cyclonic flow around the vortex. Mass transport of water is to the right of the surface wind; therefore there is a mass transport away from the vortex. This will cause cooler waters from below to ascend to the surface to replace the outflow of water from the vortex. Fig. 17 illustrates a vortex over a cold tongue on a daily SST analysis; Fig.24 illustrates one on a composite SST analysis.

G. STRATUS AND DIVERGENCE

The relative amount of isobar divergence was computed by taking the ratio of the isobar spread at one latitude to the spread at the latitude five degrees south of the reference latitude. Then a cloud divergence was computed by dividing the difference of the cloud widths at the two latitudes by the width at the southern latitude. The divergence factor for the isobars for 22 cases examined was found to range from 1.15 to 2.94. The isobar divergence was then plotted against the change in cloud width and cloud divergence, and a random scatter (no relationship) was obtained. Although divergence is necessary for stratus formation, it appears that it is not a controlling factor in the horizontal spatial dimension of the stratus.

Fig. 17a
Satellite ESSA VI - March 1, 1960.

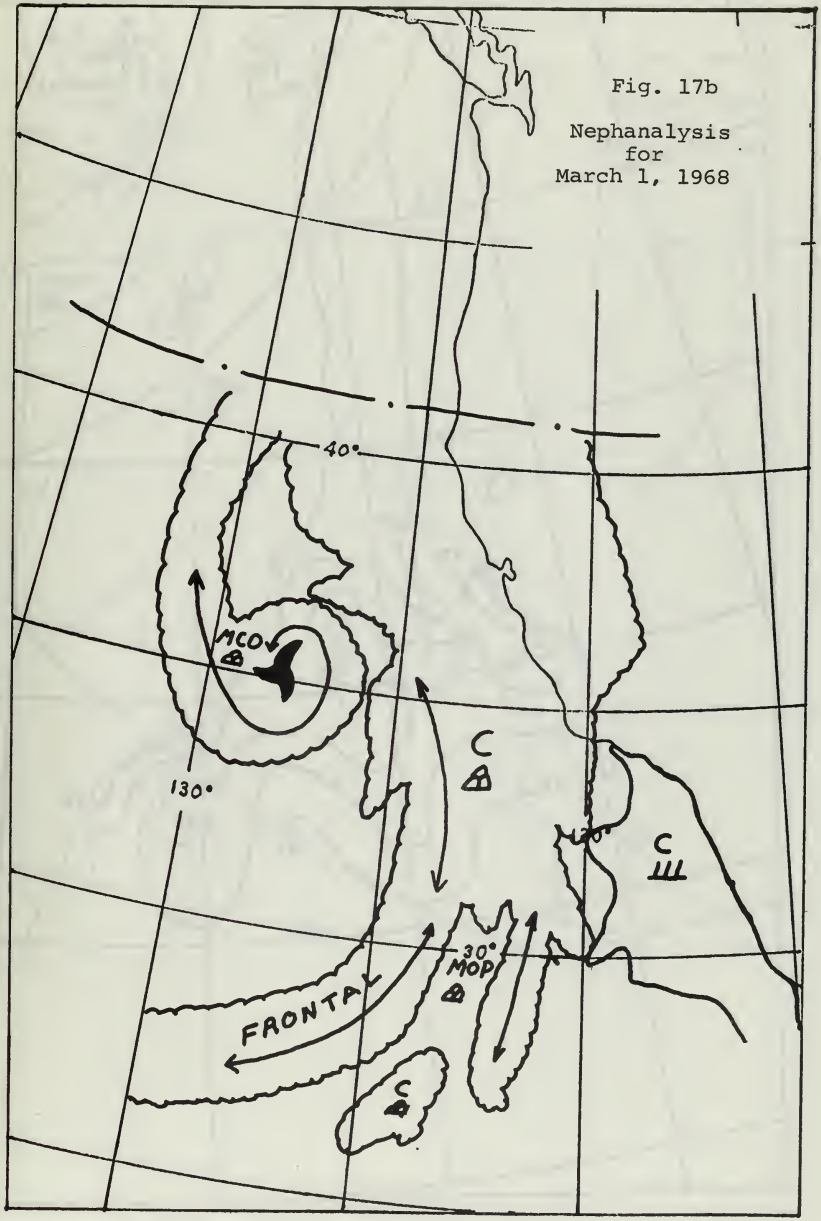

Fig. 17b

Nephanalysis
for
March 1, 1968

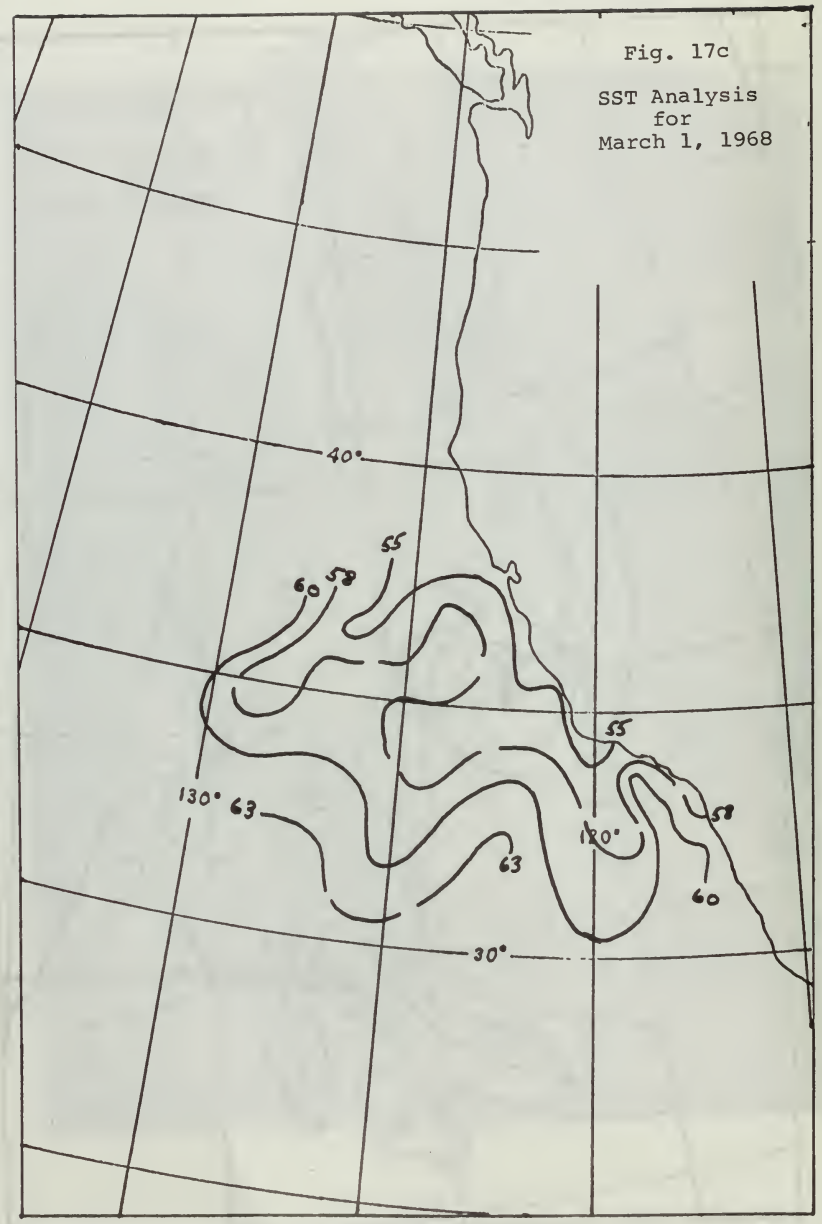

Fig. 17c

SST Analysis
for
March 1, 1968

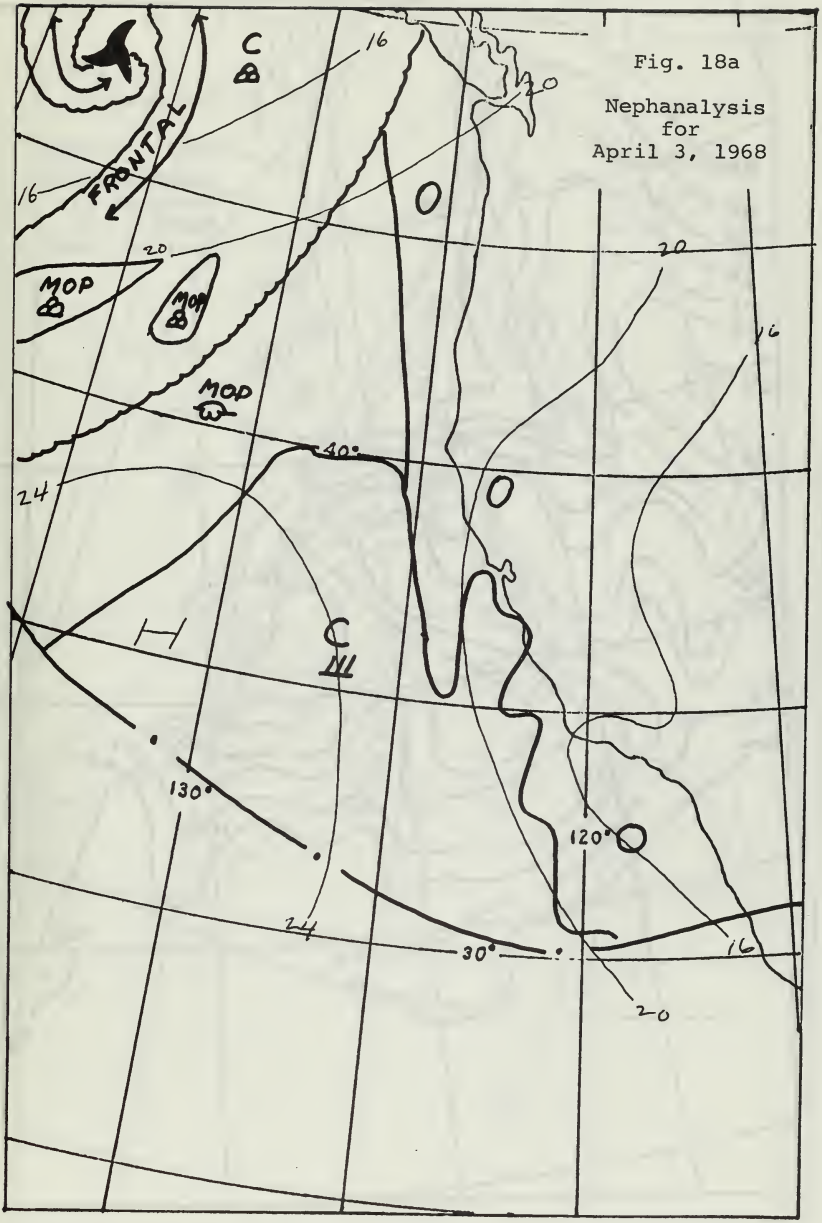

Fig. 18a

Nephanalysis
for
April 3, 1968

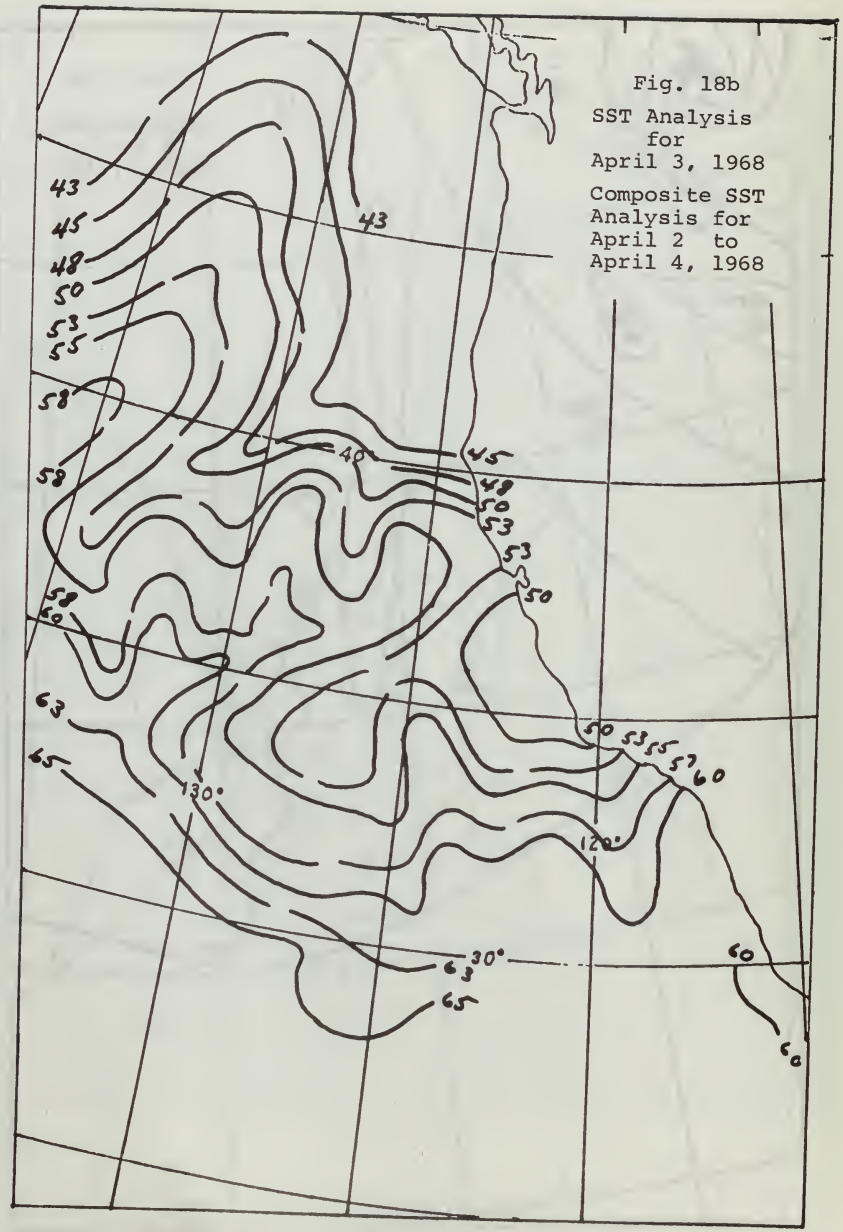

Fig. 18b
SST Analysis
for
April 3, 1968
Composite SST
Analysis for
April 2 to
April 4, 1968

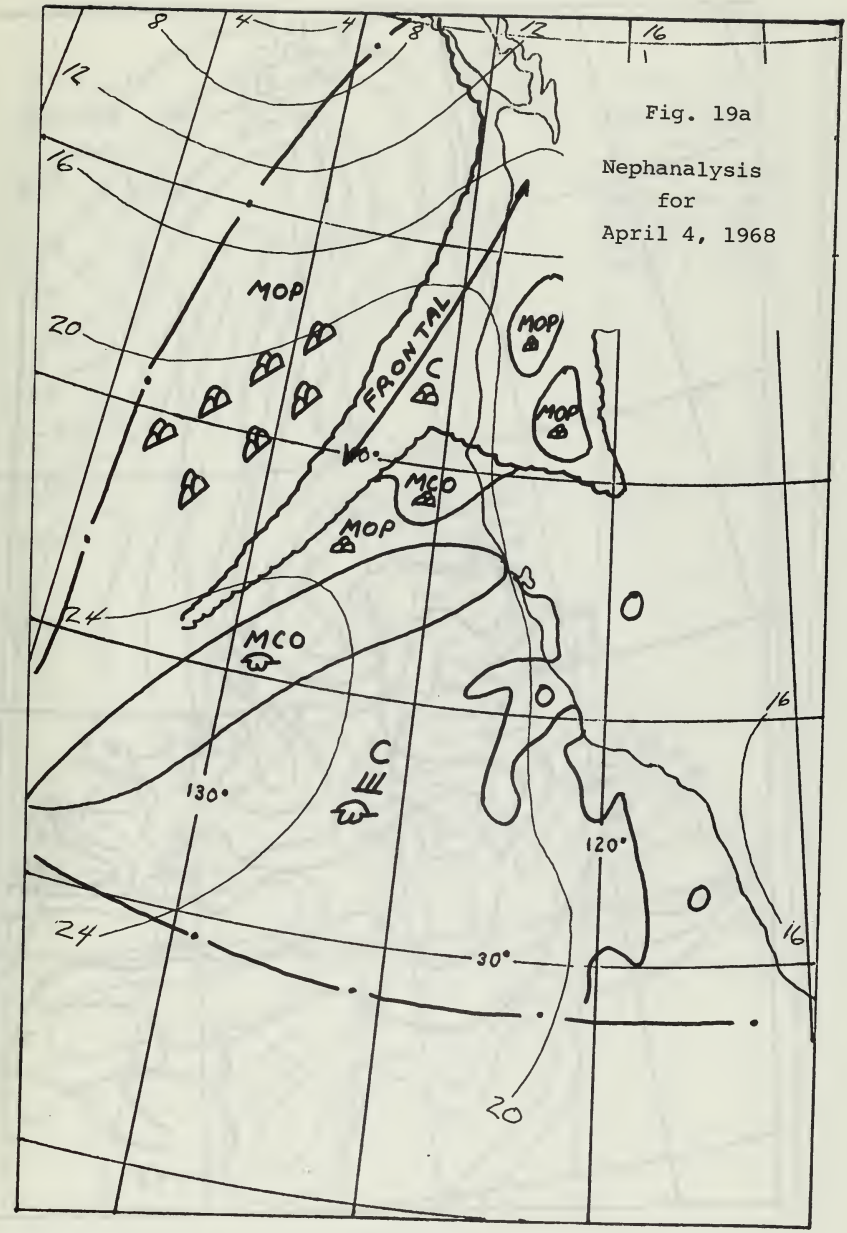

Fig. 19a

Nephanalysis
for
April 4, 1968

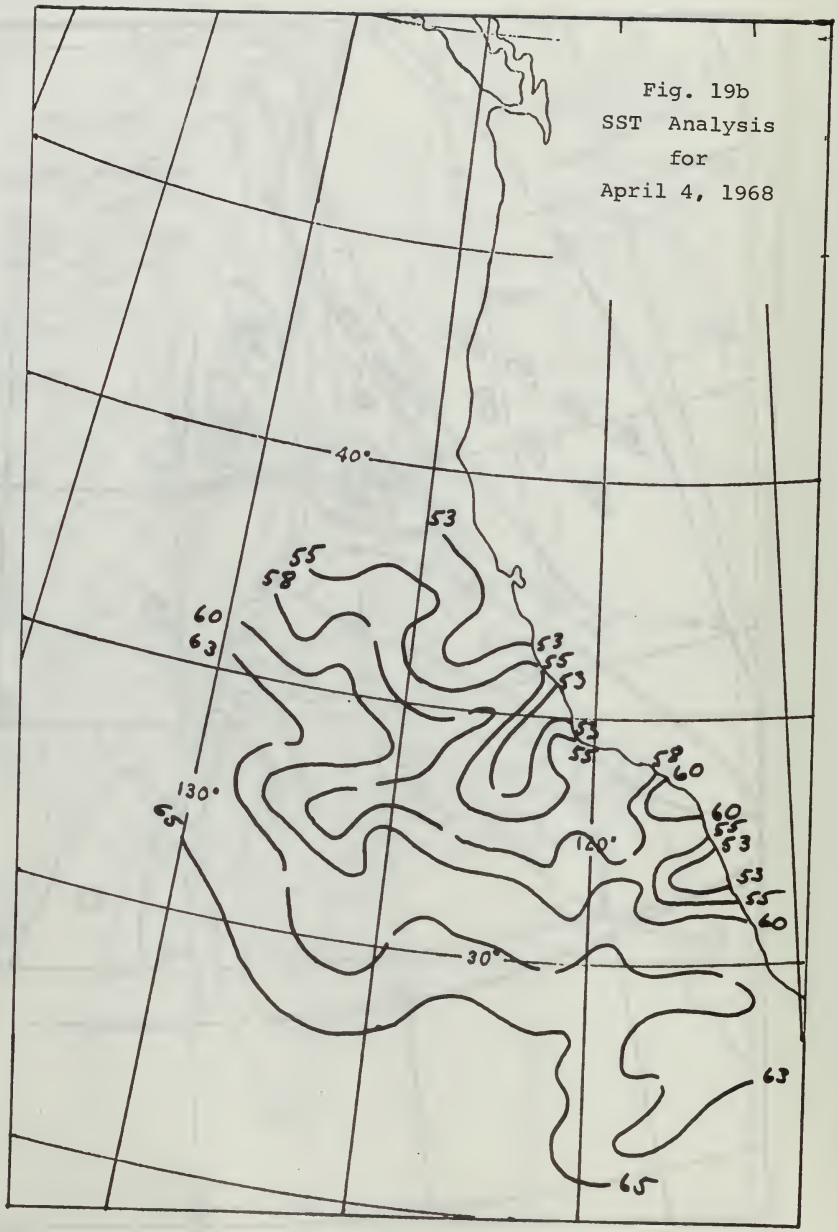

Fig. 19b
SST Analysis
for
April 4, 1968

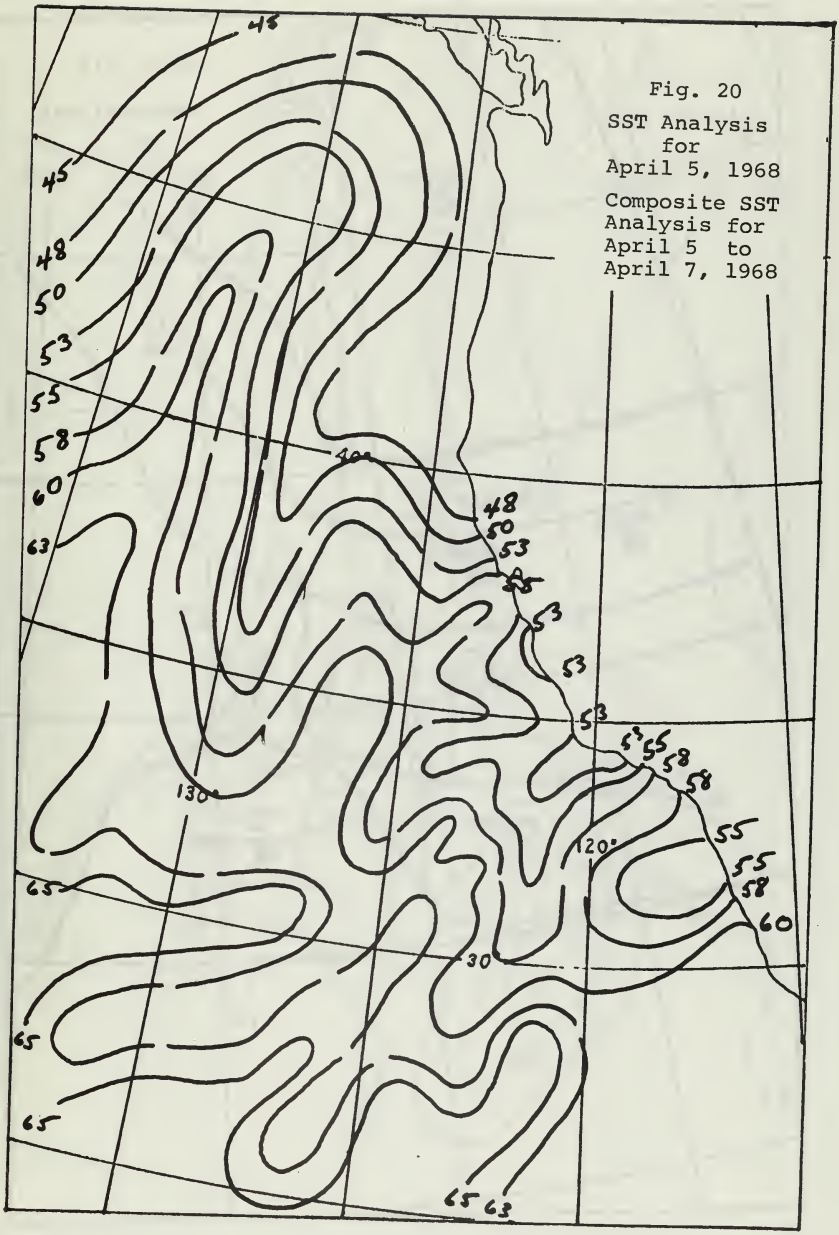

Fig. 20

SST Analysis for April 5, 1968

Composite SST Analysis for April 5 to April 7, 1968

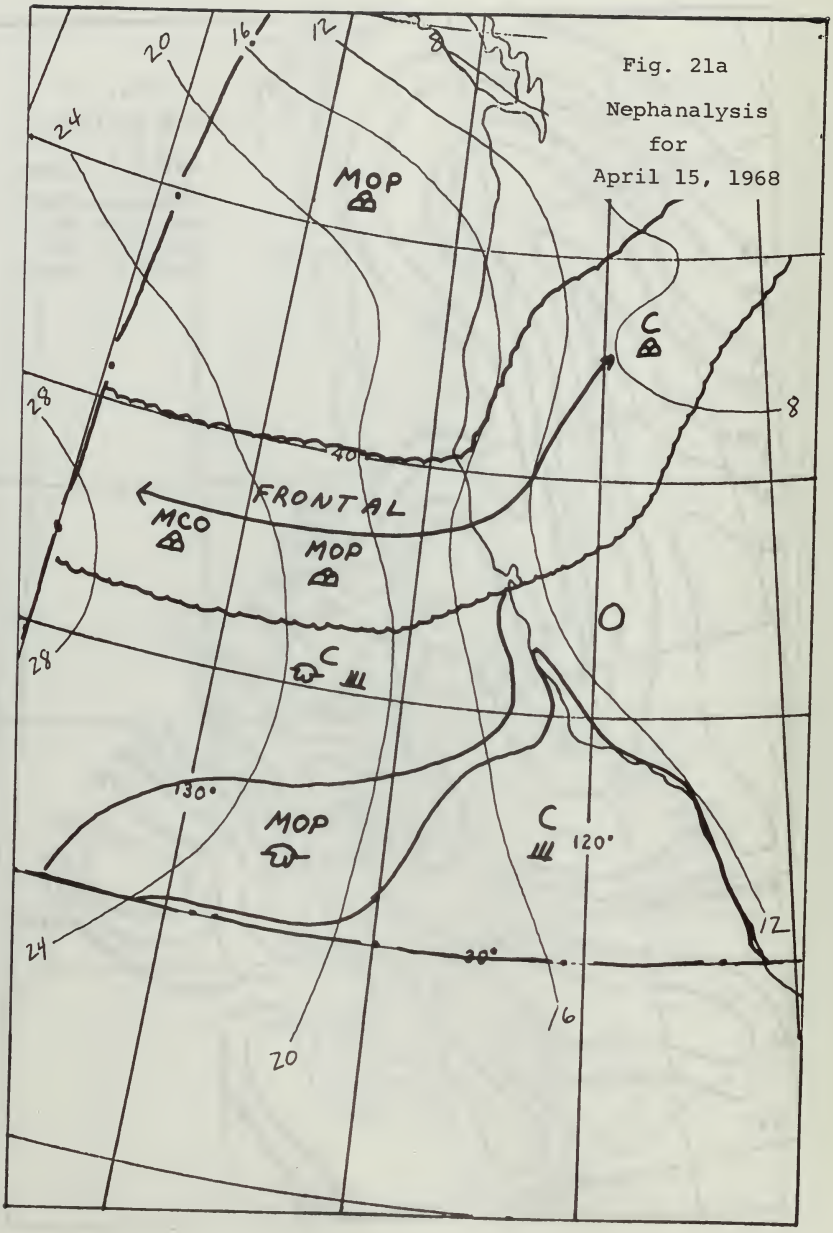

Fig. 21a
Nephanalysis
for
April 15, 1968

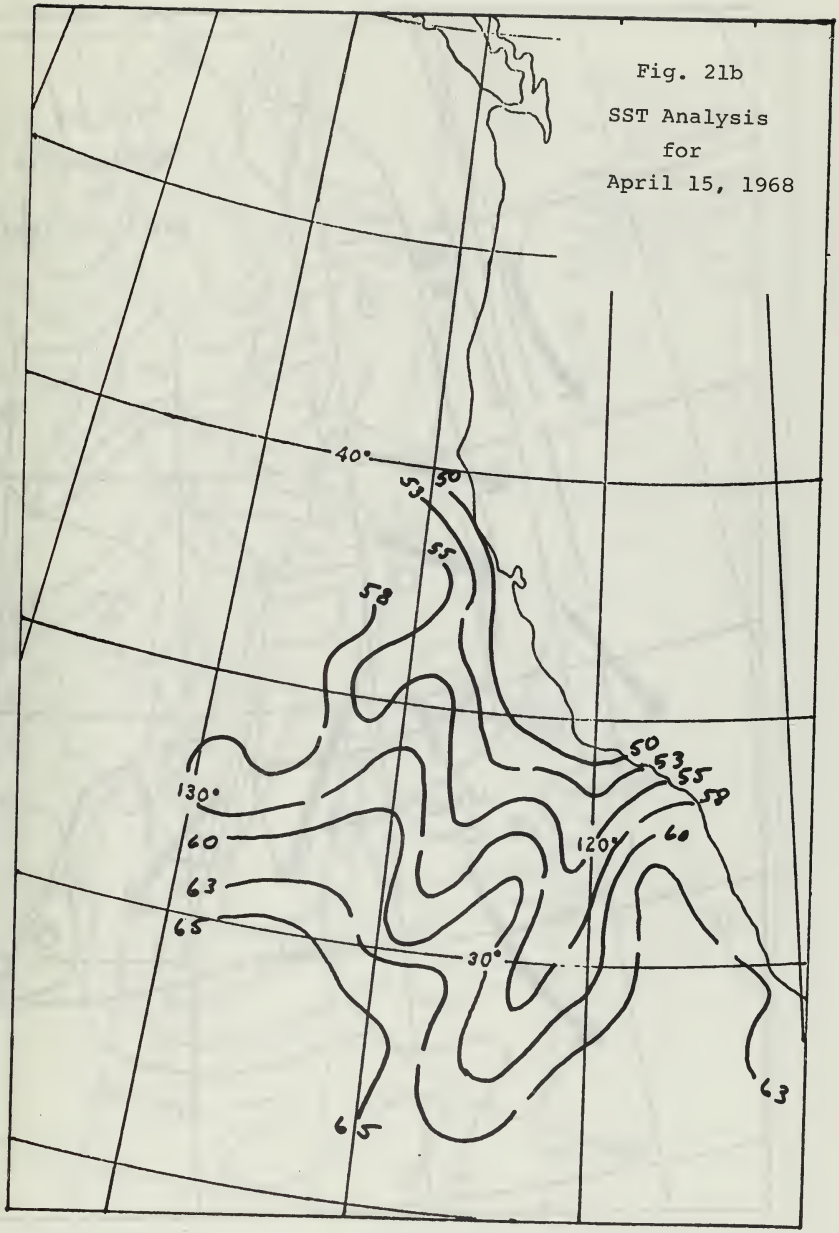

Fig. 21b
SST Analysis
for
April 15, 1968

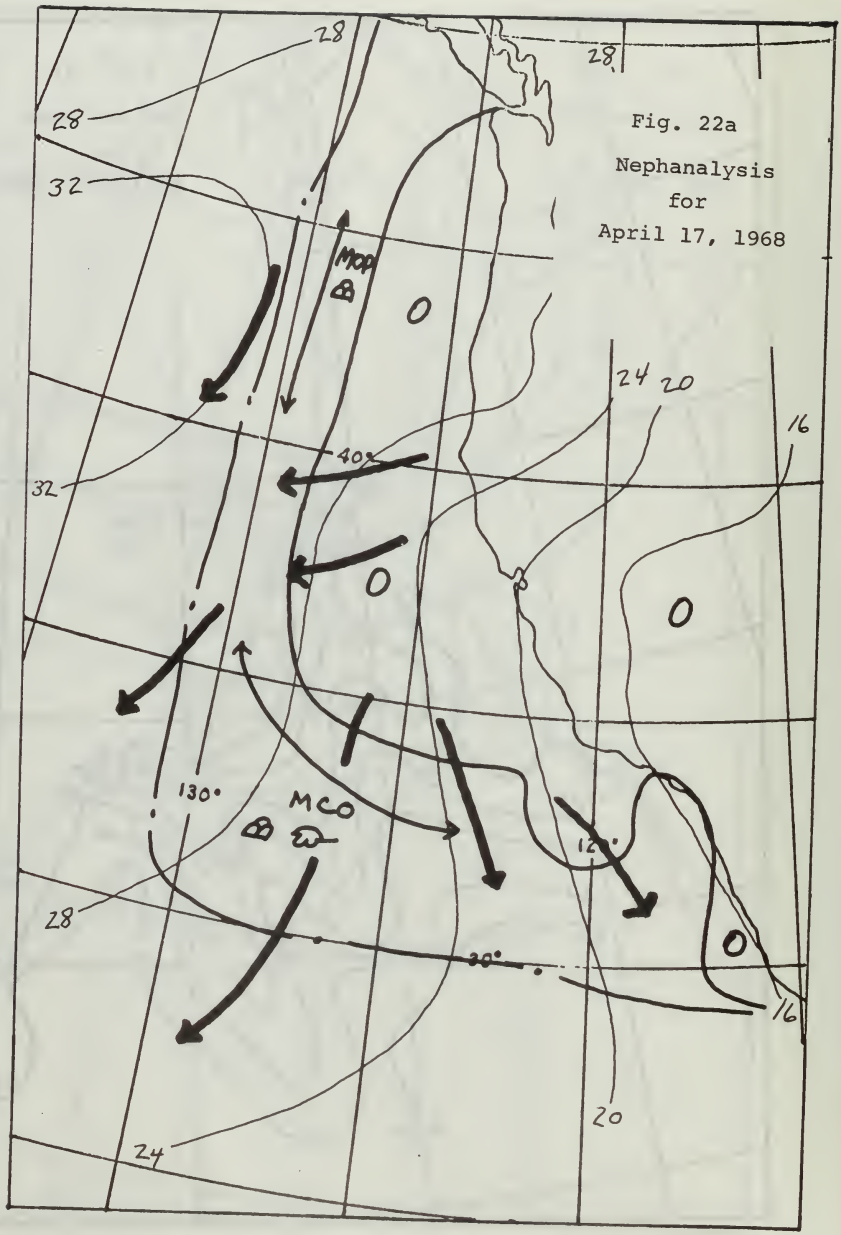

Fig. 22a
Nephanalysis
for
April 17, 1968

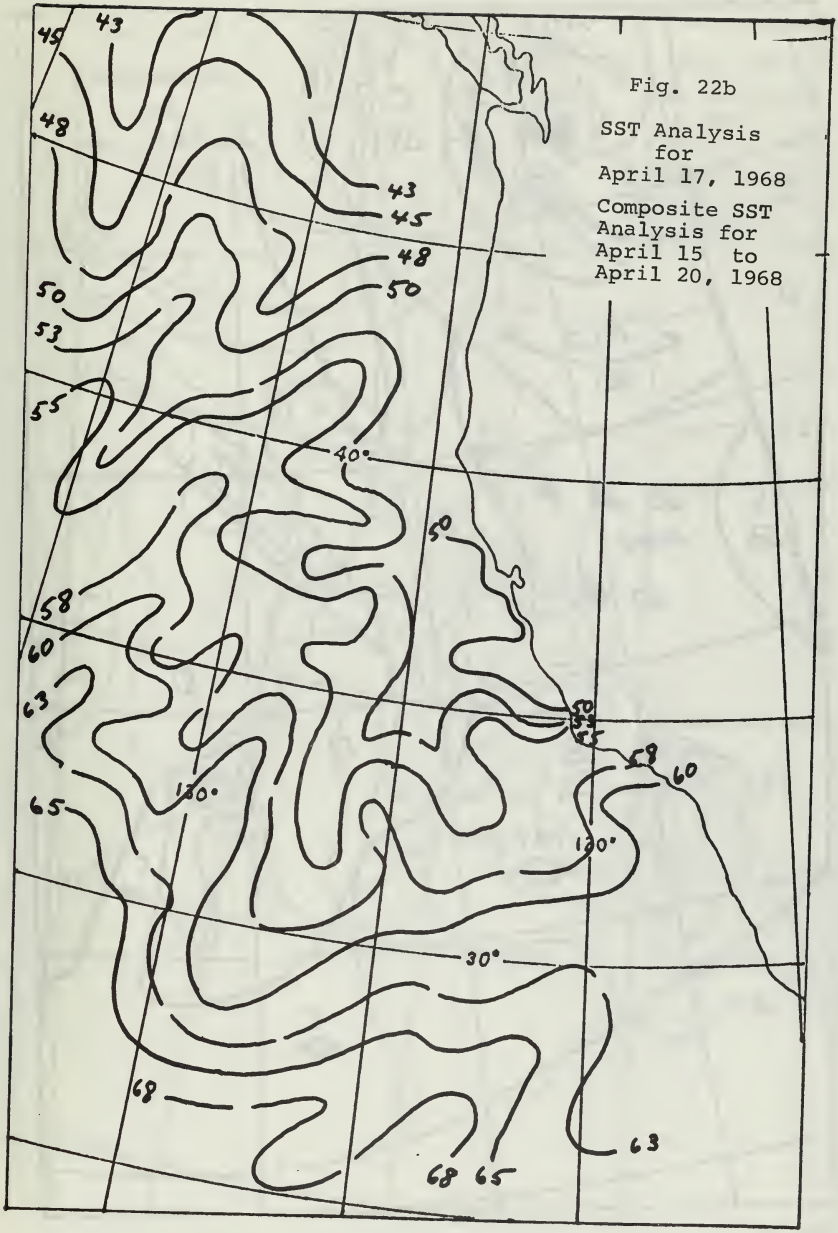

Fig. 22b

SST Analysis
for
April 17, 1968

Composite SST
Analysis for
April 15 to
April 20, 1968

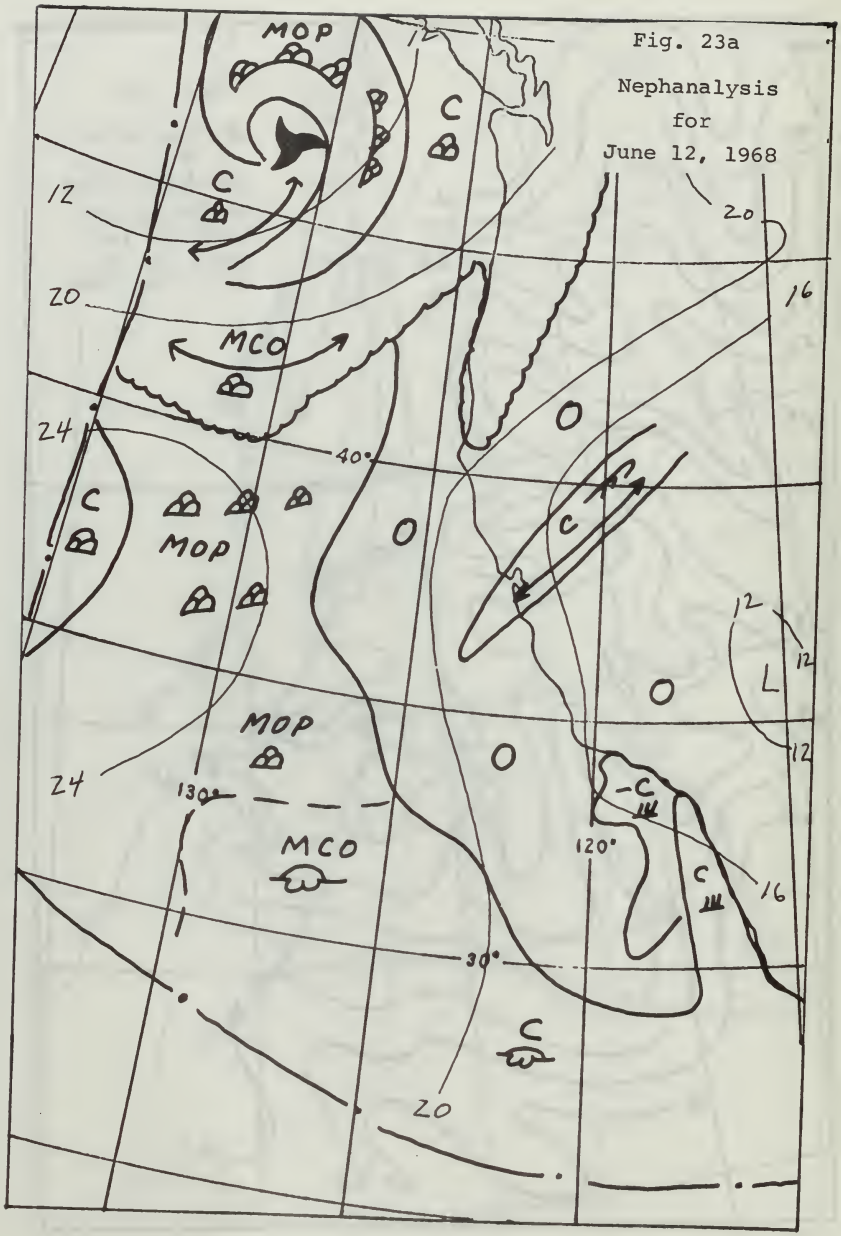

Fig. 23a
Nephanalysis
for
June 12, 1968

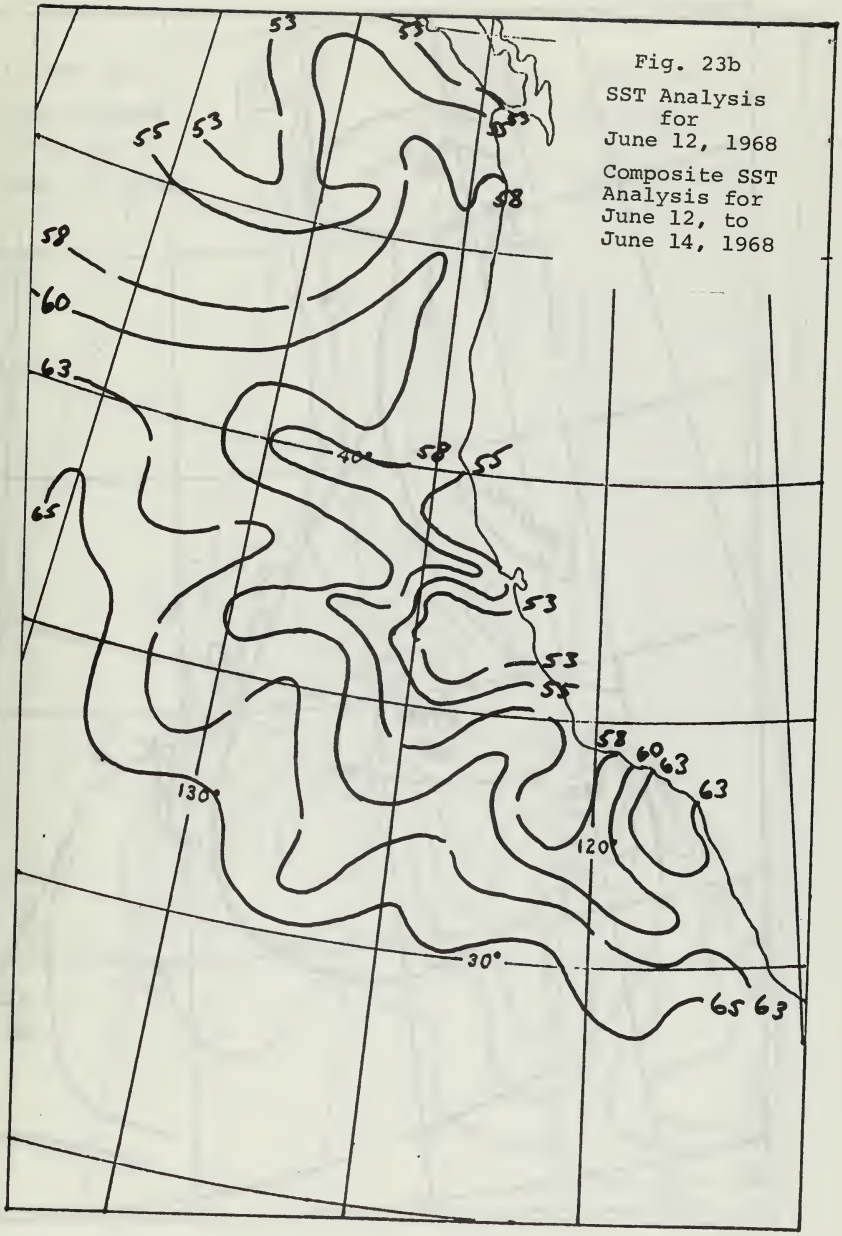

Fig. 23b
SST Analysis
for
June 12, 1968
Composite SST
Analysis for
June 12, to
June 14, 1968

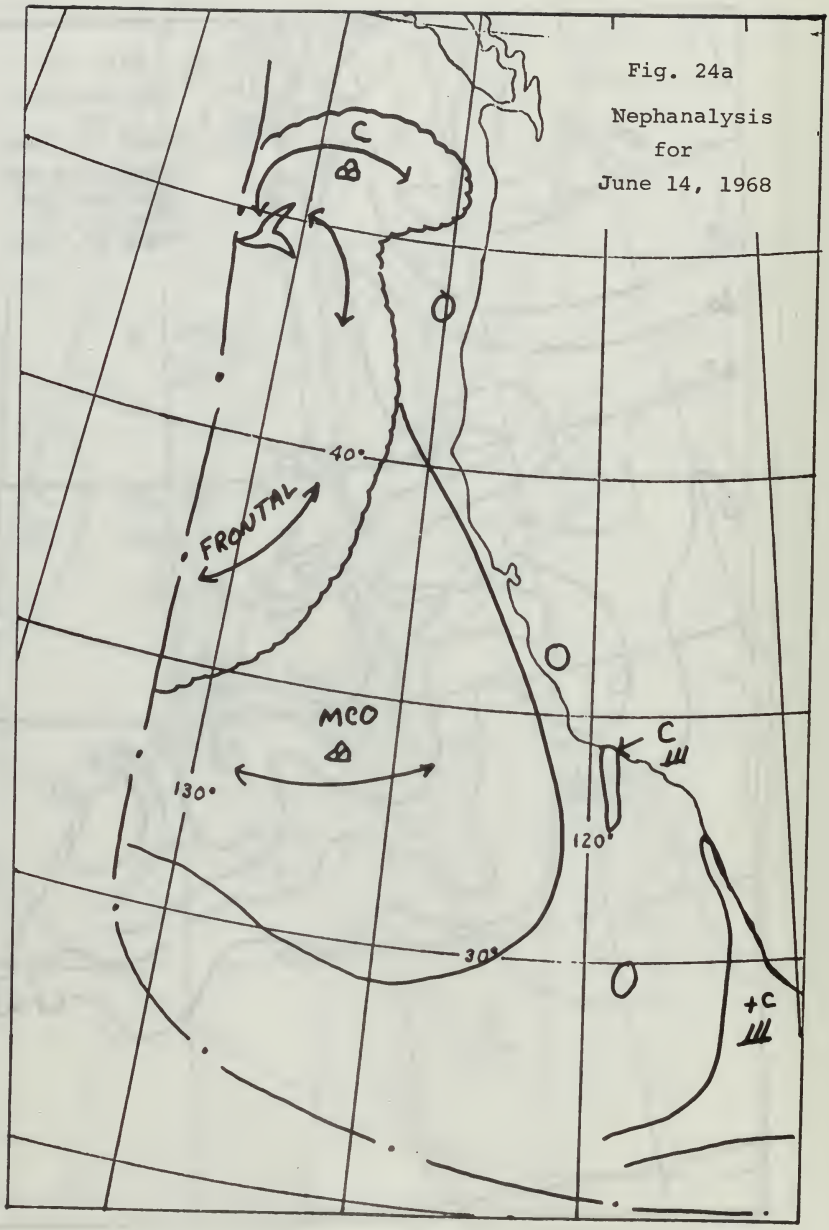

Fig. 24a
Nephanalysis
for
June 14, 1968

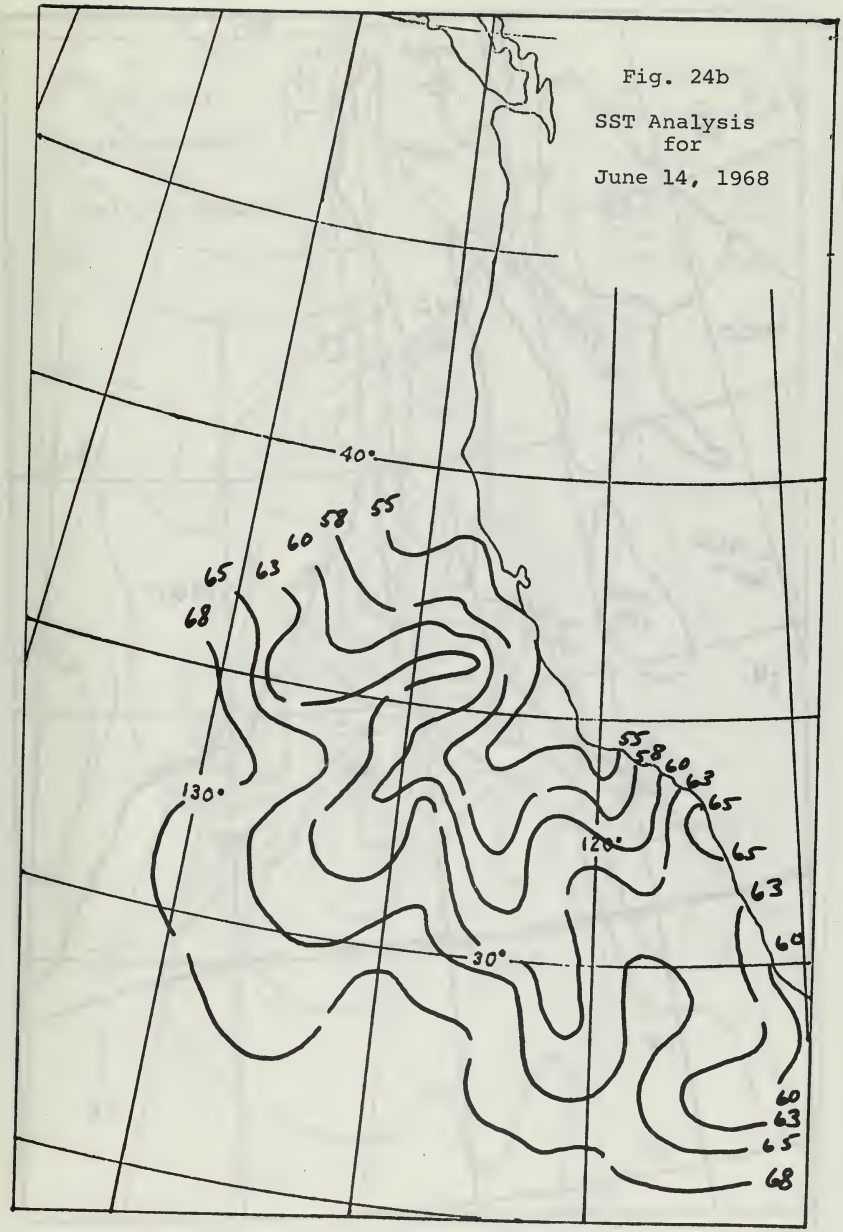

Fig. 24b

SST Analysis
for
June 14, 1968

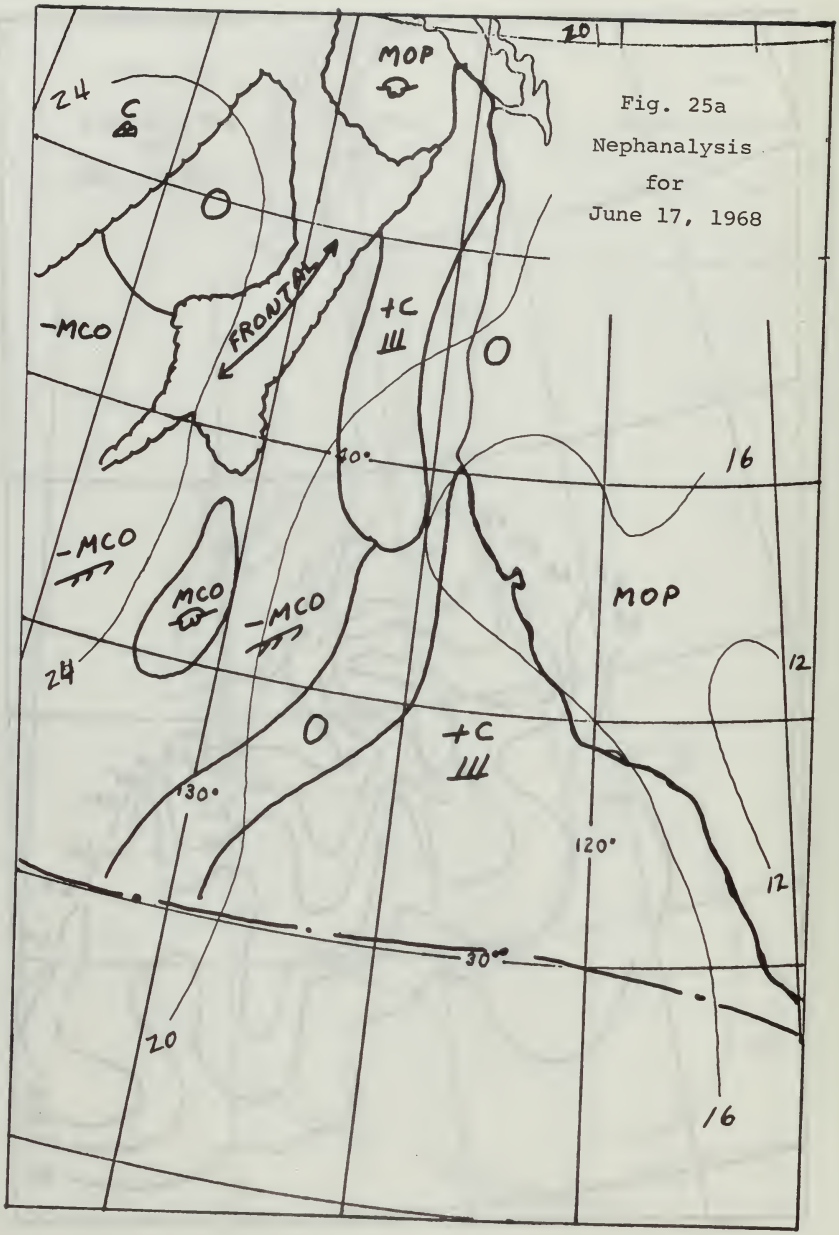

Fig. 25a
Nephanalysis
for
June 17, 1968

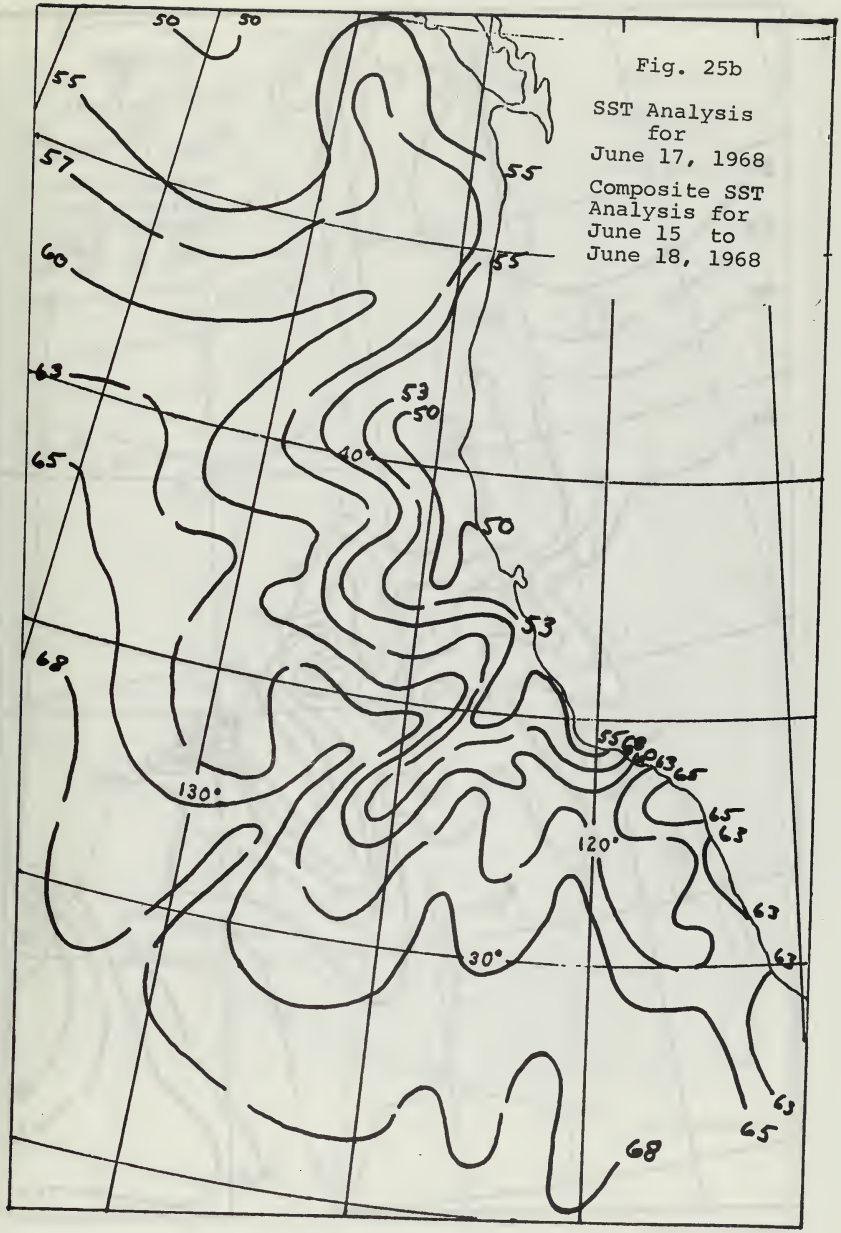

Fig. 25b

SST Analysis for June 17, 1968

Composite SST Analysis for June 15 to June 18, 1968

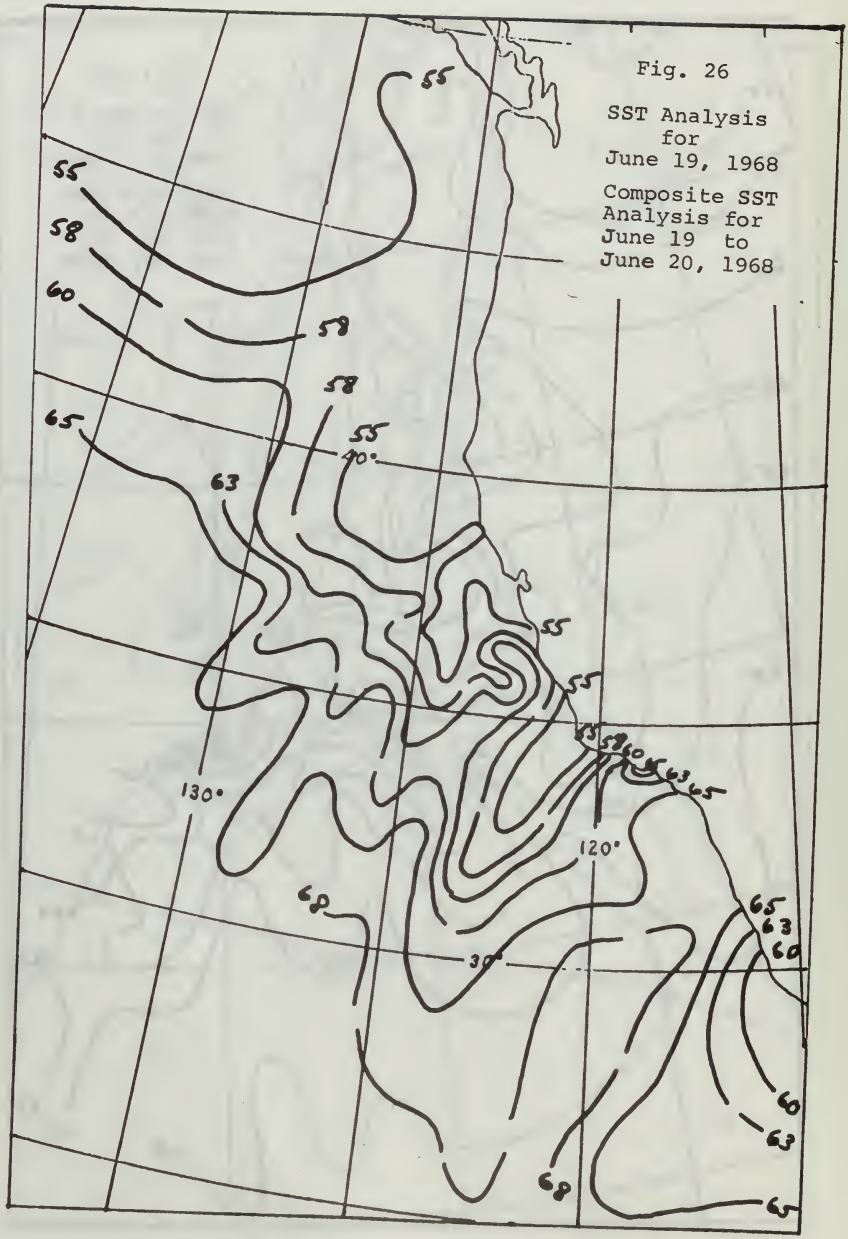

Fig. 26

SST Analysis
for
June 19, 1968

Composite SST
Analysis for
June 19 to
June 20, 1968

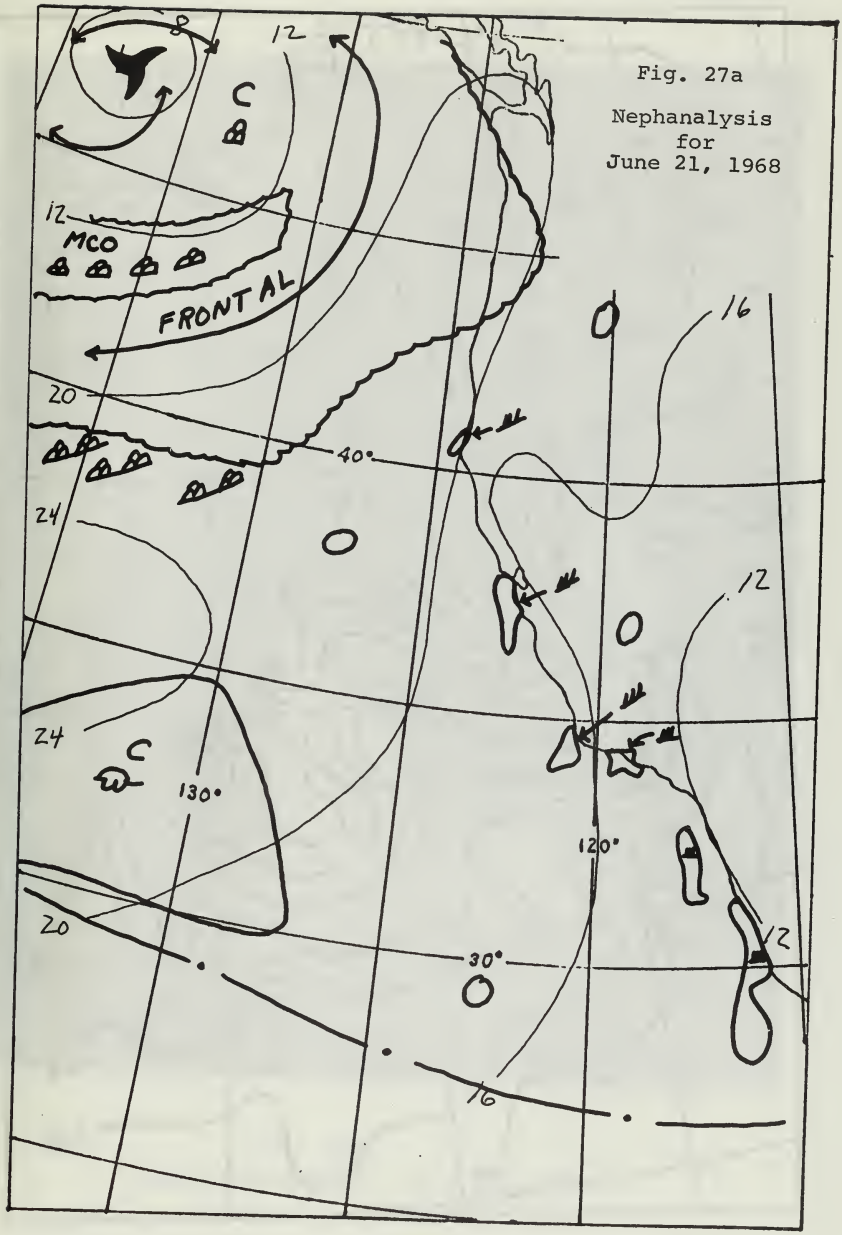

Fig. 27a

Nephanalysis
for
June 21, 1968

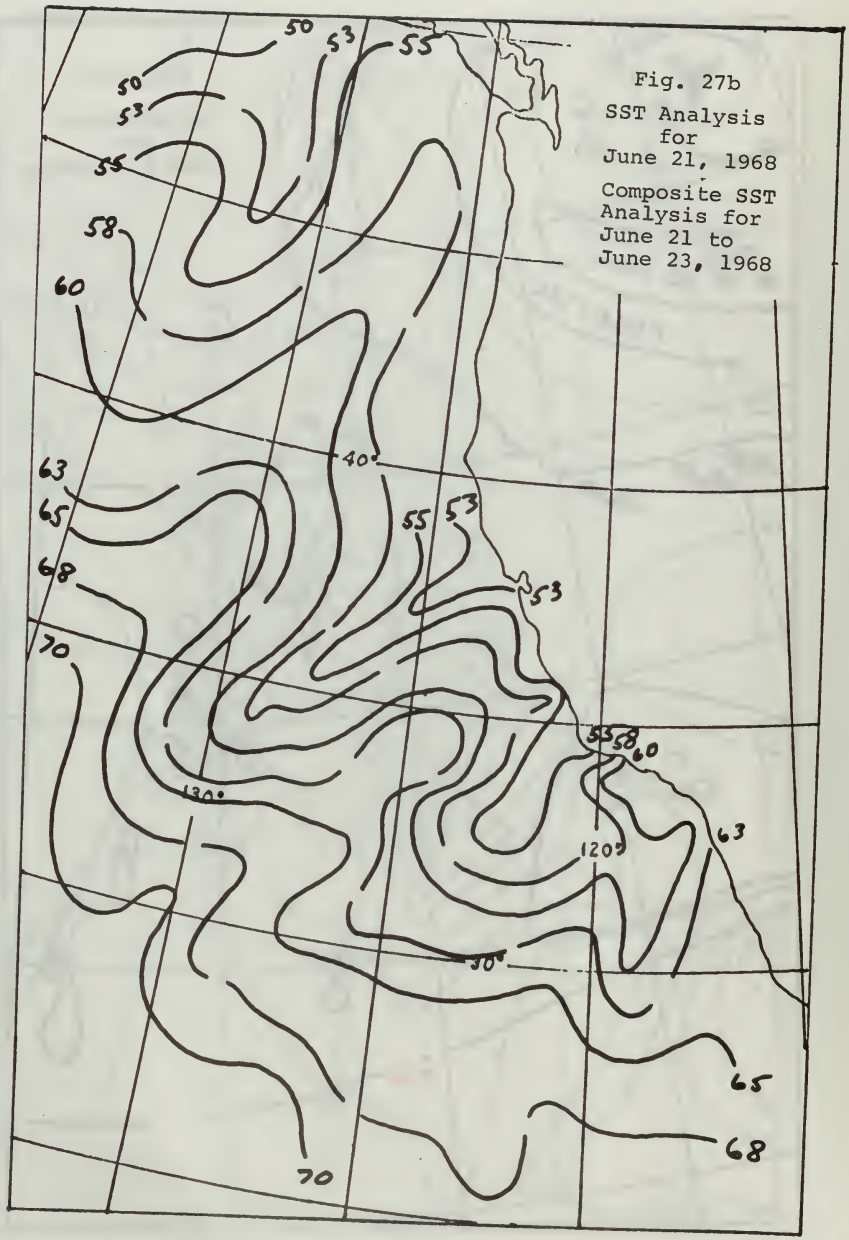

Fig. 27b
SST Analysis
for
June 21, 1968

Composite SST
Analysis for
June 21 to
June 23, 1968

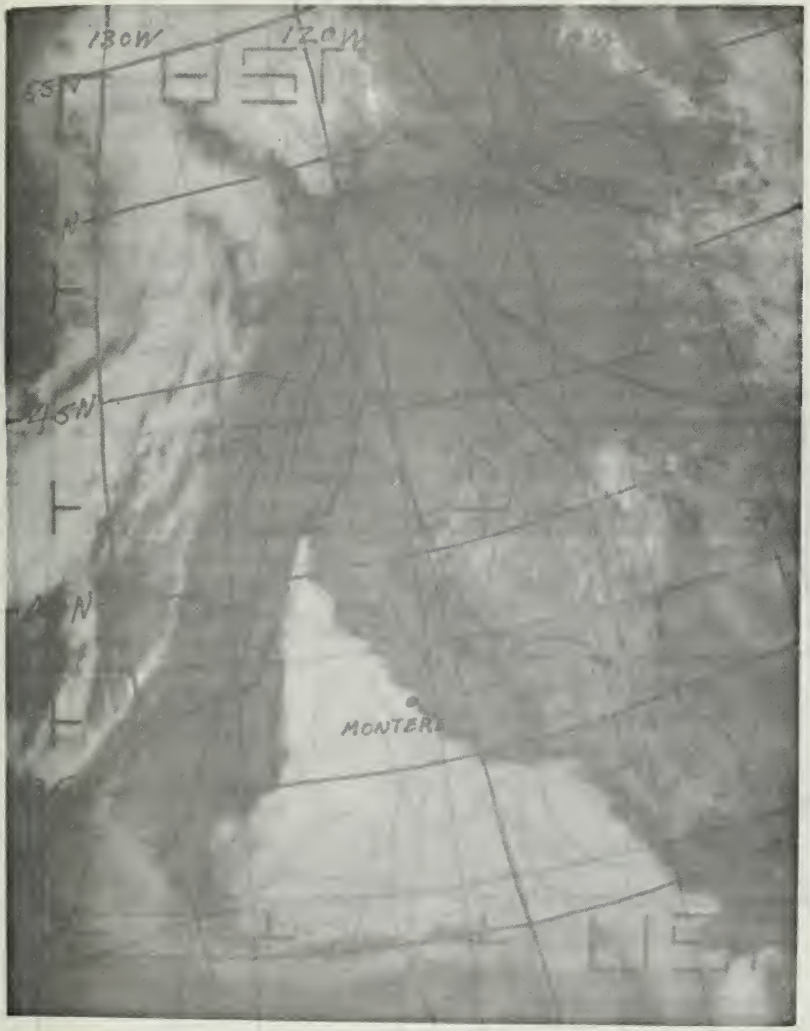

Fig. 28a
Satellite ESSA VI - June 25, 1968

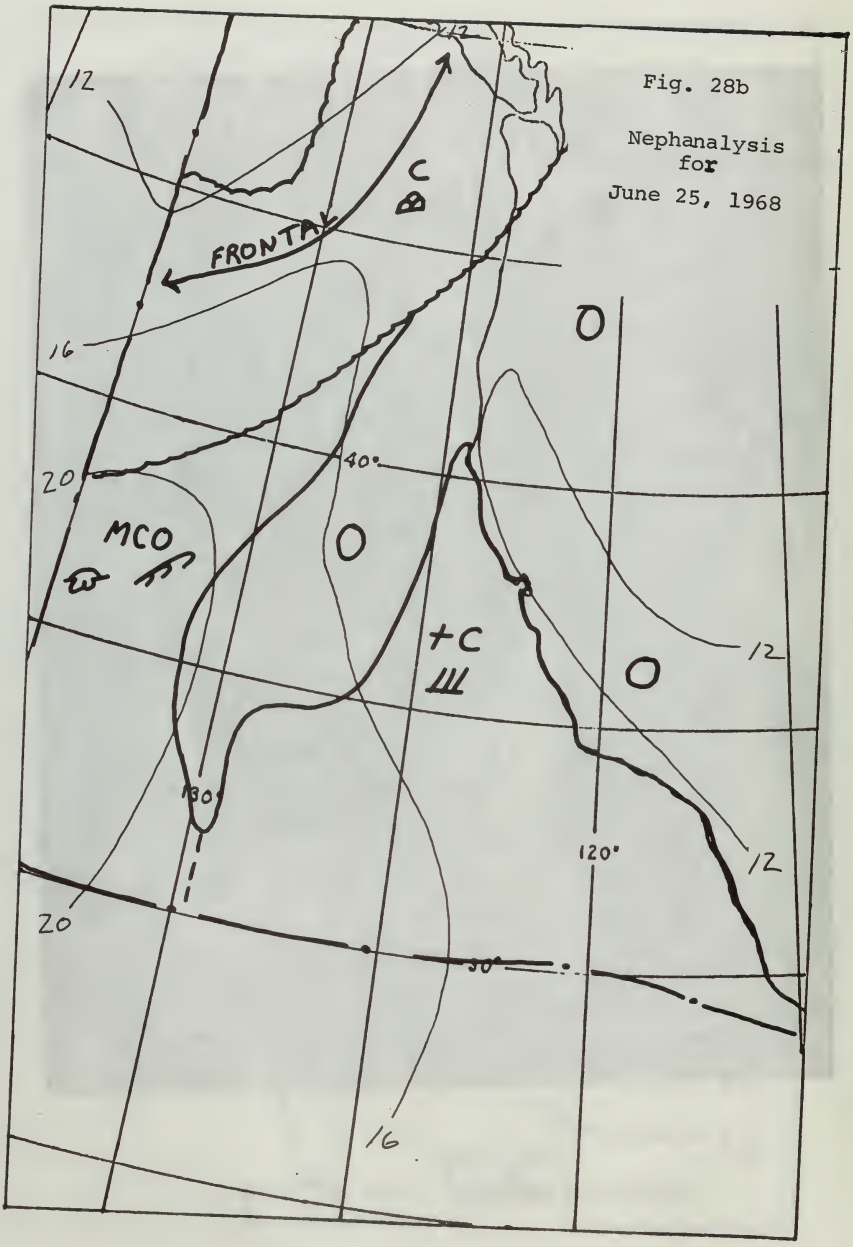

Fig. 28b

Nephanalysis
for
June 25, 1968

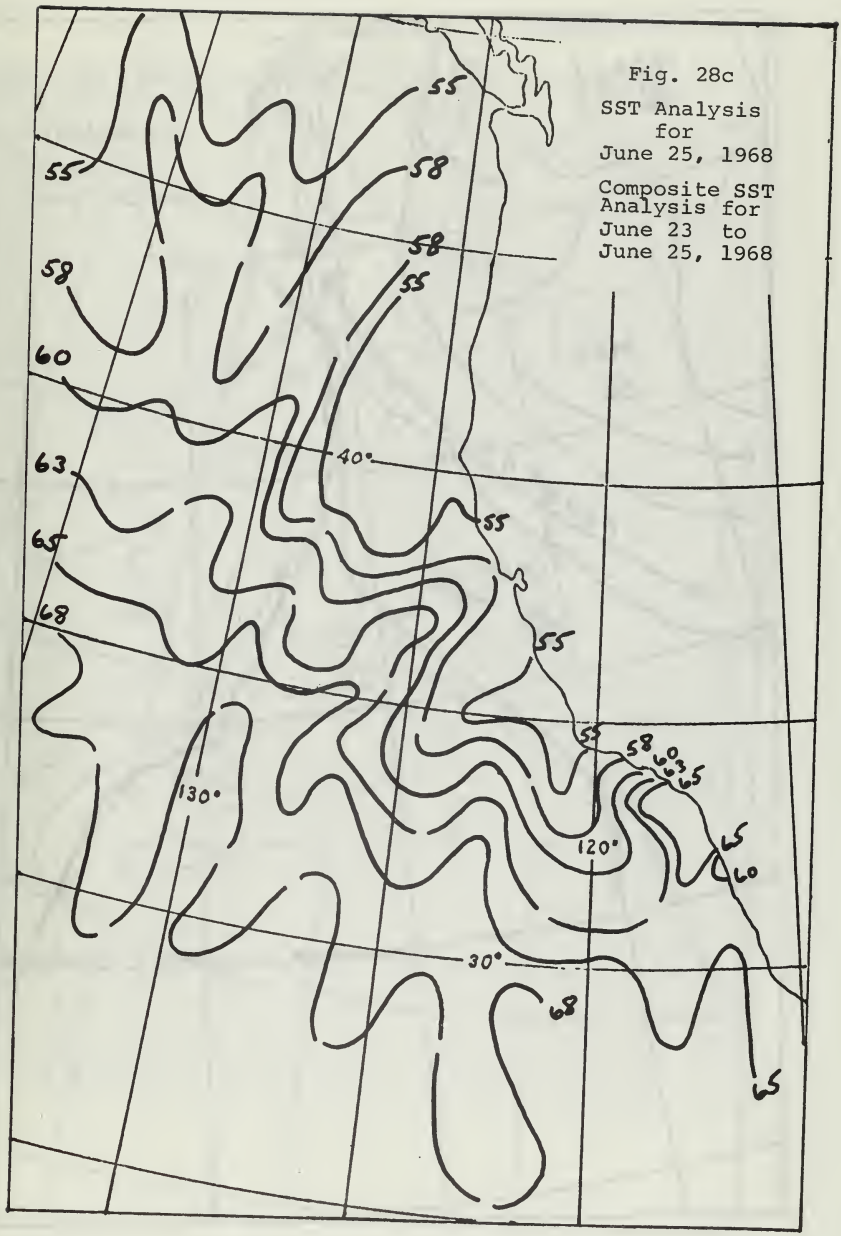

Fig. 28c

SST Analysis for June 25, 1968

Composite SST Analysis for June 23 to June 25, 1968

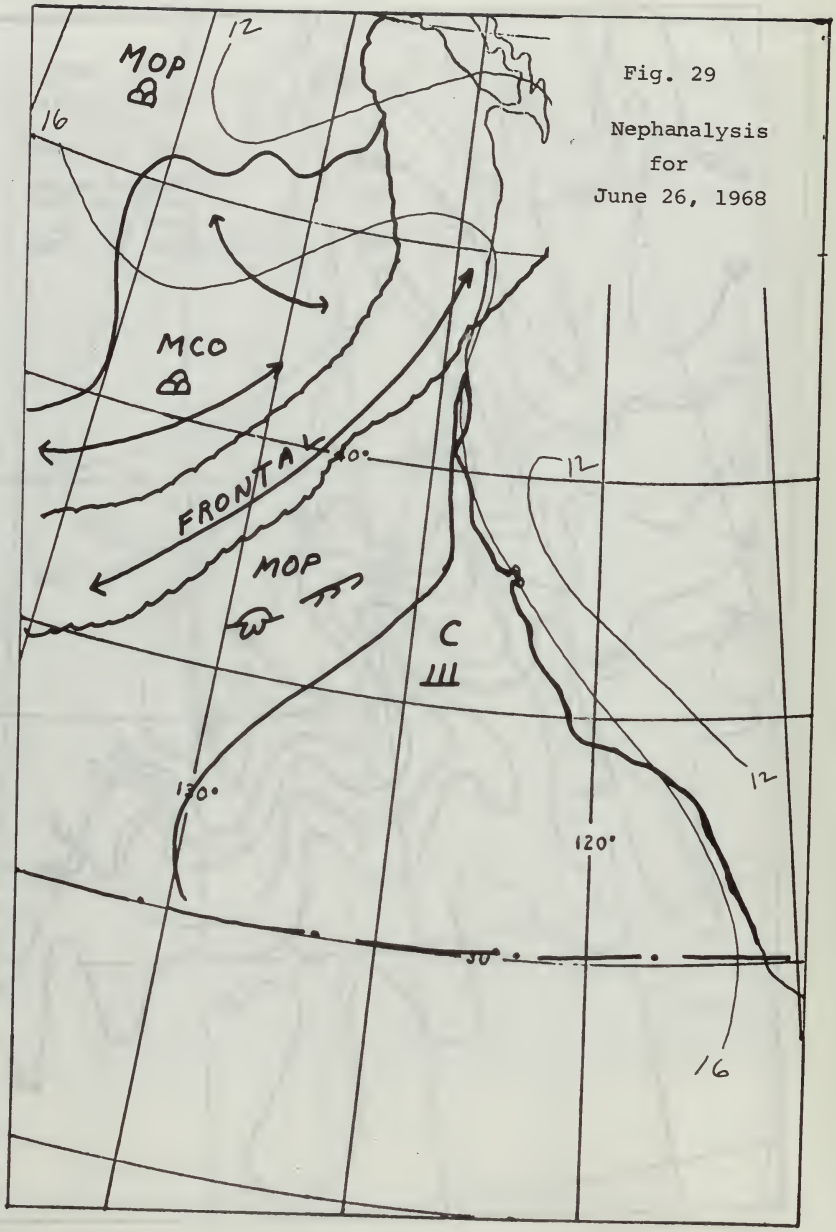

Fig. 29

Nephanalysis
for
June 26, 1968

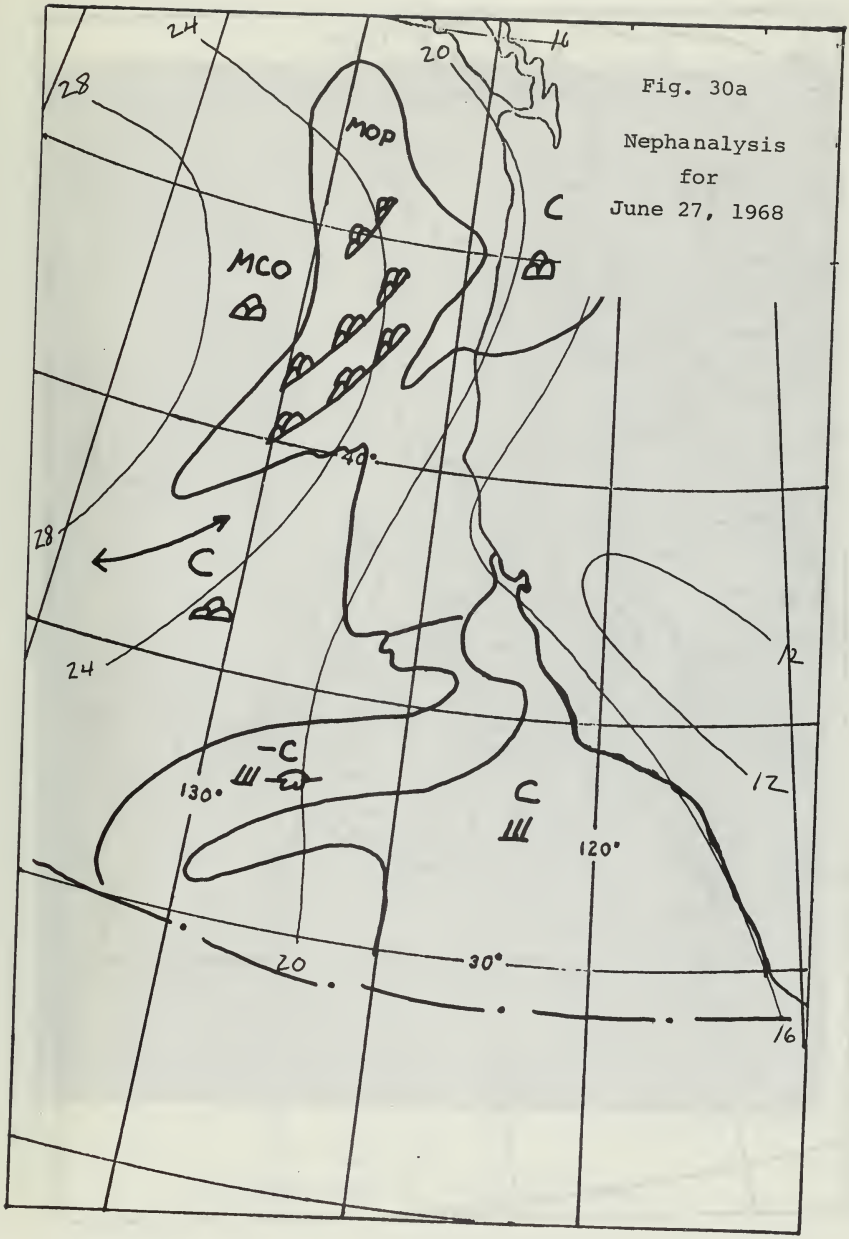

Fig. 30a

Nephanalysis
for
June 27, 1968

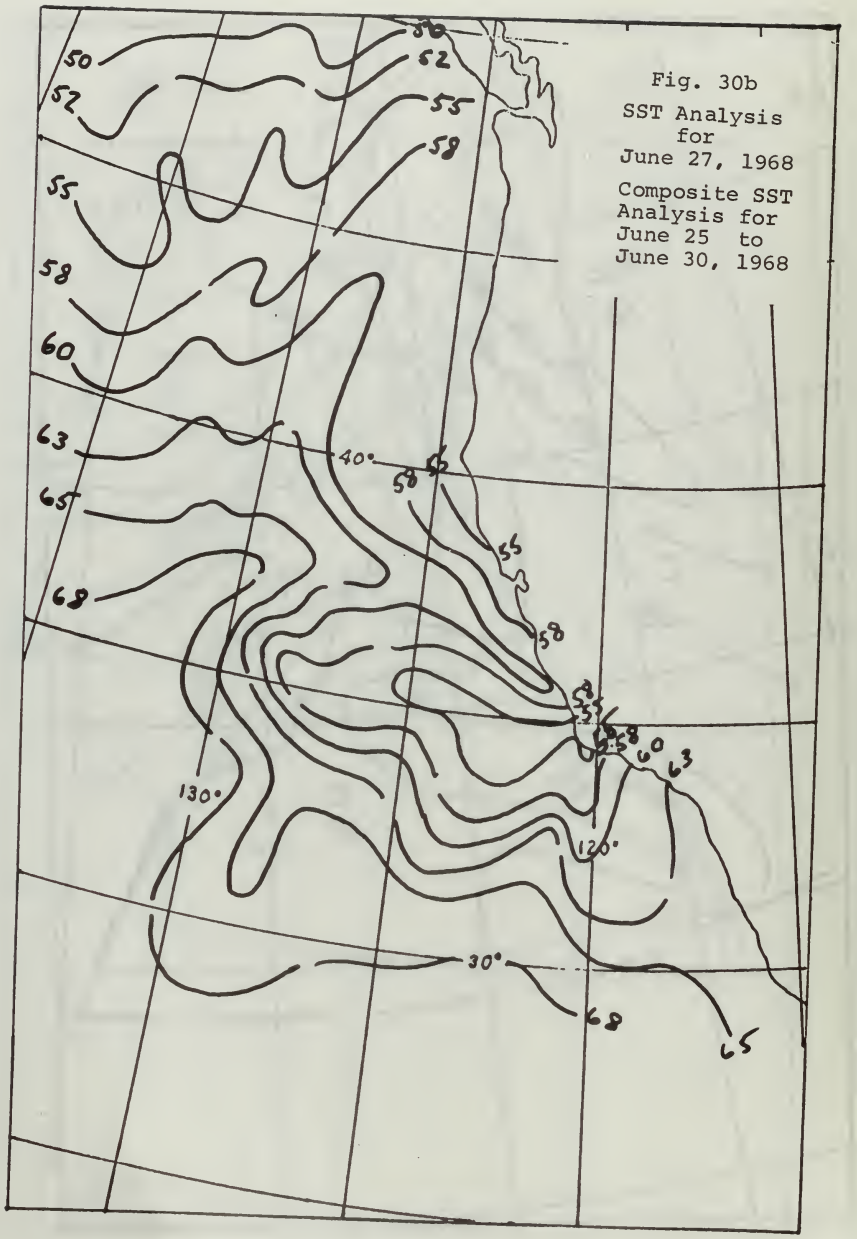

Fig. 30b
SST Analysis
for
June 27, 1968

Composite SST
Analysis for
June 25 to
June 30, 1968

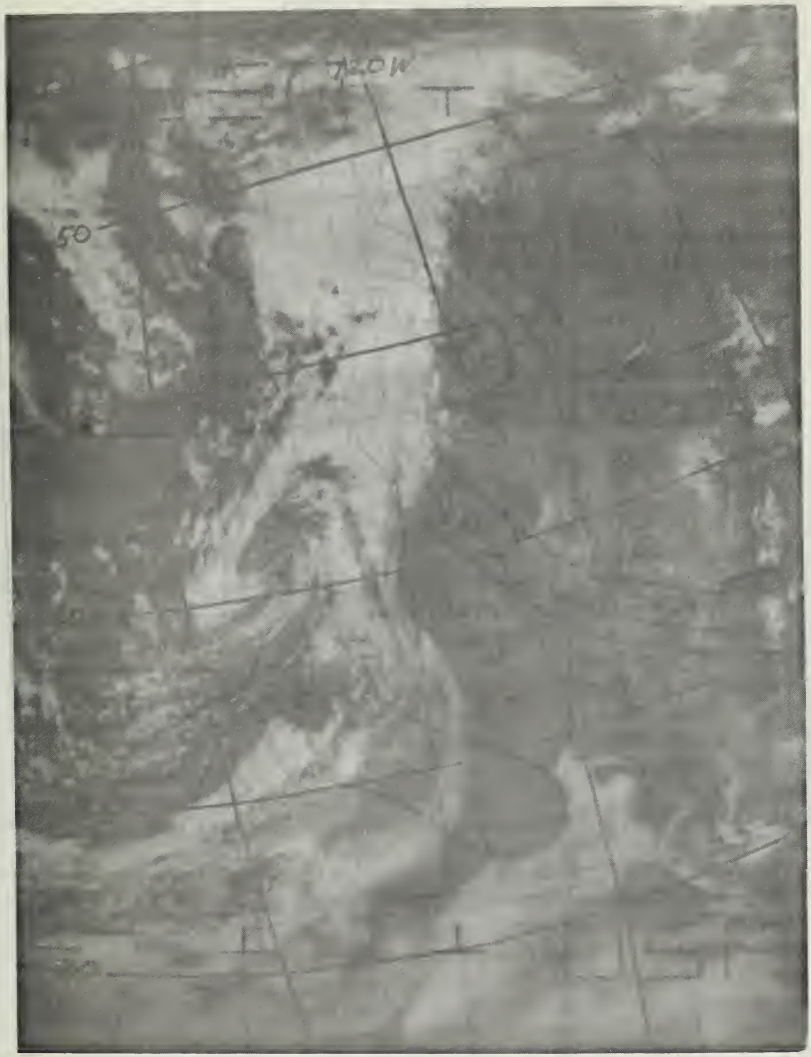

Fig. 31a
Satellite ESSA VI - July 19, 1968

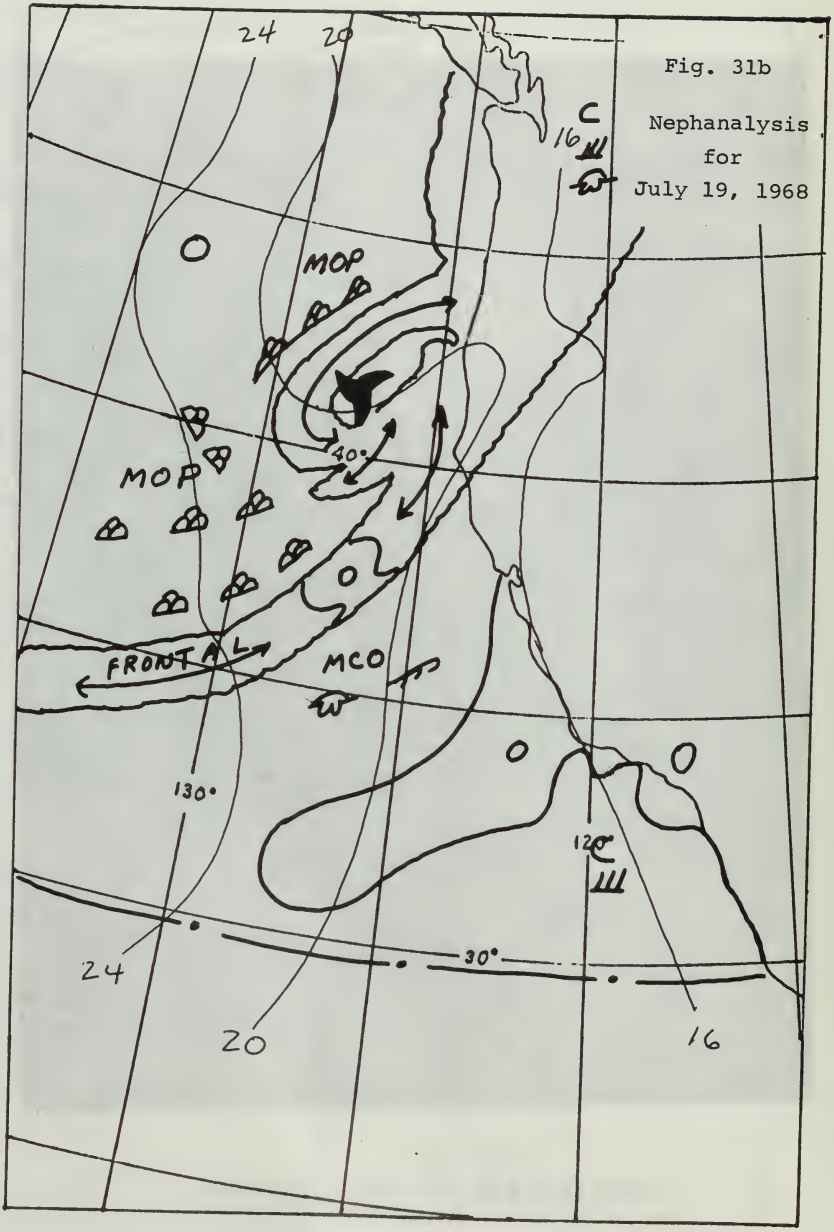

Fig. 31b

Nephanalysis for July 19, 1968

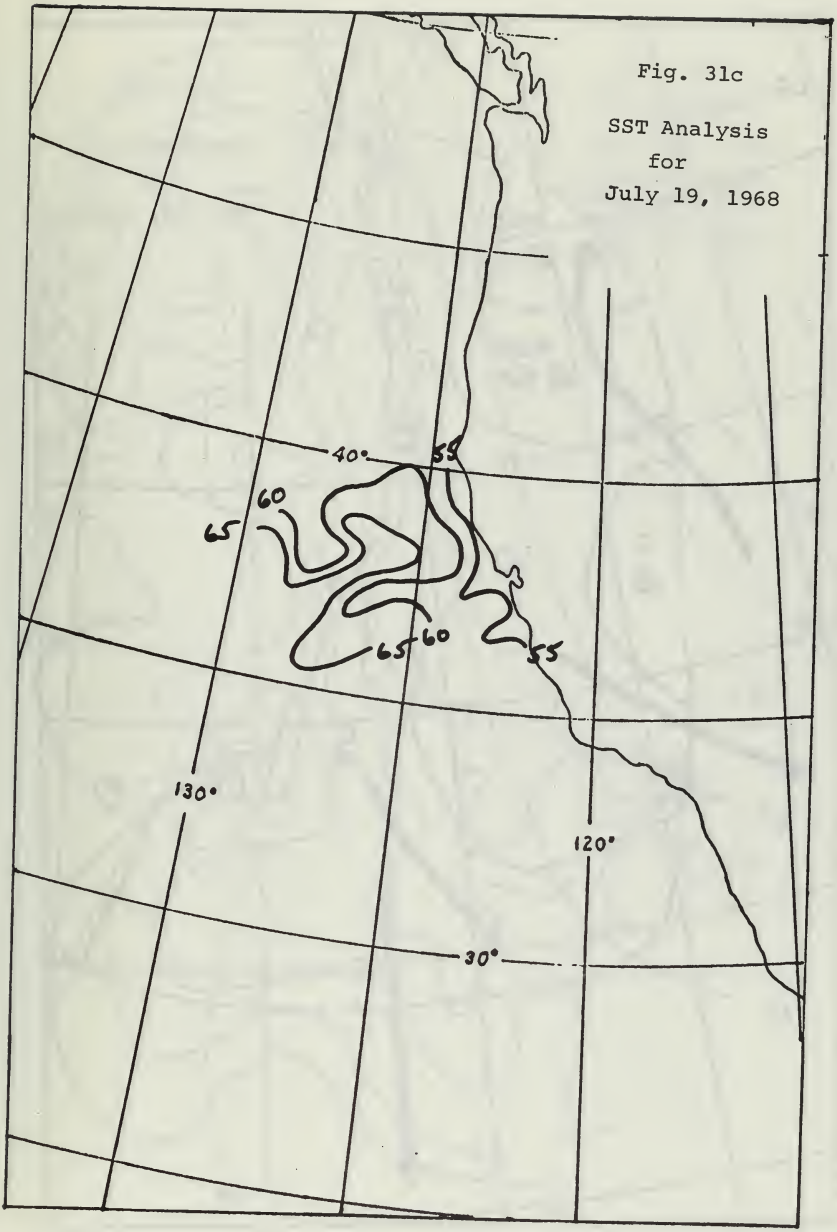

Fig. 31c

SST Analysis
for
July 19, 1968

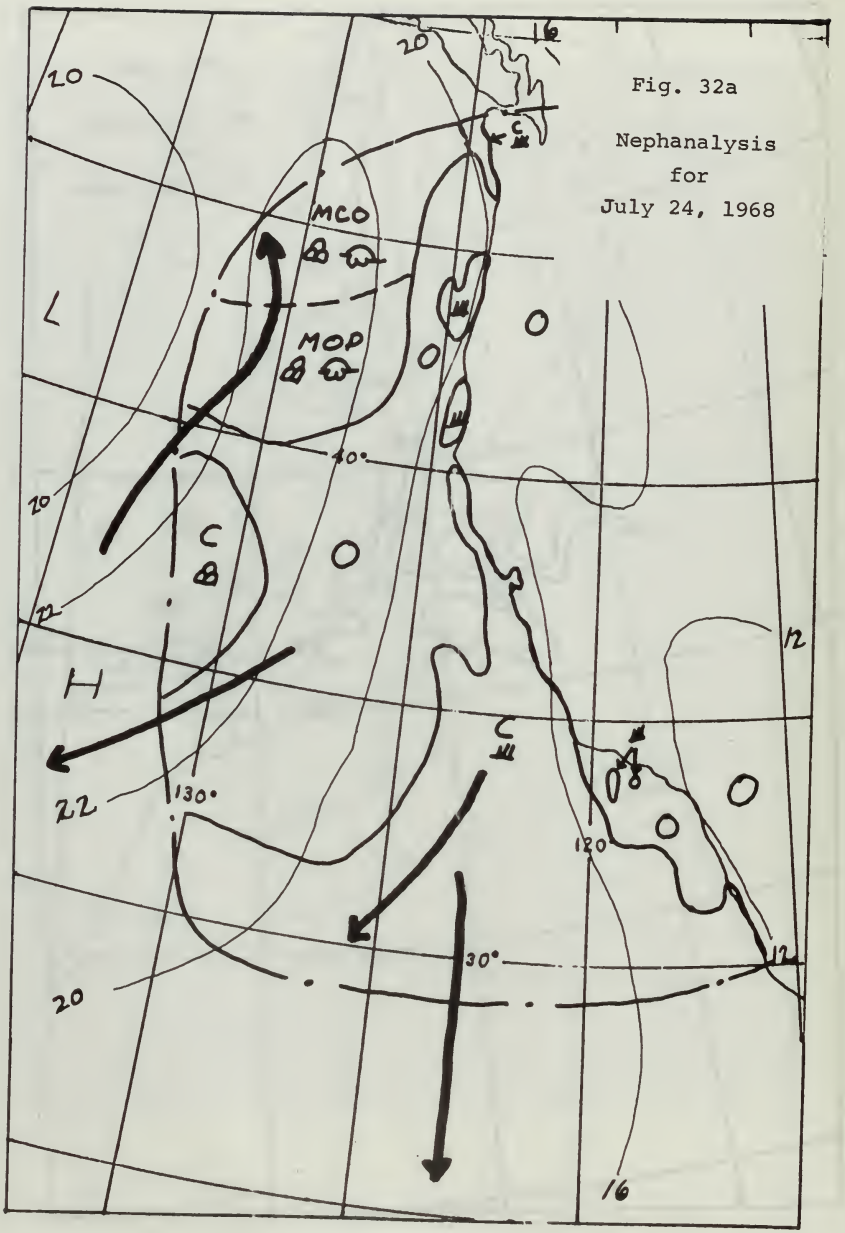

Fig. 32a

Nephanalysis
for
July 24, 1968

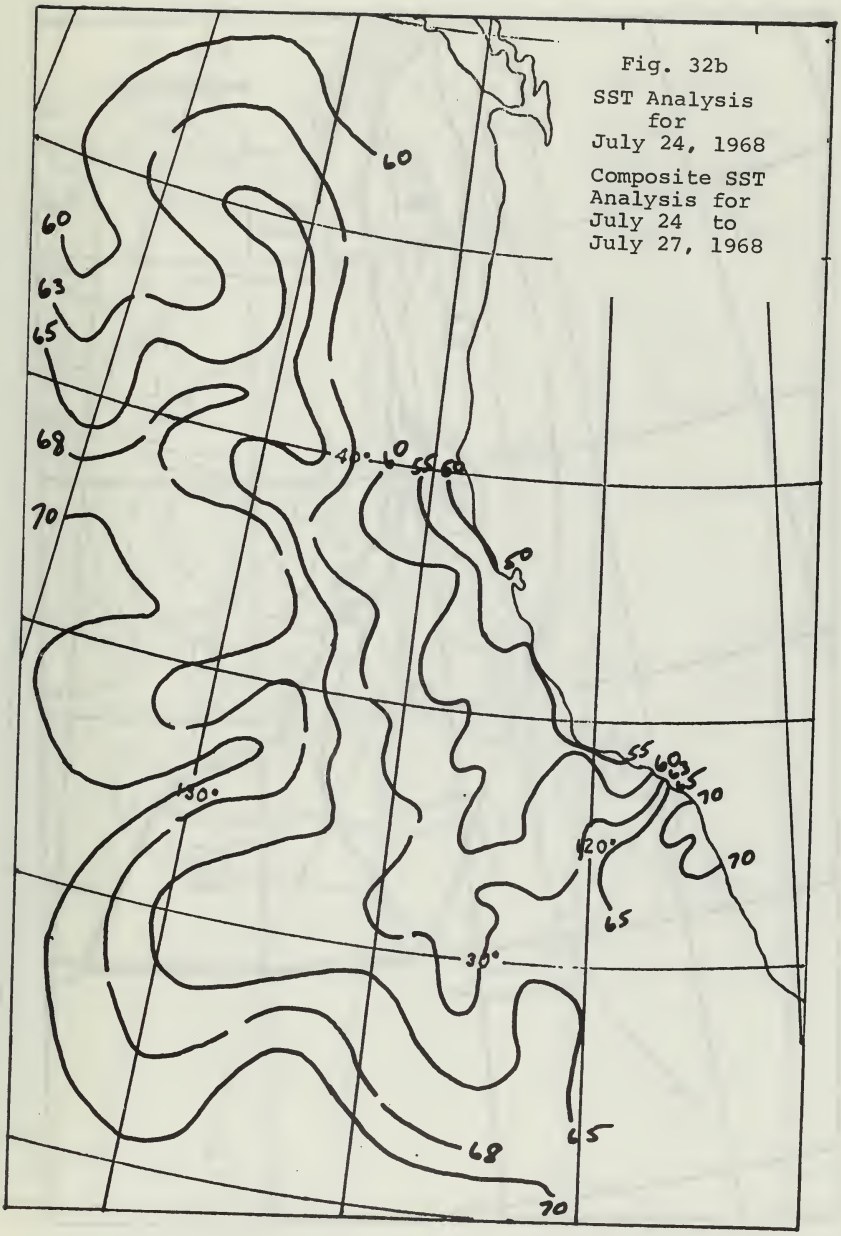

Fig. 32b
SST Analysis
for
July 24, 1968

Composite SST
Analysis for
July 24 to
July 27, 1968

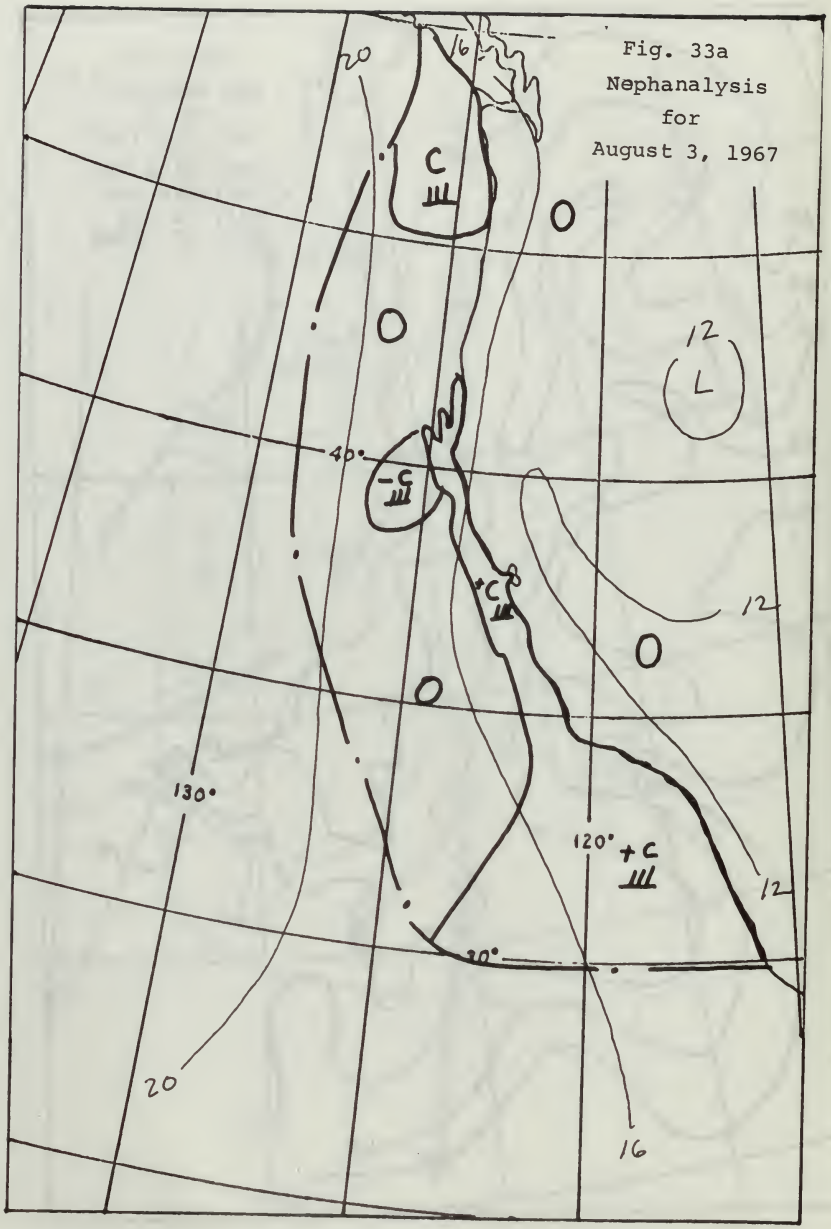

Fig. 33a
Nephanalysis
for
August 3, 1967

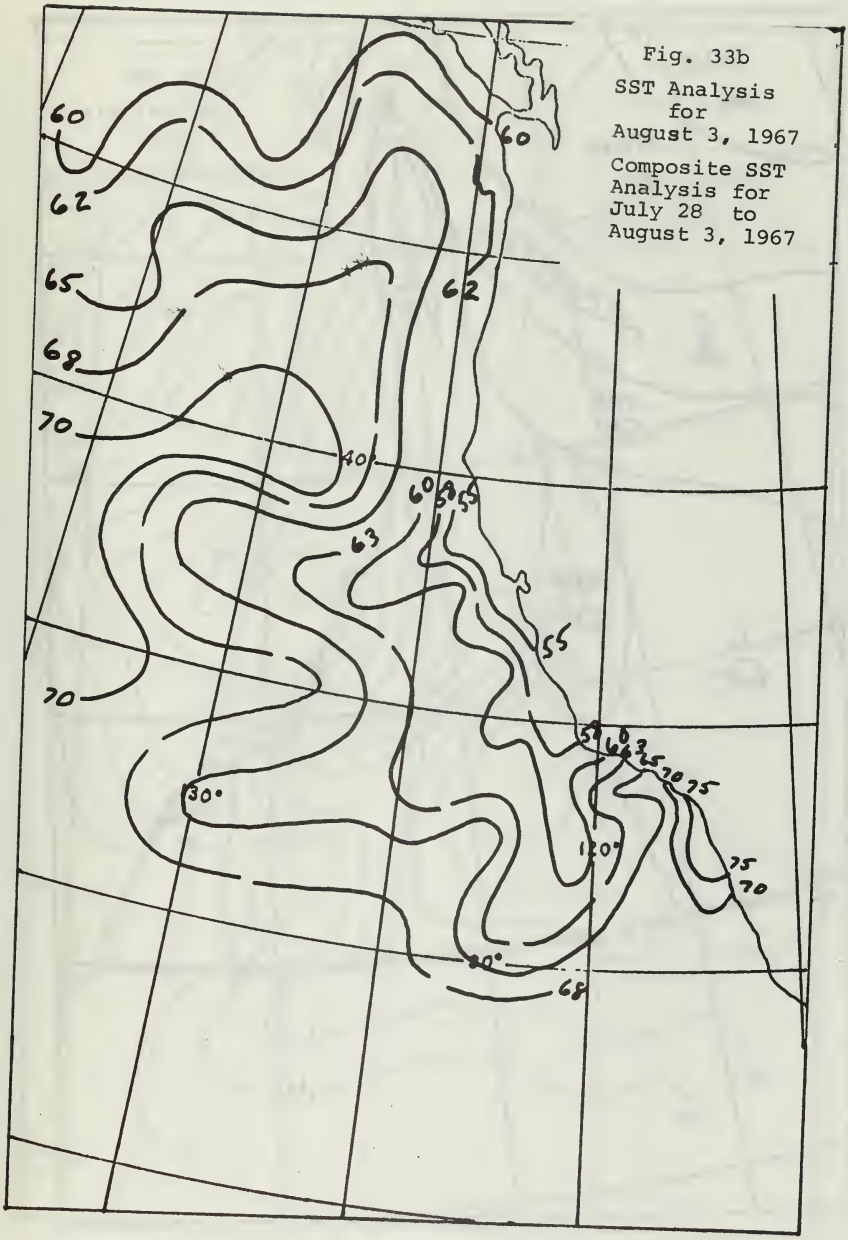

Fig. 33b

SST Analysis for August 3, 1967

Composite SST Analysis for July 28 to August 3, 1967

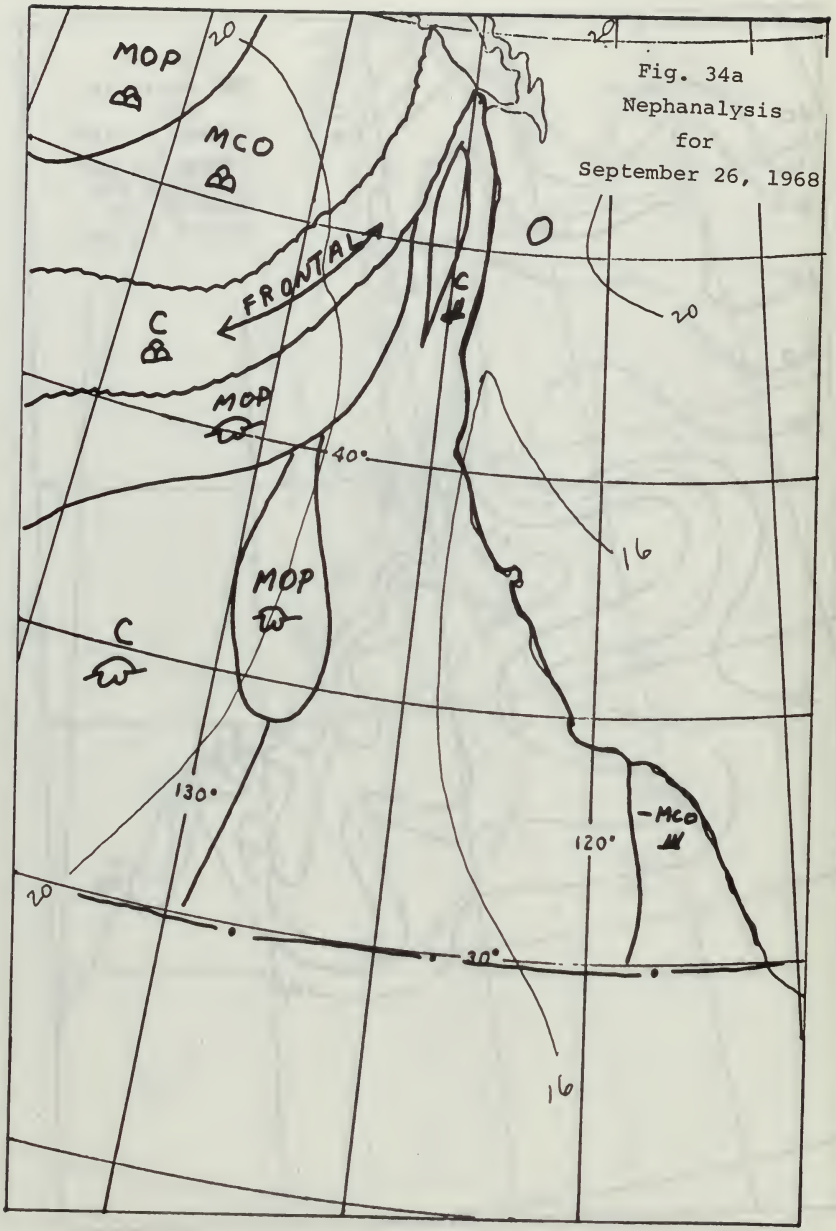

Fig. 34a
Nephanalysis
for
September 26, 1968

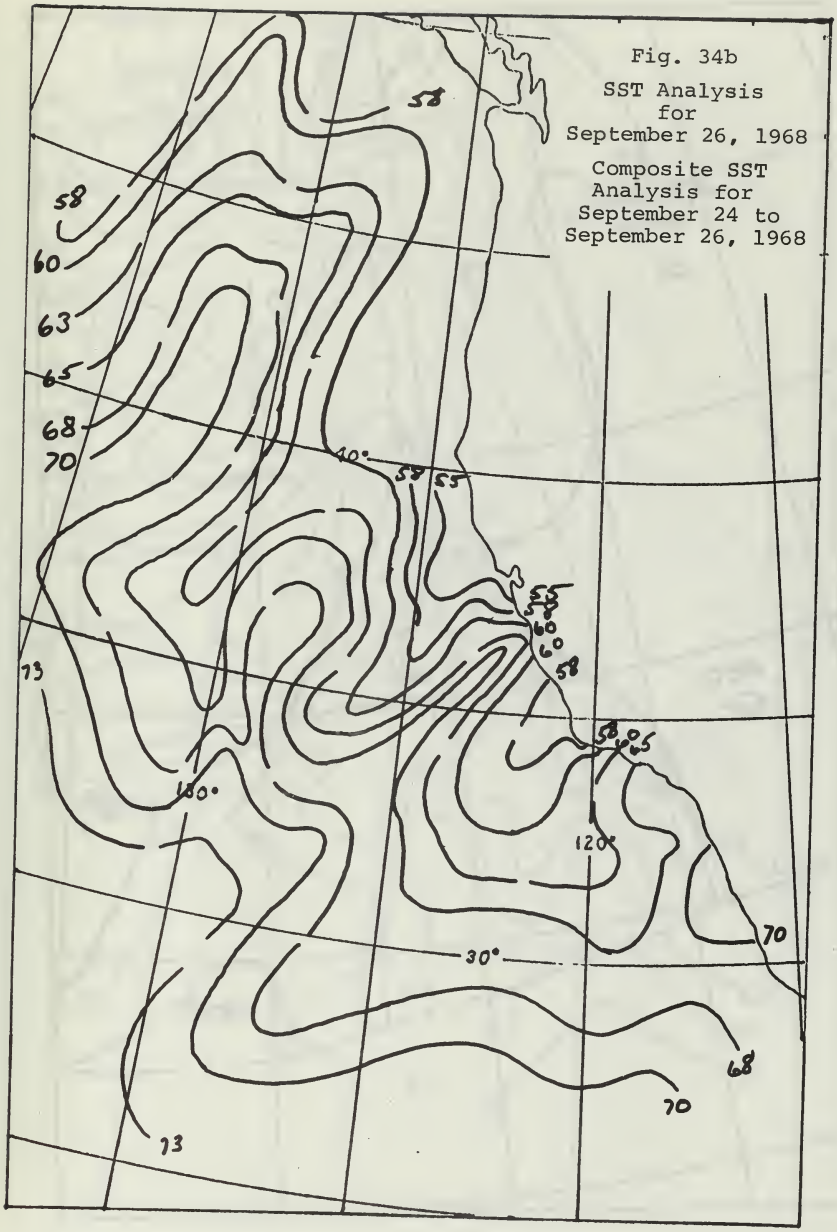

Fig. 34b

SST Analysis
for
September 26, 1968

Composite SST
Analysis for
September 24 to
September 26, 1968

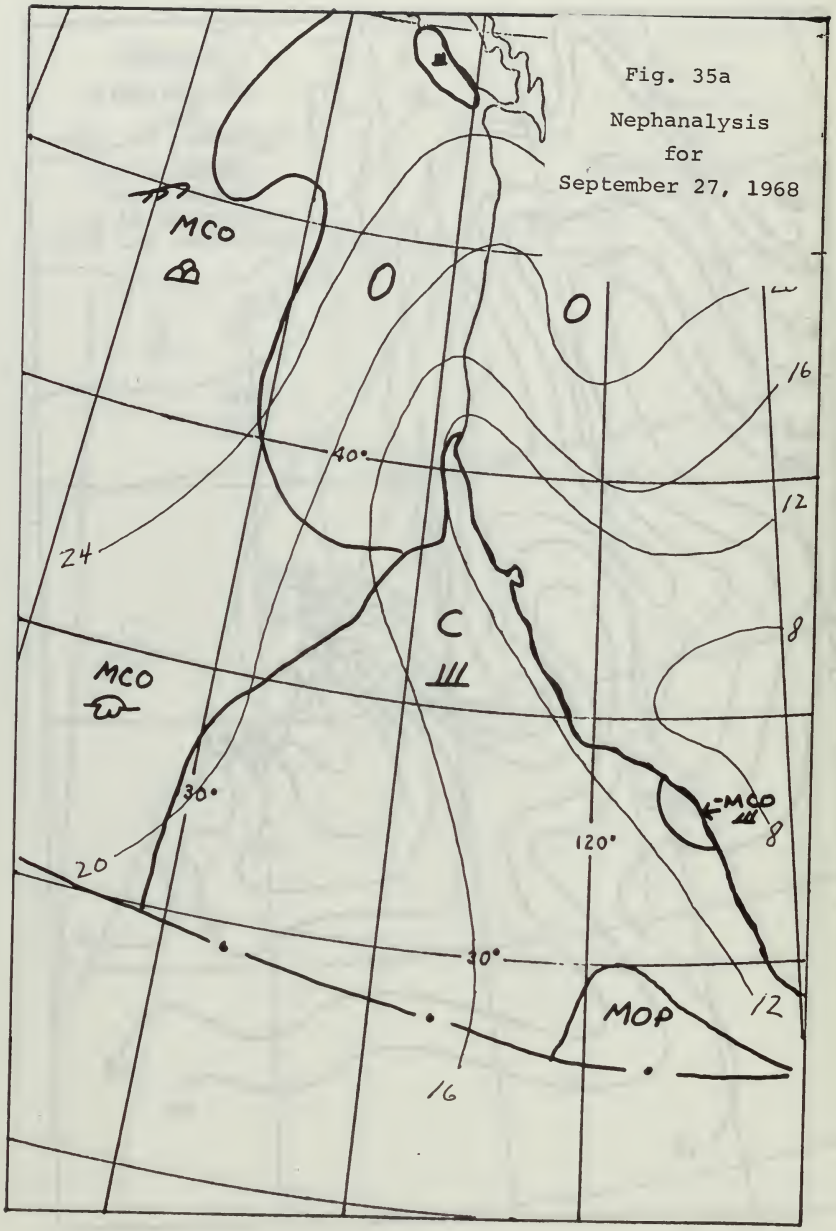

Fig. 35a
Nephanalysis
for
September 27, 1968

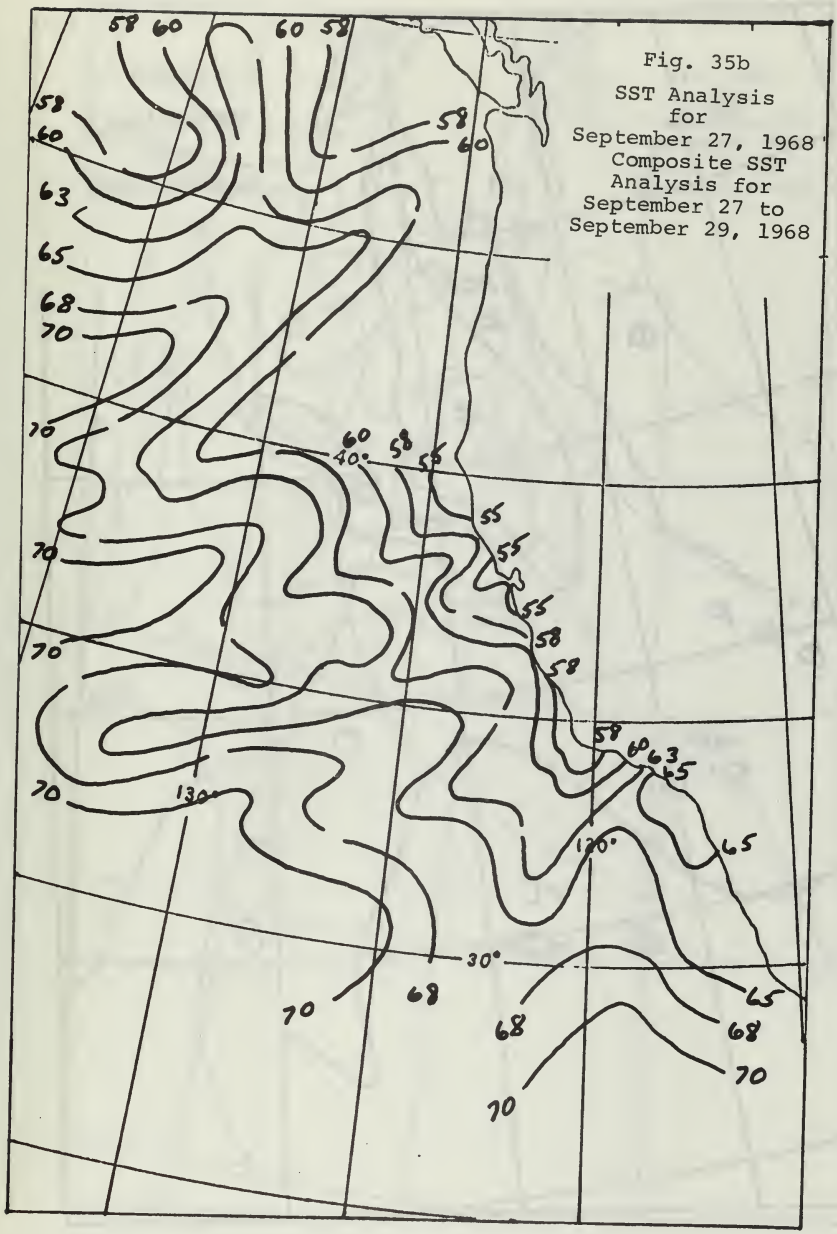

Fig. 35b

SST Analysis for September 27, 1968
Composite SST Analysis for September 27 to September 29, 1968

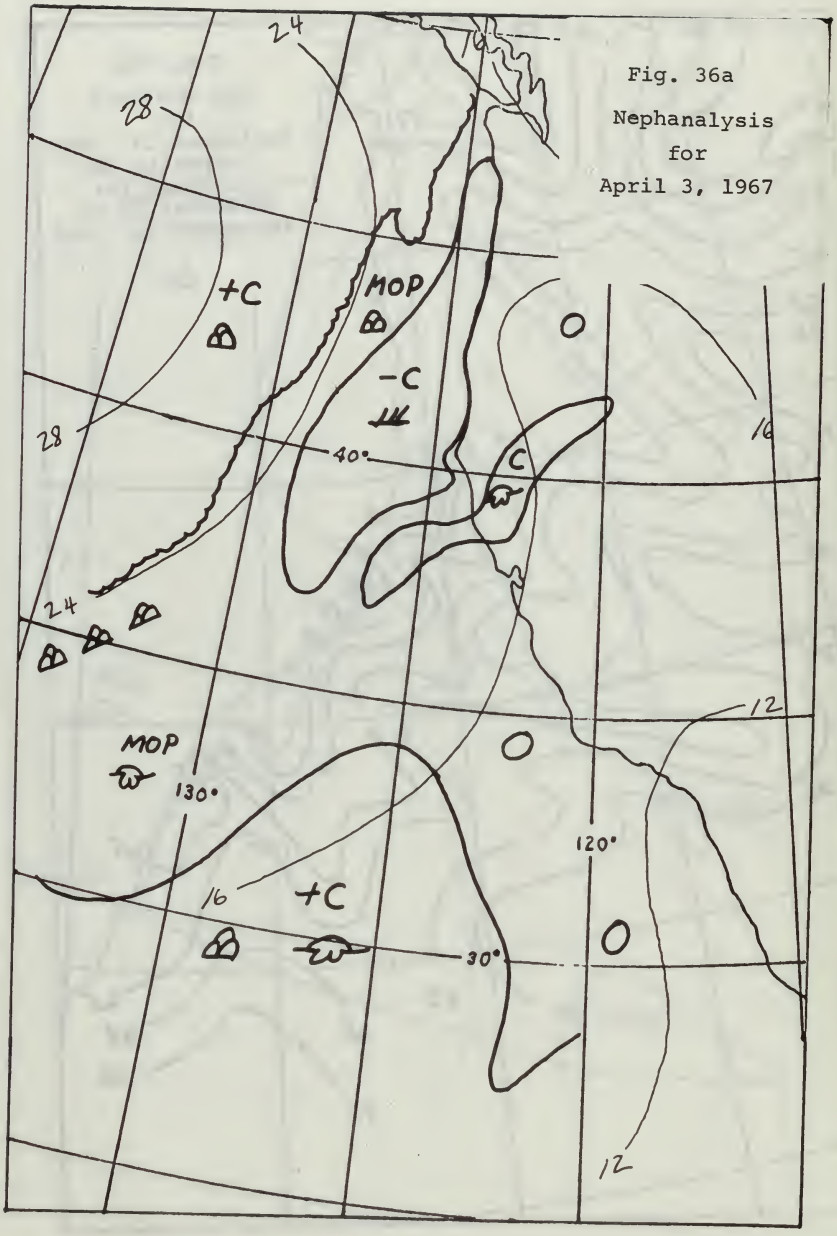

Fig. 36a
Nephanalysis
for
April 3, 1967

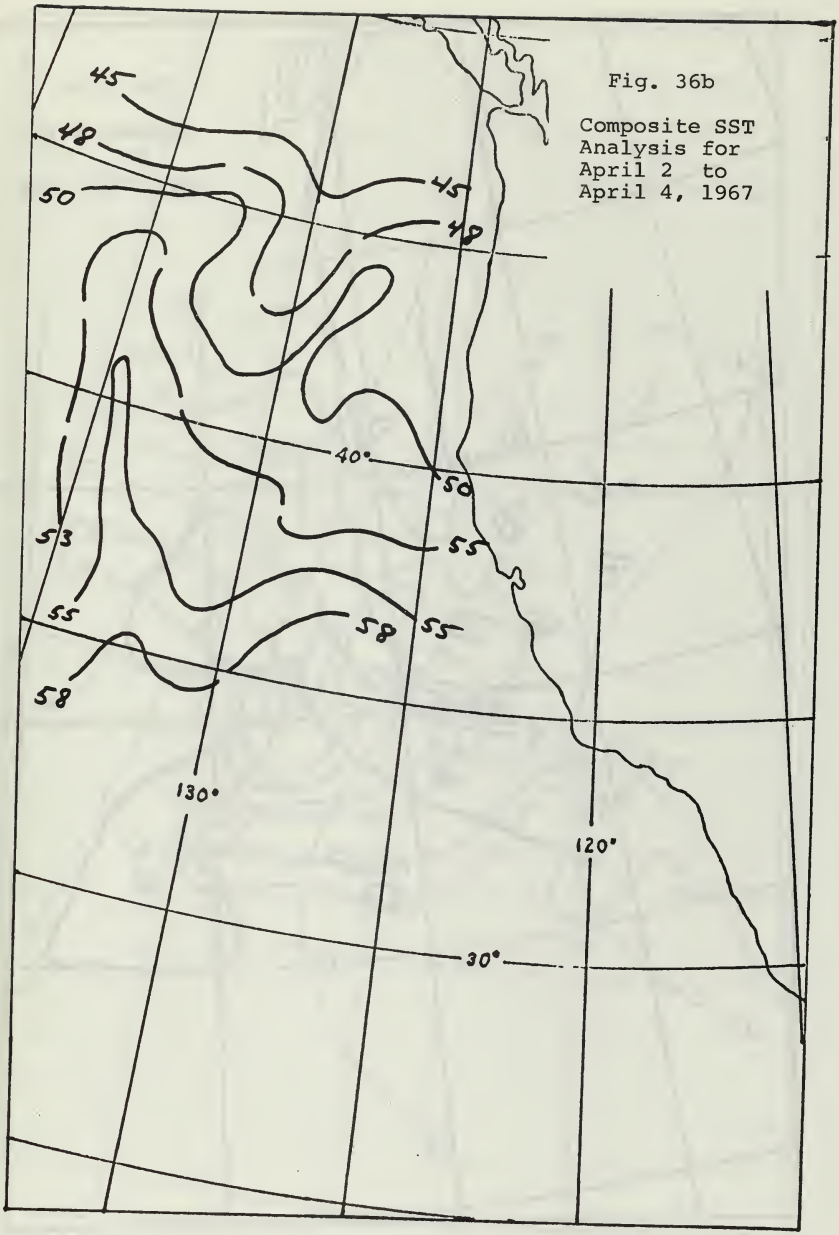

Fig. 36b

Composite SST Analysis for April 2 to April 4, 1967

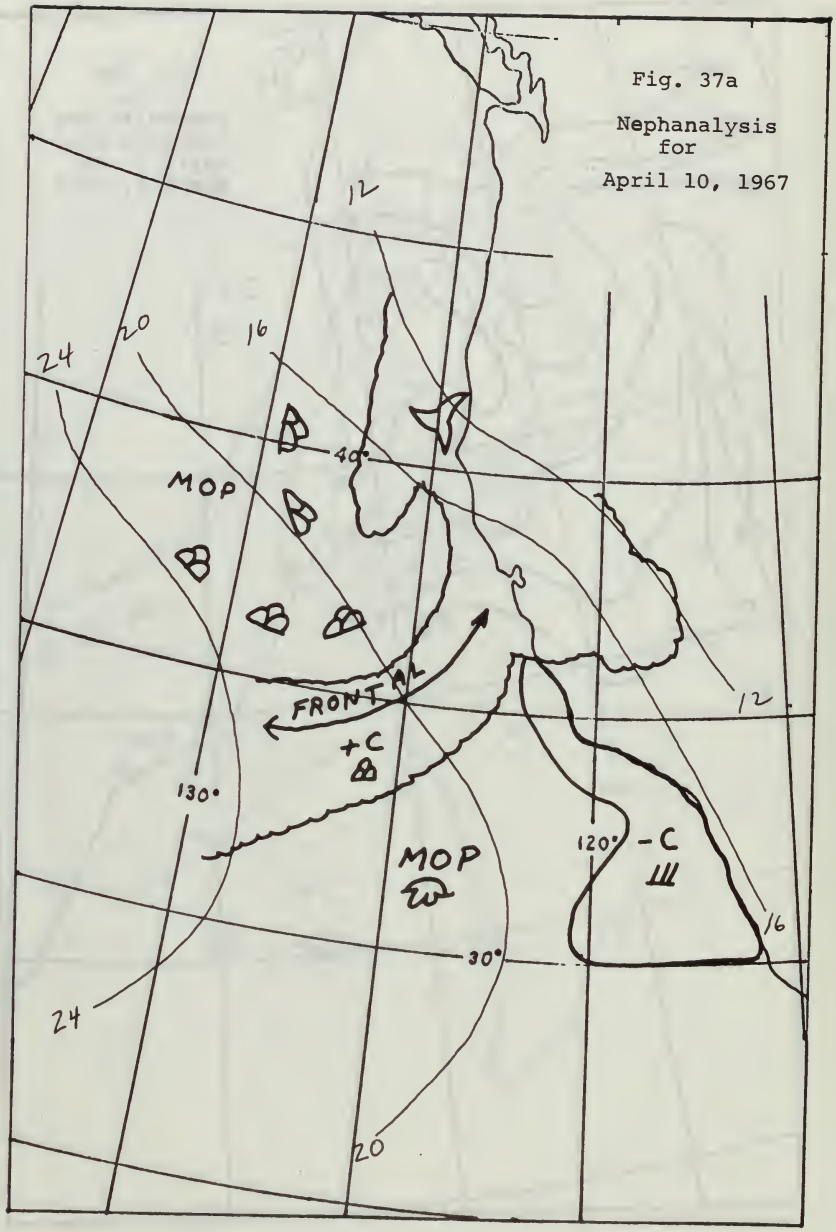

Fig. 37a

Nephanalysis
for
April 10, 1967

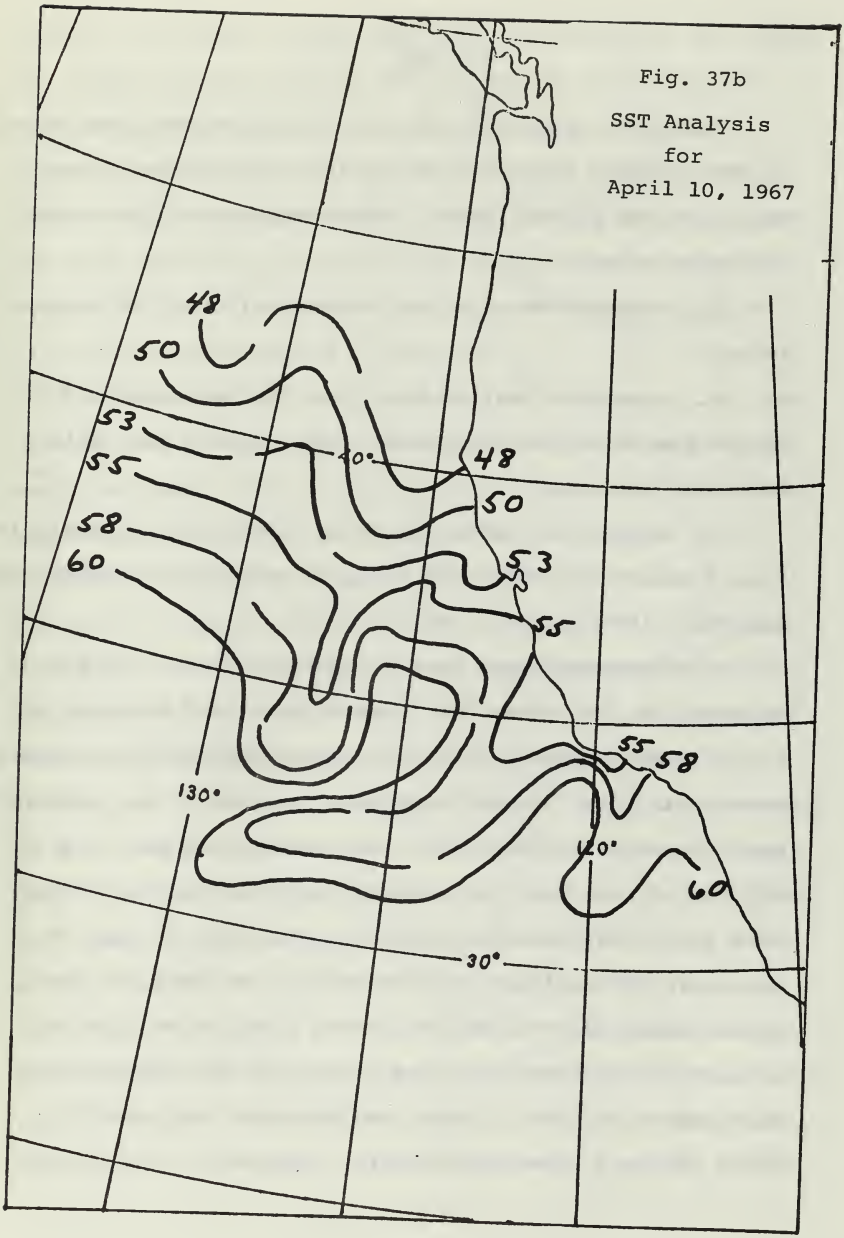

Fig. 37b
SST Analysis
for
April 10, 1967

V. TEST

Combining the six types of correlation discussed above, an SST analysis model for the California Current and upwelling areas may be formed. The necessary tools to make an analysis are:

1. a satellite photo or nephanalysis for the day concerned,

2. a surface weather chart for the day concerned (to obtain the isobaric patterns and any SST data available from ship reports),

3. a previous SST analysis or climatological analysis (e.g., the monthly mean SST analyses presented by LaViolette and Seim (1969) in Fig. 1).

Five attempts were made at construction of the SST analyses; in two cases the climatological SST analyses of Fig. 1 were employed, in three others previous SST analyses were used. Fig. 38 and 39 show the results of two attempts using previous SST analyses. In constructing Fig. 38, the SST analysis in Fig. 23b and the nephanalysis for June 17, 1968 (Fig. 25a) were utilized. In constructing Fig. 39, the daily SST analysis from August 16, 1968 and the composite analysis covering the period from the 16th to the 19th of August 1968 were used along with the nephanalysis from August 20, 1968. Each case includes four synoptic SST's obtained from ship reports. The heavy lines in the

figures are those for the analysis constructed by the model; the dashed lines are those for the actual verifying SST analysis, prepared from extensive SST data coverage. In general most of the verifying SST features were obtained in the constructed SST pattern. Positioning of the tongues was more difficult in large areas of cloud cover and large cloud-free areas. The orientation, however, was good on all of the constructed SST analyses.

A method of evaluating a model SST analysis is to compare it and the historical analysis (used to construct the model analysis) with the actual analysis, to see which best represents the actual analysis. This was done by first obtaining the average temperature difference between the actual SST analysis and the model SST analysis at a number of points; then this average was compared with the average temperature difference between the actual SST analysis and the historical SST analysis at these same points. The points were at every 2^{o} longitude between 135W and the coast of North America and at every 3^{o} latitude between 29N and 50N. The data for five attempts are presented in Table III. The number of points used in the average differs for each attempt because only areas where an analysis existed were included. The method of evaluation is crude because of the space between the points where the temperature averages were taken. Attempts one and two used mean SST analyses presented in Fig. 1. Attempts three and five are Figs. 38 and 39

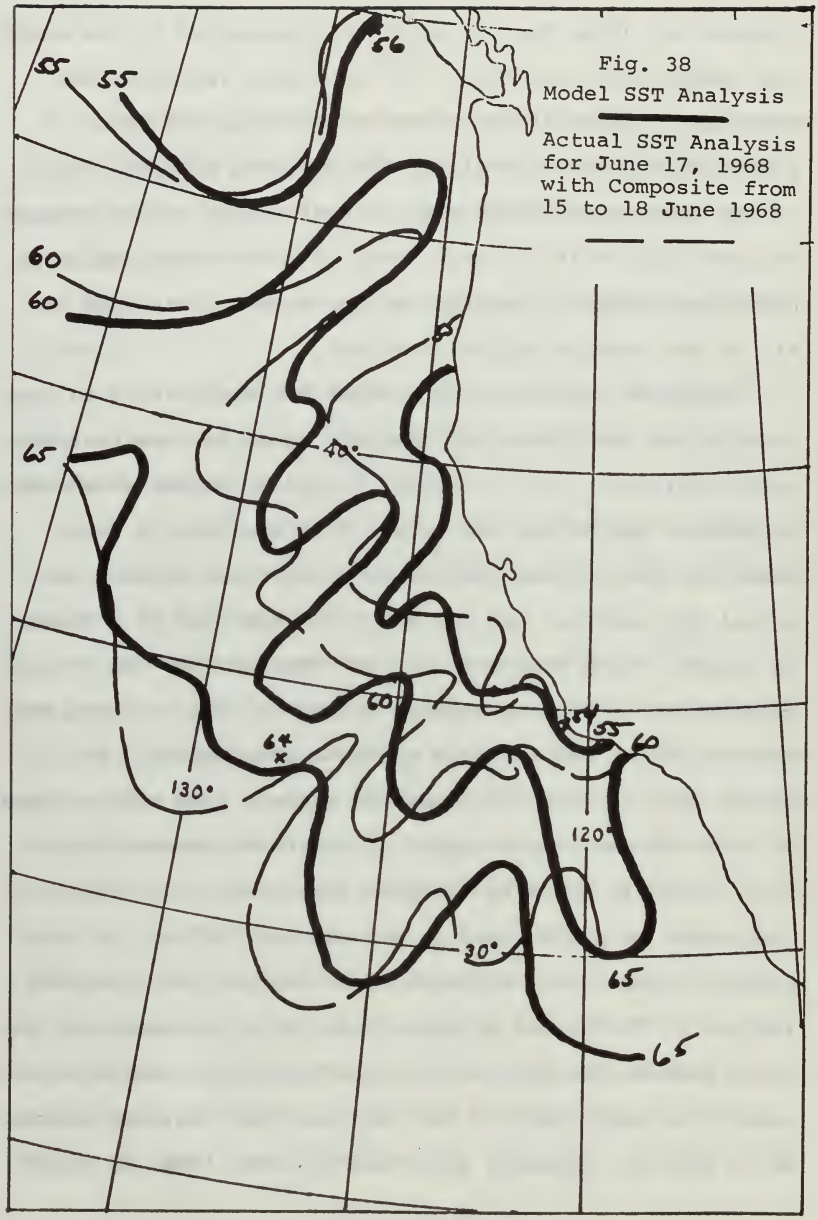

Fig. 38
Model SST Analysis

Actual SST Analysis for June 17, 1968 with Composite from 15 to 18 June 1968

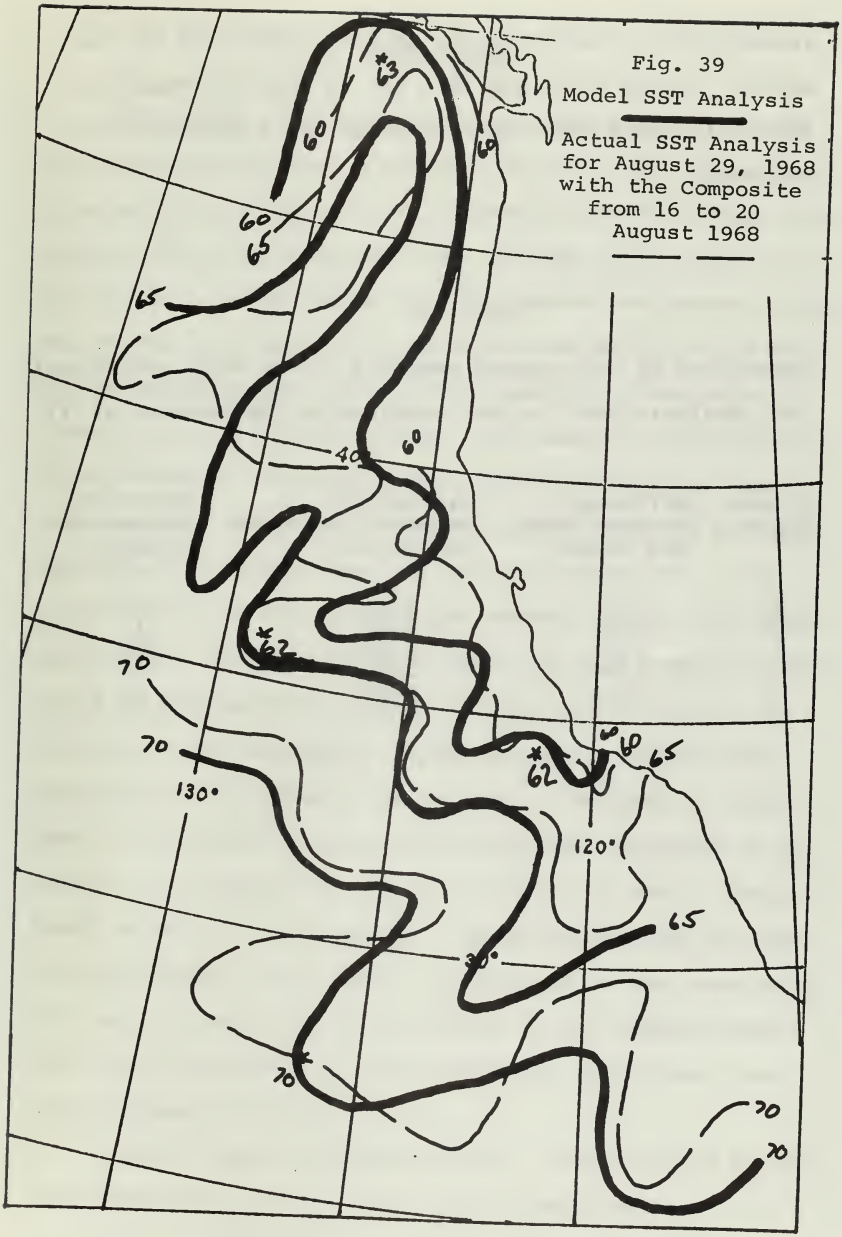

Fig. 39
Model SST Analysis

Actual SST Analysis for August 29, 1968 with the Composite from 16 to 20 August 1968

respectively; they show the greatest expertise for the model. It was felt, and that can be seen by examining Table III, that experience improves one's ability to use the model.

Table III

Comparison of Constructed Analysis by the Model and Historical Analysis Used in the Construction (Difference in ^{o}F)

Attempt Number	Difference between Model and Actual	Difference between Historical and Actual	Number of Points in Average
1	2.04	2.32	25
2	1.35	1.62	37
3	1.15	1.79	39
4	1.50	2.70	20
5	0.94	1.95	32

VI. CONCLUSIONS

Five types of correlation were found between the SST patterns and the cloud patterns. First is the correlation between the stratus and the California Current and upwelling areas. The stratus existed over a large cold tongue of water while a warm tongue of water formed the seaward boundary of the stratus. A warm spot (in the SST) existed near 33.5N, and this spot often had an associated decrease or clearing of the stratus clouds. The second correlation existed between a cloud-free area and the California Current and upwelling areas in a cold air mass. The cold air mass was normally brought into the area by passage of a cold front. Third is the correlation between stratus and upwelling areas. Although stratus occurring from upwelled water could be delineated at times, it often was masked by the stratus of the California Current or was prevented from occurring by atmospheric conditions. A variety of atmospheric conditions existing along different portions of the coast at the same time made it difficult to make a thorough study of many of the aspects of upwelling through the use of cloud photos. The fourth correlation is the association of frontal clouds with warm tongues of sea surface water. The fifth correlation is the occurrence of vortices over cold tongues of water.

Besides these five correlations, warm and cold tongues were observed to line up with the isobaric pattern. At

least a two-day time period appears to be needed to realign the SST pattern after a change in surface flow. Finally, the divergence of the surface isobars was found not to correlate with the stratus pattern.

An analysis model was formed using the correlations obtained. Although most of the features of the verifying SST patterns were obtained using the model, positioning of isotherms under completely clear or completely cloud-covered areas was found to be difficult. The skill in using the model increased with experience.

VII. RECOMMENDATIONS

The remaining months of the year, October through February, need to be investigated to see if these correlations apply all year. If they do, then the correlations could be incorporated into synoptic forecasting schemes for sea surface temperatures.

With the SST data obtained by the author, a study of the synoptic changes of sea surface temperature patterns is feasible.

LIST OF REFERENCES

1. Air Weather Service, General Aspects of Fog and Stratus Forecasting, Manual 105-44, 1954.

2. Arthur, Robert S., "Oscillation in Sea Temperature at Scripps and Oceanside Piers", Deep Sea Res., 2:107-121, 1954.

3. Arthur, Robert S., "On the Calculation of Vertical Motion in Eastern Boundary Currents from Determinations of Horizontal Motion", J. Geophys. Res.,70(12):2799-2803, 1965.

4. Bittner, Guide for Interpretation of Satellite Photography and Naphanalyses, Project FAMOS Res. Report (4-67), 1967.

5. Dawson, E.Y., "A Further Study of Upwelling and Associated Vegetation along Pacific Baja California, Mexico", J. Mar. Res., 10(1):39-58, 1951.

6. Edinger, James G., "Modification of the Marine Layer over Coastal Southern California", J. Appl. Meteor., 44:706-712, 1963.

7. Hidaka, Koji, "A Contribution to the Theory of Upwelling and Coastal Currents", Trans. Amer. Geophys. Un., 35:431-444, 1954.

8. Holly, Richard W., Temperature and Density Structure of Water along the California Coast, Master's Thesis, Naval Postgraduate School, 1968.

9. James, Richard W., Ocean Thermal Structure Forecasting, Naval Oceanographic Office, ASWEPS Manual Series, Vol. 5, SP-105, 1966.

10. LaViolette, Paul E., and Sandra E. Seim, Satellite Photography as a Means of Determining Water Temperature Structure, Informal Report No.68-76, 1968.

11. LaViolette, Paul E., and Sandra E. Seim, Satellite Capable of Oceanic Data Acquisition- A Review, Naval Oceanographic Office, Technical Report No.215, 1969a.

12. LaViolette, Paul E., and Sandra E. Seim, Monthly Charts of Mean, Minimum, and Maximum Sea Surface Temperatures of the North Pacific Ocean, Naval Oceanographic Office,SP-123, 1969b.

13. Leipper, Dale F., Sea Surface Temperature Variations Influencing Fog Formation in Southern California, Scripps Inst. of Ocean., University of California, Contract N60ri-211, Report No. 9, 1947.

14. Leipper, Dale F., "Fog Development at San Diego, California", J. Mar. Res., 8(3):337-346, 1948.

15. Leipper, Dale F., "Sea Temperature Variations Associated with Tidal Currents and Stratified Shallow Water over an Irregular Bottom", J. Mar. Res., 14(3):234-252, 1955.

16. Leipper, Dale F., "The Sharp Smog Bank and California Fog Development", Bull. Amer. Meteor. Soc., 49(4): 354-358, 1968.

17. McEwen, George F., "Rate of Upwelling in the Region of San Diego Computed from Serial Temperatures", Fifth Pac. Sci. Congr., 1933, Proc., 3:1763, 1934.

18. Neiburger, Morris, "Temperature Changes During Formation and Dissipation of West Coast Stratus", J. of Meteor., 1(1):29-41, 1944.

19. Neiburger, Morris, "The Relation of Air Mass Structure to the Field of Motion over the Eastern North Pacific Ocean", Tellus,12:29-41, 1960.

20. Neiburger, Morris, D. S. Johnson, and C. Chien, Studies of the Structure of the Atmosphere over the Eastern North Pacific in Summer, I. The Inversion over the Eastern North Pacific, University of California Pub. Meteor., 1(1):1-94, 1961.

21. Patton, C. P., Climatology of Summer Fog in the San Francisco Bay Area, University of California Pub. in Geog., 10:113-200, 1956.

22. Pattullo, June G., and Wayne Burt, The Pacific Ocean, Atlas of the Pacific Northwest,Ore.State Univ.,1960.

23. Petterssen, Sverre, "On the Causes and the Forecasting of the California Fog", Bull. Amer. Meteor. Soc., 19(2):49-55, 1938.

24. Pincock, G. L., and J. A. Turner, "Advection Fog along the British Columbia Coast and over the North Pacific Ocean during Late Summer and Early Winter", Eighth Pac. Sci. Congr., Proc., 2:955-960, 1955.

25. Reid, Joseph L., Gunnar I. Roden, and John G. Wyllie, Studies of the California Current System, Prog. Rep. CCOFI, 1 July 1956- 1 Jan. 1958, pp.27-56, 1958.

26. Reid, Joseph L., Oceanography of the Northeastern Pacific Ocean during the Last Ten Years, CCOFI Repts., 1 Jan. 1958 to 30 June 1959, 7:77-90, 1959.

27. Roden, Gunnar I., "On Statistical Estimation of Monthly Extreme Sea-Surface Temperatures along the West Coast of the United States", J. Mar. Res., 21(3):972-989, 1962.

28. Skogsberg, Tage, "Hydrography of Monterey Bay, California, Thermal Conditions, 1929-1933", Trans. Amer. Phil. Soc. 29:1-152, 1936.

29. Smith, Robert L., June G. Pattullo, and Robert K. Lane, "An Investigation of the Early Stage of Upwelling along the Oregon Coast", J. Geophys. Res., 71(4):1135-1140, 1966.

30. Smith, Robert L., "Note on Yoshida's (1955) Theory of Coastal Upwelling", J. Geophys. Res., 72(4):1396-1397, 1967.

31. Stevenson, Robert E., and Donn S. Gorsline, "A Shoreward Movement of Cool Subsurface Water", Trans. Amer. Geophys. Un., 37(5):553-557, 1956.

32. Stewart, H. B., Jr., Coastal Water Temperature and Sea Level - California to Alaska, Rept. CCOFI, 1 Jan. 1958 - 30 June 1959, Vol. 7, 1959.

33. Sverdrup, H. U., "On the Process of Upwelling", J.Mar. Res., 1:155-164, 1938

34. Sverdrup, H. U., and R. H. Fleming, The Waters off the Coast of Southern California, March to July 1937, Bull.Scripps Inst. Oceanogr., 4:261-378, 1941.

35. Sverdrup, H. U., M. W. Johnson, and R. H. Fleming, The Oceans, Prentice-Hall, Inc., New York, 1087 pp., 1942.

36. Tabata, Susumu, Heat Exchange between Sea and Atmosphere along the Northern British Columbia Coast, Prog. Repts. Pac. Coast Sta., Fish. Res. Bd. of Canada, 108:18-20, 1957.

37. U.S. Department of the Interior Fish and Wildlife Service, Cruise Report, August 20 to December 18, 1968.

38. Wood, Floyd B., "The Formation and Dissipation of Stratus Clouds beneath Turbulence Inversions", Bull. Amer. Meteor. Soc., 19(3):97-103, 1938.

39. Wyrtki, Klaus, Summary of the Physical Oceanography of the Eastern Pacific Ocean, Inst. of Mar. Res., IMR Ref. 65-10, UCSD - 34P99 - 11, 1958.

40. Yoshida, Kozo, and Han L. Mao, "A Theory of Upwelling of Large Horizontal Extent", J. Mar. Res., 16:40-54, 1957.

41. Yoshida, Kozo, "Coastal Upwelling off the California Coast", Rec. Oceanogr. Wks., Japan, 2(2):8-20, 1955.

42. Yoshida, Kozo, "A Study of Upwelling", Rec. Oceanogr. Wks., Japan, 4(2):186-192., 1958.

INITIAL DISTRIBUTION LIST

		No. Copies
1.	Defense Documentation Center Cameron Station Alexandria, Virginia 22314	20
2.	Library, Code 0212 Naval Postgraduate School Monterey, California 93940	2
3.	Dr. Glenn H. Jung Department of Oceanography Naval Postgraduate School Monterey, California 93940	3
4.	Dr. Dale F. Leipper, Chairman Department of Oceanography Naval Postgraduate School Monterey, California 93940	1
5.	LT. Anthony L. Gerst 98 Brahm Street Pittsburgh, Pennsylvania 15212	2
6.	Naval Weather Service Command Washington Navy Yard Washington, D.C. 20390	1
7.	Officer in Charge Navy Weather Research Facility Naval Air Station, Bldg. R-48 Norfolk, Virginia 23511	1
8.	Commanding Officer Fleet Weather Central Naval Air Station Alameda, California 94501	1
9.	Commanding Officer U.S. Fleet Weather Central COMNAVMARIANAS, Box 12 FPO San Francisco, California 96630	1
10.	Commanding Officer U.S. Fleet Weather Central Box 31 FPO San Francisco, California 09540	1

		No. Copies
11.	Commanding Officer Fleet Numerical Weather Central Naval Postgraduate School Monterey, California 93940	1
12.	Commanding Officer Fleet Weather Facility Naval Air Station, North Island San Diego, California 92135	1
13.	Commanding Officer and Director Navy Undersea R&D Center (NUC) Attn: Code 2230 San Diego, California 92152	1
14.	Atmospheric Sciences Library Environmental Science Service Administration Silver Spring, Maryland 20910	1
15.	Department of Oceanography Code 58 Naval Postgraduate School Monterey, California 93940	3
16.	Department of Metereology Code 51 Naval Postgraduate School Monterey, California 93940	1
17.	Oceanographer of the Navy The Madison Building 732 N. Washington Street Alexandria, Virginia 22314	1
18.	Naval Oceanographic Office Attn: Paul LaViolette Washington, D.C. 20390	1
19.	National Oceanographic Data Center Washington, D.C. 20390	1
20.	Director, Coast & Geodetic Survey Department of Commerce Attn: Office of Oceanography Washington, D.C. 20235	1
21.	Mission Bay Research Foundation 7730 Herschel Avenue La Jolla, California 92038	1

		No. Copies
22.	Director, Maury Center for Ocean Sciences Naval Research Laboratory Washington, D.C. 20390	1
23.	Office of Naval Research Department of the Navy Attn: Undersea Warfare (Code 466) Washington, D.C. 20360	1
24.	Office of Naval Research Department of the Navy Attn: Geophysics Branch (Code 416) Washington, D.C. 20360	1
25.	Commanding Officer ATTN: Corbeille Pacific Missile Range Point Mugu, California 93041	1

Unclassified
Security Classification

DOCUMENT CONTROL DATA - R & D

(Security classification of title, body of abstract and indexing annotation must be entered when the overall report is classified)

1. ORIGINATING ACTIVITY *(Corporate author)*

Naval Postgraduate School
Monterey, California 93940

2a. REPORT SECURITY CLASSIFICATION

Unclassified

2b. GROUP

3. REPORT TITLE

Correlation of Sea Surface Temperature with Cloud Patterns off the West Coast of North America during the Upwelling Season

4. DESCRIPTIVE NOTES *(Type of report and, inclusive dates)*

Master's Thesis; October 1969

5. AUTHOR(S) *(First name, middle initial, last name)*

Anthony L. Gerst

6. REPORT DATE	7a. TOTAL NO. OF PAGES	7b. NO. OF REFS
October 1969	121	42

8a. CONTRACT OR GRANT NO.	9a. ORIGINATOR'S REPORT NUMBER(S)
b. PROJECT NO.	
c.	9b. OTHER REPORT NO(S) *(Any other numbers that may be assigned this report)*
d.	

10. DISTRIBUTION STATEMENT

This document has been approved for public release and sale; its distribution is unlimited.

11. SUPPLEMENTARY NOTES	12. SPONSORING MILITARY ACTIVITY
	Naval Postgraduate School Monterey, California 93940

13. ABSTRACT

The possibility of a correlation between sea surface temperature (SST) and cloud patterns was investigated using cloud photos from the satellites NIMBUS II (1967) and ESSA VI (1968). Five types of correlation were found to exist: the correlation between stratus and the California Current and upwelling areas in a warm air mass, between clearing and the California Current and upwelling areas in a cold air mass, between stratus and the upwelling areas under favorable conditions, between frontal clouds and warm tongues of surface water, and between vortices and cold tongues of surface water. A sixth type of correlation was found between the surface isobaric pattern and the orientation of cold and warm tongues of surface water. Finally, the divergence of the surface isobars was found not to correlate with the stratus pattern. An awareness of the physical conditions off the coast was vital to seeing and understanding these correlations. A model SST analysis, using the six types of correlation observed, represented the actual SST analysis significantly better than the historical SST analysis.

DD FORM 1 NOV 65 1473 (PAGE 1)
S/N 0101-807-6811

Unclassified
Security Classification

A-31408

14 KEY WORDS	LINK A		LINK B		LINK C	
	ROLE	WT	ROLE	WT	ROLE	WT
Sea Surface Temperature						
Stratus						
Upwelling						
Satellite Cloud Photos						
Analysis Model						